IDENTIFICATION AND CHARACTERISATION OF *SORGHUM BICOLOR* HEME OXYGENASE-1 (*SB*HO1) GENE AND ITS ROLE IN CONFERRING BIOTIC AND ABIOTIC STRESS TOLERANCE TO PLANTS

Vivian Ikebudu

3206244

A thesis submitted in fulfilment of the requirements for the degree of

MAGISTER SCIENTIAE

In the

Department of Biotechnology

Faculty of Science

University of the Western Cape

Supervisor: Dr. Takalani Mulaudzi-Masuku

Co-Supervisors: Prof. Emmanuel Iwuoha & Dr. Andrew Faro

December 2019

GENERAL PLAGIARISM DECLARATION

Name: Vivian Ikebudu

Student number: 3206244

1. I hereby declare that I know what plagiarism entails, namely, to use another's work and to present it as my own without attributing the sources in the correct way (Refer to University Calendar part 1 for definition).
2. I know that plagiarism is a punishable offence because it constitutes theft.
3. I understand the plagiarism policy of the Faculty of Natural Science of the University of the Western Cape.
4. I know what the consequences will be if I plagiarise in any of the assignments for my course.
5. I declare therefore that all work presented by me for every aspect of my course, will be my own, and where I have made use of another's work, I will attribute the source in the correct way.

Signature Date: 27/01/20

ACKNOWLEDGEMENT

I would like to thank **The Almighty God**, the way maker, the God of possibilities for the gift of life to be able to undertake this project.

I would like to thank my supervisor **Dr. Takalani Mulaudzi-Masuku** for all her efforts, assistance, guidance and patience in her kind supervision. I am honored to work under her supervision.

I thank my co-supervisors, **Prof. Emmanuel Iwuoha** and **Dr. Andrew Faro** for their guidance and support in my research.

My appreciation extends to my colleagues in the Molecular Sciences and Biochemistry laboratory; **Miss Thembeka Mabiya, Miss Kaylin Hendricks, Mr Gershwin Sias, Miss Chelsea Aries** and **Miss Siphosethu Mazitshana** for availing their time even when they had their own projects to undertake.

I wish to express my profound thanks to my husband **Mr. Charles Nnaemeka** for encouraging me to go on with my studies and providing a loving environment for me. My sincere love to my children **Gabriella Ifeyinwa Nnaemeka, Emmanuel Chukwuelotam Nnaemeka and Gianna Amarachukwu Nnaemeka** for their understanding that mummy had to study for the better.

I thank my late father **Pastor Marcel Ikebudu**, my mom **Mrs Florence Ikebudu,** my brothers and sisters, friends and In-laws for their support and encouragement and patience. I pray that the good Lord, will bless you all abundantly. Amen!!!

Lastly, I would like to thank the **National Research Foundation (NRF)** grant holder link (2018) and the **Ada & Bertie Levenstein** (2019) for the tuition and project funds granted.

PEER-REVIEWED PUBLICATION

- Mulaudzi-Masuku, T., Ikebudu, V.C., Muthevhuli, M., Faro, A., Gehring, C.A & Iwuoha, E. 2019. Characterization and expression analysis of heme oxygenase genes from *Sorghum bicolor*. *Journal of Bioinformatics and Biology Insights*, 13: 1-11.

Table of Contents

LIST OF ABBREVIATIONS

AA	Ascorbic acid
ABA	Abscisic acid
APX	Ascorbate peroxidase
ATP	Adenosine triphosphate
BV	Biliverdin
CAT	Catalase
CDD	Conserved Domain Database
CO	Carbon monoxide
CO_2	Carbon dioxide
$CuCl_2$	Copper (II) chloride
DHAR	Dehydroascorbate reductase
DNA	Deoxyribose nucleic acid
ETC	Electron transport system
FE	Iron
FtH	Ferritin heavy chain
GA	Gibberelic acid
GPX	Guaiacol peroxidase
GR	Glutathione reductase
GSH	Glutathione
HO1	Heme oxygenase-1
H_2O_2	Hydrogen peroxide
HSP	Heat shock protein
MEGA	Molecular Evolutionary Genetics Analysis
MEME	Maximaization for Motif Elicitation
MDA	Malondialdehyde
MDHA	Monodehydroascorbate
MDHAR	Monodehydroascorbate reductase
Mn-AOX	Mitochondrial alternative oxidase
Mn-SOD	Mitochondrial superoxide dismutase
MS	Murashige & Skoog
NADP	Nicotinamide adenine diphosphate
NADPH	Nicotinamide adenine dinucleotide phosphate hydrogen

$^1O_2$	Singlet oxygen
O_2^-	Superoxide radical
OH^-	Hydroxyl radical
PDB	Protein data bank
PEPC	Phosphoenolpyruvate carboxylase
PSI	Photosystem I
PSII	Photosystem II
qRT-PCR	Quantitative real-time polymerase chain reaction
ROS	Reactive oxygen specie
SNP	Sodium nitroprusside
SOD	Superoxide dismutase
UBQ	Ubiquitin
UV	Ultraviolet
XOD	Xanthine oxidase

LIST OF TABLES

LIST OF FIGURES

Chapter 1

Literature Review

1.1 Introduction

Biotic and abiotic stresses such as herbivore attack, pathogen infection, salinity, drought, cold, heat and UV radiation, are unfavourable conditions that affect plant growth and productivity globally (Fedoroff *et al*., 2010). Agricultural productivity and food security are severely limited by salinity, drought and temperature. These environmental factors occur as a result of climate change, which is predicted to cause an increase in the occurrence of severe weather and may stimulate increased damage to plants (Zhu, 2016). Pathogen and herbivore attacks caused a 31 - 42 % loss in crop yield and about 6 - 20 % post-harvest loss (Tesfaw & Feyissa, 2014). Estimates have shown that over 50 % loss of crop yield worldwide is as a result of abiotic stresses (Lobell *et al.*, 2011) and their severity would lead to an increase in loss of arable land yearly. Population growth and migration to these arable lands further increases the issue of land desiccation and by 2050, food production will have to be increased by at least 70 % to meet the growing demand for quality, nutritious and sustainable food. Various biotic and abiotic stresses lead to the increased production of reactive oxidative species (ROS) in plants that cause damage to proteins, lipids and nucleic acids, resulting in cell death (Choudhury *et al.*, 2017).

ROS are second messengers in cellular processes; they act as signaling molecules or damaging molecules depending on the equilibrium between their production and scavenging. The ability of plants to survive stress depends on the duration and severity of the stress, changes in growth conditions and plant's adaptation capacity to changes in the energy equation (Sharma *et al.*, 2012). It has been estimated that about 1 - 2 % of oxygen consumed by plant cells leads to the production of ROS (Karuppanapandian *et al.,* 2011). Reactive oxygen species (ROS) include singlet oxygen ($^1O^2$), hydrogen peroxide (H_2O_2), hydroxyl (OH^-) and superoxide radical (O_2^-) (Des & Roychoudhury, 2014). These types of ROS are generated as unwanted by-products of O_2 used up by plants (Karuppanapandian *et al.,* 2011). Overproduction of ROS in plant results in imbalance in the redox homeostasis and leads to oxidative stress, which affects crop production (Sharma *et al.,* 2017).

Plants have adaptive mechanisms to prevent oxidative stress and these include photosynthetic pathway changes, over-expression of regulatory genes, antioxidant enzyme induction, synthesis of compatible solutes and accumulation or exclusion of ions (Tan *et al.,* 2013). The enhancement of the antioxidant defence can increase a plant's tolerance against the majority of biotic and abiotic stresses (Jin *et al.,* 2012). Non-enzymatic and enzymatic antioxidant mechanisms scavenge and detoxify excess ROS, thereby preventing oxidative damage (Sharma *et al.,* 2012). Some of the antioxidant enzymes include guaiacol peroxidase (GPX), catalase (CAT), superoxide dismutase (SOD), glutathione-S-transferase (GST) and ascorbate peroxidase (APX), while the non-enzymatic antioxidants include reduced glutathione (GSH), carotenoids, ascorbic acid (AA), proline, flavonoids, α-tocophenol and phenolics (Gill *et al.,* 2011).

Heme oxygenase 1 (HO1) is another enzymatic antioxidant in plants and animals that has attained research interest as a result of its ability to detoxify ROS and free radicals by providing cytoprotection against oxidative stress (Shekhawat *et al*., 2010). HO1 oxidatively degrades heme to produce biliverdin, carbon monoxide and free iron (He & He, 2014) and play a role in the biosynthesis of phytochrome chromophore in plants (Muramoto *et al*., 2002). HO1 has also been shown to respond to different stresses including herbicides (Xu *et al*., 2012), heavy metals (Han *et al*., 2014, Wang *et al*., 2017), salt and drought stresses (Xu *et al*., 2011). Stress tolerance in plants involves a number of genes, from the perception of stress by signal transduction pathways to the activation and control of stress-responsive genes in response to environmental stresses (Redondo-Gomez, 2013).

1.2 Biotic and abiotic stress

Stress in plants refers to external conditions that affect the growth and development or the productivity of plants. This is usually as a result of changes in environmental conditions, which triggers various responses in plants such as changes in growth rate, cellular metabolism, altered gene expression and crop yields (Gull *et al*., 2019). Plant stresses can be divided into biotic and abiotic stress. Biotic stress is caused by living organisms such as pathogens (bacteria, fungi, virus) while abiotic stress is caused by environmental factors such as salinity, drought, temperatures, and heavy metals among others (Gull *et al*., 2019).

1.2.1 Biotic stressors

1.2.1.1 Pathogens

Biotic stresses are caused by pathogens such as bacteria, viruses and fungi, which alter plants primary metabolism and affects plant growth and development (Berger *et al*., 2007). Pathogenic changes to plant metabolism comprise reallocation of photoassimilates and suppression of plants defense responses. Pathogen attack to plants leads to leaf and fruit wilt, root and stem rot, chlorosis and necrosis, photosynthetic disruption that can result in low crop yield or plant death (Selvaraj & Fofana, 2012). Examples of pathogen attacks are by bacterial wilt of tomatoes

(*Ralstonia solanacearum*), *Fusarium* wilt of tomatoes (Bawa, 2016) and root knot disease of beans caused by *Phaesariopsis griseola* (Nay *et al*., 2019) due to attack on the xylem vessel.

1.2.2 Abiotic stressors

1.2.2.1 Salinity stress

Salinity stress is one of the abiotic factors that affect agricultural crop productivity leading to over 50 % yield loss for crops. Globally, about 20 % of irrigated land is affected by salinity and there is a daily increase, which has been estimated that by 2050, about 50 % of this land will be salinised (Rasool *et al.,* 2013; FAO, 2009). Salinity stress is caused by metabolic and physiological changes inhibiting crop production depending on the severity and the length of the stress. Ionic and osmotic stresses are the secondary effect arising from salinity stress and they affect plant's processes such as nutrient uptake, metabolism and photosynthesis (Kadar, 2010). The osmotic phase occurs as a result of the presence of salt outside the root areas of a plant and leads to the inhibition of cell expansion, cell division, stomata closure and root growth. The ionic phase occurs due to the effect of salt in a plant that causes premature senescence in the adult leaves and leading to growth reduction in the photosynthetic area and enzyme activities (Munn & Tester, 2008).

1.2.2.2 Drought stress

Drought stress is an environmental stress and occurs due to various reasons including salinity, low rainfall, high and low temperatures. Drought stress causes morphological, physiological, biochemical and molecular changes in plants (Salehi-Lisar & Bakhshayeshan-Agdam, 2016). Drought occurs when there is reduced water availability in the soil and atmospheric conditions that result in water loss by evaporation or by transpiration. It causes stomata closure, water content reduction, decreased growth, cell enlargement, photosynthetic and metabolic disruption and eventually leads to plant death and thus affects food production (Jaleel *et al*., 2009).

1.2.2.3 Temperature

Plants can be affected by high, chilling or freezing temperatures which lead to physiological, molecular and morphological and biochemical changes in plants, which affect food production (Bita & Gerats, 2013). Change in temperature occurs naturally during plant growth and development; however, very high temperature damages intramolecular interactions for growth and impairs plant development leading to loss of crop productivity. Hence food security for human population is challenged (Bita & Gerats, 2013).

Low temperatures may also affect plants growth and productivity and lead to crop losses (Sanghera *et al*., 2013). Chilling (0 – 15 °C) and freezing (< 0 °C) injuries are as a result of low temperature in plants and they both interfere with non-photosynthetic and photosynthetic processes in a plant cell. Chilling and freezing stress leads to reduced crop yield and plant death (Shewfelt, 1992).

1.3 Types of reactive oxygen species

Reactive oxygen species (ROS) are reactive molecules, groups of free radicals and ions from oxygen, that are regarded as by-products from aerobic metabolism, which when produced in the cell at high amounts, results in cellular damages such as inactivation of enzymes, protein degradation, genetic alteration and programmed cell death amongst others (Sharma *et al*., 2012).

They are also beneficial in plants when produced in moderate quantities, mediating numerous responses in plants as second signaling messengers. ROS include singlet oxygen ($^1O_2$), superoxide radical (O_2^-), hydrogen peroxide (H_2O_2) and hydroxyl radical (OH^-) (Choudhury *et al.*, 2013).

Singlet oxygen ($^1O_2$) is a harmless molecule unless activated, its activation occurs by adsorption of energy to form O_2 or by stepwise mono-valent reduction to O_2^-, H_2O_2 and OH^-. Singlet oxygen can cause serious damage to photosystem I (PSI) and photosystem II (PSII) and may disrupt the photosynthetic system in plant cells. Abiotic stresses like drought and salinity cause the stomata to close, reducing the concentration of intercellular carbon dioxide (CO_2) in the chloroplast and forms singlet oxygen. Despite the short half-life of singlet oxygen which is 3 µs, it is able to diffuse through the cell and damage molecules like nucleic acids, pigments, lipids and proteins (Das & Roychoudhury, 2014). Singlet oxygen is the main reactive oxygen species that results in loss of activity of the PSII and cell death. It also up-regulates genes that protect plant cells against oxidative stress. Also, plants scavenge singlet oxygen with the aid of plastoquinone, β-carotene and tocopherol (Das & Roychoudhury, 2014).

Transfer of energy to oxygen or the partial reduction of oxygen results in the constant production of ROS in the chloroplasts. Superoxide radical (O_2^-) is formed during the non-cyclic electron transport chain (ETC) in the thylakoid localised in the photosystem I and other compartments in the cell. Superoxide radical is the first ROS to be formed by the interaction between various ETC components and oxygen, and further reaction also generates other ROS family members. Transformation reaction of O_2^- produces toxic singlet oxygen and hydroxyl radicals and leads to lipid peroxidation in the membrane (Das & Roychoudhury, 2014).

Hydrogen peroxide (H_2O_2) is produced in plant cells under normal or stress conditions such as salinity, ultraviolet (UV) irradiation, drought, cold and pathogens. Major locations of H_2O_2 production in cells are in the mitochondria, chloroplast, plasma membrane and endoplasmic reticulum. H_2O_2 can readily diffuse from its site of production through biological membranes and cause oxidative damage. High levels of H_2O_2 in cells lead to programmed cell death (Sharma *et al.*, 2012), whereas at low levels, it acts as a signaling molecule to biotic and abiotic stresses. H_2O_2 acts as a regulator in photorespiration and photosynthesis, cell cycle, senescence, stomatal movement, growth and development.

Hydroxyl radical (OH^-) production depends on O_2^- and H_2O_2 at neutral pH and temperature in the presence of transition metals. Its production is inhibited by superoxide dismutase (SOD) and catalase (CAT). Hydroxyl radical (OH^-) is the most reactive of all reactive oxygen species and its interaction with biological molecules leads to cellular damages such as protein and membrane damage as well as lipid peroxidation. Cells do not have the mechanism to scavenge OH^- enzymatically and increased production leads to cell death (Yadav & Sharma, 2016).

1.4 Sites where ROS are produced in plant cells

ROS formation occurs in stressed and unstressed cells and is formed by leakage of electrons from electron transport activities at sites located in the chloroplast, mitochondria, plasma membrane, perixosome, cell walls, apoplasts, and the endoplasmic reticulum. The main sources of ROS accumulation are the peroxisomes and chloroplast under light conditions while the main ROS producer is the mitochondrion in dark conditions (Choudhury *et al.*, 2013).

1.4.1 Chloroplast

In the chloroplast, there are thylakoid membrane systems that are ordered and house the photosynthetic machinery (Asada, 2006). ROS occur in different forms and are produced in different locations in the chloroplast. The main sites of ROS are the photosystem I (PSI) and photosystem II (PSII) electron transport systems (ETCs) in the chloroplasts. Salt, drought and temperature stress enhance ROS production in chloroplasts in the electron transfer chain (ETC) of the PSI and PSII. In normal conditions, electrons that flow from PS in an excited state centers on nicotinamide adenine diphosphate (NADP) and this is reduced to nicotinamide adenine dinucleotide phosphate hydrogen (NADPH); it then goes into the Calvin cycle and CO_2, the electron acceptor, is reduced. Under stress conditions, NADP is decreased, overloading the ETC, causing ferredoxin leakage, which leads to the reduction of O_2 to O_2^-. This then leads to the increased production of ROS (Sharma *et al.*, 2012).

1.4.2 Mitochondria

Harmful ROS can be produced in the mitochondrial ETC, which houses charged electrons that reduces O_2 to O_2^- (Arora *et al.*, 2002). Complex I and complex II are components of the mitochondrial ETC that produce ROS. Reduction of O_2 to O_2^- takes place in the nicotinamide adenine dinucleotide (NADH) dehydrogenase part of the respiratory chain in the flavoprotein region (Arora *et al.*, 2002). When substrates for complex I are depleted, reverse electron flow occurs from complex II to I and this process increases the accumulation of ROS in complex I under the regulation of adenosine triphosphate (ATP) hydrolysis (Turrens, 2003). The ETC and ATP synthases are coupled under normal aerobic conditions in plants but different stress factors modify and inhibit their components reducing the electron carrier and thus, leading to the production of ROS (Murphy, 2009). Mitochondrial superoxide dismutase (Mn-SOD) and mitochondrial alternative oxidase (Mn-AOX) are enzymes used by plants to neutralize the effect of oxidative stress.

1.4.3 Plasma membrane

The plasma membrane plays an important role with environmental changes that occur in the cell and it provides necessary information for the continuous survival of the plant cell. The NADPH-dependent oxidases localised in the plasma membrane are exposed due to the way their genes are expressed and different homologs present under stress conditions (Apel & Hirt, 2004). The NADPH-dependent oxidase mediates electron transfer from NADPH in the cytoplasm to O_2 to form superoxide radical (O_2^-). The O_2^- formed is spontaneously dismutated or the activity of superoxide dismutase (SOD) dismutates O_2^- to form hydrogen peroxide (H_2O_2). It has been supported that NADPH oxidase plays a significant role in the plant's defence against biotic and abiotic stress conditions (Apel & Hirt, 2004).

1.4.4 Peroxisomes

Peroxisomes are micro-bodies bound by a lipid bilayer membrane. Peroxisomes in plants function in the biosynthesis of auxin and jasmonic acid, photomorphogenic degradation of branched amino acids and the production of glycine betaine. It has also been suggested that regulatory proteins in the peroxisomes like kinases, heat shock proteins (HSPs) and phosphatases also exist (Grant *et al.,* 2000). Peroxisomes have an important oxidative metabolism and are the main sites for intracellular H_2O_2 production. During metabolism in the peroxisomes, superoxide radicals (O_2^-) are made at two different sites. In the first location, xanthine and hypoxanthine are metabolised to uric acid by xanthine oxidase (XOD) present in the peroxisome matrix. In the second location where the membrane is dependent on NADPH, O_2^- is produced as a by-product.

The production of H_2O_2 in peroxisomes result from metabolic processes catalysed by flavine oxidases, photo-respiratory glycosate oxidase, disproportionation of O_2^- radicals and fatty acid β-oxidation (Del Rio *et al.,* 2006). The increased production of O_2^- and H_2O_2 leads to oxidative damage while low amounts of O_2^- and H_2O_2 act as mediators in the signalling of pathogen-induced programmed cell death in plants.

1.5 Targets of reactive oxygen species

1.5.1 Proteins

Production of reactive oxygen species damages proteins, lipids and DNA as shown in Figure 1. Plants that are stressed produce ROS, which causes oxidation of proteins, thereby varying protein activity directly through nitrosylation, disulphide bond formation, carbonylation and glutathionylation, or indirectly through the breakdown of products from fatty acid peroxidation by conjugation (Moller *et al.,* 2007). Excessive ROS, result in site-specific amino acid modification, changes in electric charge, cross-linking reaction product aggregation and sensitivity of proteins to proteolysis. Different amino acids in a peptide differ in their sensitivity to attacks by ROS. Sulfur containing amino acids and thiol groups are the most vulnerable for ROS attack and their oxidation is reversible. Cysteine and methionine are susceptible to damage by hydroxyl (OH^-) and singlet oxygen ($^1O_2$) (Moller *et al.,* 2007). Enzymes with sulphur-iron centers are irreversibly inactivated once oxidized by O_2^-. Oxidized proteins are predisposed to ubiquitination and are a target for proteasomal degradation (Das & Roychoudhury, 2014).

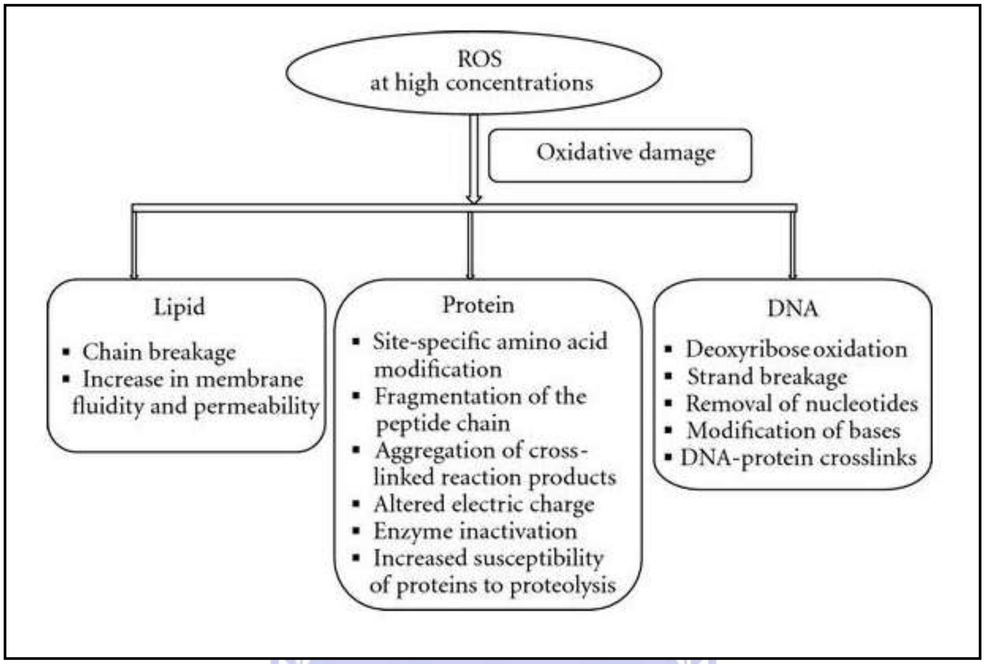

Figure 1: Target of ROS. Production of reactive oxygen species leads to protein, lipid and DNA damage (Sharma *et al.*, 2012).

1.5.2 Lipids

Cells in the plasma membrane are enveloped by lipids and are able to adapt to environmental changes. Lipid peroxidation occurs in organelles and cellular membranes and affects the cellular function when ROS level increases above threshold. Lipid peroxidation is thought to be the most damaging action known in living organisms (Gill & Tuteja, 2010). Lipid peroxidation intensifies oxidative stress by producing lipid radicals that are able to react with and damage proteins and DNA. Malondialdehyde (MDA) is one of many cytotoxic products of lipid peroxidation and causes damage to cell membranes (Wahsha *et al*., 2012). Lipid peroxidation caused by ROS can result in destabilisation and increased fluidity and permeability in the cell membrane (Sharma *et al*., 2012).

1.5.3 DNA

Reactive oxygen species are the main cause of DNA damage and cause oxidative harm to mitochondrial, chloroplastic and nuclear DNA. DNA is a cell's genetic material and when it is damaged, it can cause encoded protein changes and result in inactivation or malfunction of the protein. Oxidative stress on DNA leads to strand breakage, nucleotide removal, deoxyribose oxidation, protein-DNA crosslinks and organic base modification. Mutations also occur as a result of mismatches with nucleotides due to changes in one strand. It has been observed that plants exposed to salinity and metal toxicity undergo DNA degradation (Sharma *et al*., 2012). The hydroxyl radical reacts with purine and pyrimidine bonds and also damages the deoxyribose backbone by removal of hydrogen atoms, which further react and cause strand breaks in the DNA (Halliwell, 2006). Products generated from oxidative damage are C-8 hydroxyquanine, thymine glycol, hydroxylmethyl urea, adenine and opened thymine ring. Hydroxyl radical reacts with DNA or proteins creating DNA-protein crosslinks that are lethal to plants and are not easily reparable (Das & Roychoudhury, 2014).

1.6 Plant defence mechanism against ROS

The reactive oxygen species (ROS) defence mechanism is made up of antioxidants that aid in the alleviation of stress-induced oxidative damages. Plants have defence mechanisms comprising of non-enzymatic and enzymatic mechanisms to detoxify or scavenge ROS.

1.6.1 Non-enzymatic antioxidant mechanism in plants

Non-enzymatic antioxidants comprise of the main redox buffers; ascorbic acid, glutathione (GSH), flavonoids, α-tocopherol, carotenoids and alkaloids (Das & Roychoudhury, 2014). These antioxidants protect components of the cell and function in plant growth and development by altering cellular processes such as mitosis, elongation, senescence and cell death (De Pinto & De Gara, 2004). Mutants that have low levels of ascorbic acid or modified glutathione (GSH) content are highly sensitive to stress. Ascorbic acid is oxidized by ROS to form oxidized monodehydroascorbate (MDA) and dehydroascorbate (DHA), while glutathione (GSH) is oxidized to glutathione disulfide (GSSG). The MDA, GSSG, and DHA can be reduced through the ascorbate-glutathione cycle to improve GSH and ascorbate levels. In response to various stresses, GSH levels and the activity of GSH biosynthetic enzymes in plants are increased (Vernoux *et al*., 2002). A balance of reduced to oxidized GSH and ascorbate is important for ROS scavenging in plant cells. Antioxidants in their reduced state are sustained using NADPH as a reducing agent by monodehydroascorbate reductase (MDHAR), glutathione reductase (GR) and dehydroascorbate reductase (DHAR).

Flavonoids are secondary ROS scavengers that scavenge for damaged photosynthetic apparatus caused by energy excitation. They also scavenge singlet oxygen and improve damages caused to the chloroplast outer membrane (Agati *et al.*, 2012). Carotenoids antioxidant mechanisms protect the photosynthetic system by scavenging singlet oxygen and heat generation, reaction with lipid peroxidation products to stop the chain reaction, disperse increased energy excitation through the xanthophylls cycle and prevent the production of singlet oxygen.

1.6.2 Enzymatic antioxidant mechanism in plants

Enzymatic antioxidant mechanisms in plants include superoxide dismutase (SOD), catalase (CAT), ascorbate peroxidase (APX), glutathione reductase (GR), guaiacol peroxidase (GPX), monodehydroascorbate reductase (MDHAR) and dehydroascorbate reductase (DHAR) (Filiz *et al.*, 2019). These enzymes function in sub-cellular locations and scavenge stress-induced ROS produced in plants.

1.6.2.1 Superoxide dismutase

Superoxide dismutase (SOD) belongs to the metalloenzyme family found in aerobic organisms and plays a protective role against oxidative damages. SOD catalyses the dismutation of O_2^- into H_2O_2 and O_2 and is found in sub-cellular segments where activated oxygen is produced (Berwal & Ram, 2018). There are three types of metal-based cofactor isozymes; Mn-SOD, which is localised in the mitochondria, Fe-SOD localised in the chloroplasts and Cu/Zn-SOD localised in peroxisomes, the cytosol and chloroplasts (Mittler, 2002). These three isozymes are encoded by the nucleus and are upregulated by various abiotic stresses as a result of increased ROS formation. It has been reported that the increased production of SOD in plants leads to improved oxidative stress tolerance (Gupta *et al*., 1993).

1.6.2.2 Catalase (CAT)

Catalase is a heme-containing enzyme that catalyses the synthesis of O_2 and H_2O through the dismutation of H_2O_2 and it is present in many organisms from plants to mammals (Glorieux & Calderon, 2017). Catalase plays a role in the removal of H_2O_2 produced in the peroxisomes during oxidative stress by oxidases that are involved in purine catabolism, β-oxidation of fatty acids and photorespiration (Vellosillo *et al*., 2010). In angiosperms, isoforms *CAT1, CAT2 and*

CAT3 have been reported; *CAT1* and *CAT2* are localised in the cytosol and peroxisomes and *CAT3* is localised in the mitochondria. *CAT1* is expressed in seeds and pollens, while *CAT2* is expressed in photosynthetic tissues, roots and seeds. *CAT3* is expressed in vascular tissues and in leaves (Das & Roychoudhury, 2014). Increased catabolism produces H_2O_2, a stressful condition requiring increased energy production and outflow of the cell. CAT gets rid of H_2O_2 in an energy effective way.

1.6.2.3 Ascorbate peroxidase (APX)

Ascorbate peroxidase (APX) reduces the levels of H_2O_2 in the cytosol and chloroplasts of plant cells (Karuppanapandian *et al*., 2011). Ascorbate is used as a hydrogen donor by APX to degrade H_2O_2 to form monodehydroascorbate (MDHA) and H_2O (Karuppanapandian *et al*., 2011). Ascorbate peroxidases (APX's) are a class I family of the heme peroxidases. On the basis of different amino acid sequences, it has five isoforms that are found in different sub-cellular locations in plants. The five isoforms of APX are stromal, cytosolic, thylakoidal, peroxisomal and mitochondrial (Sharma & Dubey, 2004). The APX's have higher affinity for H_2O_2 than CAT and hence, are more efficient at scavenging H_2O_2 than CAT. Reports have shown that in response to abiotic stresses, the activity of APX increased (Hefny *et al*., 2009; Maheshwari & Dubey, 2009). Overexpression of the cytosolic APX gene derived from pea (*Pisum sativum* L.) in transgenic tomato plants (*Lycopersicon esculentum* L.) ameliorated oxidative damage induced by cold and salt stress (Wang *et al*., 2005).

1.6.2.4 Glutathione reductase (GR)

Glutathione reductase is an important low molecular-weight thiol compound present in most cells. GR plays a role in the protection of the thiol group of enzymes, reacts with OH^- and $^1O_2$ and regenerates ascorbate by acting as a disulphide reductant (Karuppanapandian *et al*., 2011). Glutathione reductase makes use of NADPH to reduce GSSG to GSH. As an antioxidant, reduced GSH is oxidised to GSSH and it regenerates ascorbic acid (AA) from monodehydroascorbate (MDHA) and dehydroascorbate (DHA). The GR activity is predominant in the chloroplast and present in small amounts in mitochondria, the cytosol and peroxisomes. The importance of GR and GSH in scavenging H_2O_2 has been ascertained in the Halliwell-Asada pathway (Asada, 2000). Increased GR activity in plants leads to an increase in GSH and confers salt tolerance to plants. Studies have shown that GR activity increased in peas under abiotic stress (Hernandez *et al.,* 2001), as well as in French bean (*Phaseolus vulgaris*) (Nagesh & Devraj, 2008) and cowpea (Contour-Ansel *et al*., 2006).

1.7 Heme oxygenase-1

Enzymatic antioxidants play a role during oxidative damage by scavenging ROS produced in plant cells. Heme oxygenases are enzymes that catalyse the oxidative conversion of heme iron (Fe) protoporphyrin (IX) into biliverdin, carbon monoxide (CO) and ferrous iron (Fe^{2+}) in the presence of a reducing agent (NADPH/FNR/Fd) (Figure 2). Three heme oxygenase (HO) isoforms have been identified in mammals, namely heme oxygenase 1 (HO1), heme oxygenase 2 (HO2) and heme oxygenase 3 (HO3) (He & He, 2014). Heme oxygenase 1 (HO1) is an inducible

32 kDa isoenzyme whose up-regulated expression is induced in response to oxidative stress and prevents programmed cell death by increasing the rate of catabolism of free heme (Gozzelino *et al.*, 2010). Heme oxygenase 2, a 36 kDa isoenzyme and (HO3), a 33 kDa isoenzyme are both constitutively expressed with low activity.

Heme contains a Fe^{2+} atom, which can act as a Fenton reactor to produce OH^- radicals from H_2O_2 (Gozzelino *et al*., 2010). Heme catabolism is a process that allows for the production of iron (Fe) from the protoporphyrin ring, which induces the expression of the ferritin H chain (FtH) and forms a complex that stores Fe (Figure 2). Heme catabolism by HO1 also generates biliverdin, which can be converted by biliverdin reductase to bilirubin, an antioxidant. Carbon monoxide (CO), a modulator of cellular signal transduction such as up-regulation of anti-apoptotic effectors and anti-inflammatory cytokines, is also produced by heme catabolism catalysed by HO1 (Gozzelino *et al.*, 2010). Carbon monoxide also acts as a modulator of the mitogen protein kinase (MAPK) pathway (Otterbein, *et al.*, 2000), activates soluble guanyl cyclase (sGC) and up-regulates cyclic guanosine monophosphate (cGMP) (Morita *et al.*, 1995). The end products of heme catabolism have cytoprotective effects such as being anti-inflammatory, anti-proliferation and anti-apoptotic. While the protective role of HO1 has been shown in a number of studies, its mechanism of action has not been fully elucidated.

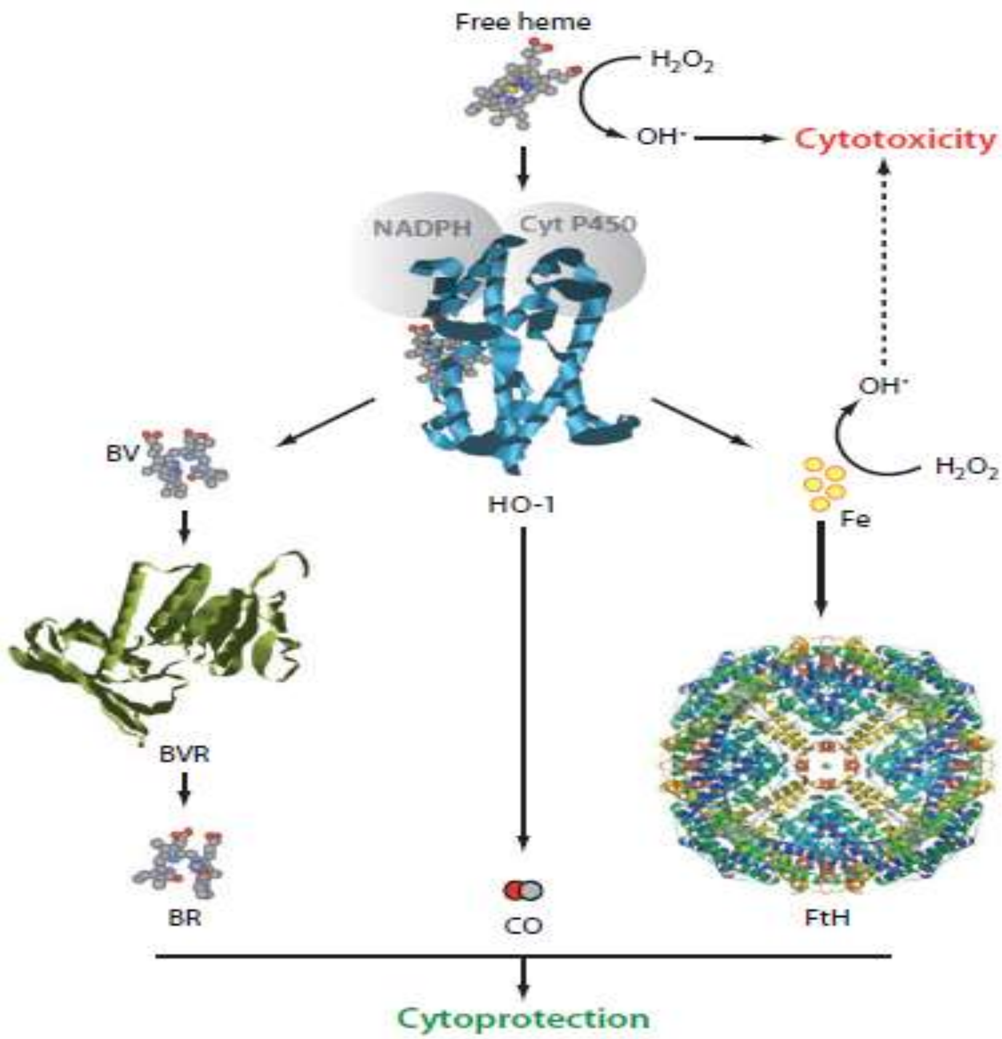

Figure 2: The heme oxygenase-1 degradation system. Free heme can catalyse the formation of cytotoxic hydroxyl radical from hydrogen peroxide. Biliverdin is synthesised from the cleavage of free heme by HO1, with the release of CO and Fe^{2+} and bilirubin (BR) is synthesised from BV by BV reductase (BVR) (Gozzelino *et al.*, 2010). Ferritin (Fe) is stored in the ferritin heavy chain (FtH) complex that stores iron.

1.7.1 Heme oxygenase-1 in plants

Heme oxygenase-1 was first identified in rat liver (Tenhunen *et al.*, 1968) as a heme degrading enzyme. Its role and cellular localisation was later characterised (Tenhunen *et al.*, 1969). Heme oxygenase has since then been identified in organisms such as algae, bacteria, insects, mammals and humans and the enzyme performs various cellular and enzymatic functions, depending on the organism (Oritz de Montellano & Wilks, 2001). Heme oxygenase in some pathogenic bacteria is used to scavenge iron from infected hosts. In algae and cyanobacteria, heme oxygenase is needed for the production of phycobilin chromophores for light harvesting photosynthesis (Beales, 1993). In mammals, heme oxygenase plays a role in the heme degradation pathway and also offers cytoprotection against oxidative susceptibility and tissue injury (Muramoto *et al*., 2002). The different enzymatic functions played by heme oxygenase in these organisms occur in different cell locations (Shekhawat & Verma, 2010). The role of heme oxygenase-1 in mammals has been well characterised as a main factor of cellular stress tolerance but its roles in plants have not been well studied and very few studies have been able to describe its antioxidative features (Shekhawat & Mahawar, 2017).

The function of heme oxygenase in plants was analysed in mutants that are not capable of producing phytochrome chromophore establishing the role that phytochromes play in various developmental responses from photo-adaptation to light and hormones interactions (Terry, 1997). Cloning of an *Arabidopsis* mutant *HYI* sequence showed similarity of the mutant gene *HYI* to that of the cyanobacteria and mammalian heme oxygenases (Muramoto *et al*., 1999). Homologues of HYI in *yg-2* (yellow-green 2) mutant of tomato, *sec-5* mutant of rice and *pcd-1* (phytochrome chromophore deficient 1) mutant of pea have been identified to function in the biosynthesis of a phytochrome chromophore (Shekhawat & Verma, 2010). Heme oxygenase genes have been identified in higher plants such as rice, maize, wheat, barley, cotton, pea, tomato and in the model plant *Arabidopsis thaliana* (Davis *et al*., 2001). Study on the characterisation of the heme oxygenase protein family in *Arabidopsis thaliana* reveals a diversity of functions such as the biosynthesis of phytochrome chromophore (Gisk *et al.*, 2010). In *Arabidopsis,* four heme oxygenase genes, HO1, HO2, HO3 and HO4 have been identified and classified into two subfamilies. The HO1, HO3 and HO4 belong to the HO1-like subfamily while the HO2 is the only member of the HO2 subfamily (Emborg *et al.*, 2006). The classification of these genes into subfamilies is based on their sequence alignment. The HO1 has the highest level of expression followed by HO2, whereas HO3 and HO4 are expressed at relatively low levels (Matsumoto *et al*., 2004).

1.7.2 The role of heme oxygenase products

Heme oxygenase oxidative degradation produces biliverdin, carbon monoxide and free iron. Biliverdin is an antioxidant and its further degradation by biliverdin reductase produces bilirubin, which is a more potent antioxidant. In animals, biliverdin produced from heme degradation reacts with biliverdin reductase and acts as a cytoprotectant by producing anti-inflammatory cytokine interferon 10, inhibits hepatitis B replication *in vitro* and inhibits nitrosylation-dependent pro-inflammatory TLR4 (Toll-like receptor 4) expression (Chen *et al*., 2012). Biliverdin is produced in plants, red algae and cyanobacteria and serves as a precursor for photosensitive tetrapyrroles like phycoerythrobilin and phycocyanobilin (Chen *et al*., 2012).

Carbon monoxide is known to be a poisonous gas. However, in animals, it is endogenously produced through induction by various stress stimuli such as heavy metals, hypoxia, heat shock and ROS (Dulak & Jozkowicz, 2003). Like nitric oxide, carbon monoxide is a signalling molecule that produces cyclic guanosine monophosphate (cGMP) by activating soluble guanylate cyclase (sGC) in animals. In plants, carbon monoxide also plays an important physiological role in regulating growth and development (Guo *et al*., 2009) as well as stomatal closure (Garcia-Mata & Lamattina, 2013), in response to environmental factors. A low level of carbon monoxide in plants enhances root and seed germination and seed dormancy breaking (He

& He, 2014). Free iron is released in a Fenton reaction with superoxide radical sequestered into ferritin, an iron storage protein (Shekhawat & Mahawar, 2017). Studies have shown that the pro-oxidant state of the cell is lowered through the upregulation of ferritin under oxidative stress (Balla *et al*., 1992), (Vile & Tyrell, 1993). While the role of free iron in animals is well studied, in plants its role has not been fully established.

1.7.3 Heme oxygenase-1 and abiotic stresses

In animals and plants, HO1 can be induced by its own substrate heme; it is also up-regulated by various stressors such as hypoxia (Motterlini *et al*., 2000), salinity (Xie *et al.*, 2011), UV radiation (Yannarelli *et al.*, 2006), heavy metals (Han *et al.*, 2008) and hydrogen peroxide (Chen *et al.*, 2009). Hematin and hemin, which are heme-containing compounds, induced heme oxygenase 1 expression in wheat (Wu *et al*., 2011), alfalfa (Han *et al*., 2007), cabbage (Duan *et al*., 2016) and tomato (Xu *et al.*, 2010). HO1 induction by β-cyclodextrin-hemin lowered the accumulation of cadmium (Cd), thereby preventing Cd-induced oxidative damage (Fu *et al.*, 2011).

1.8 *Sorghum bicolor* as the model plant

Sorghum bicolor L. (Moench) is the fifth most important cereal crop adapted to the subtropical and tropical regions of the world (Dalal *et al*, 2012). Sorghum is a diploid and has a small genome size of 750 Mbp with germplasm diversity and is a useful model cereal for structural and functional genomic studies to facilitate improved agromonically useful traits (Reddy *et al*., 2019). Its biomass can be used for animal feed and human food consumption, forages, production of green fuels that include bioethanol and biogas with less greenhouse emission.

Sorghum biomass is also used in the production of alcoholic beverages by the alcohol and liquor industry (Ignacimuthu & Premkuumar, 2014). Sorghum is the fifth most important cereal crop after wheat (*Triticum aestivum* L.), rice (*Oryza sativa* L.), maize (*Zea mays* L.) and Barley (*Hordeum vulgare* L.) (Medina *et al*., 2019). Sorghum world production was about 65.24 million tons in 2016, representing an increase of 5.42 million tons which was a 9.06 % increase from 2015 (FAO, 2016). It is one of the main staple foods of the people affected by food security, supporting over 300 million lives in Asia and Africa (Ignacimuthu & Premkuumar, 2014). In comparison to other cereal crops, sorghum produces its grain in unfavourable conditions by adaptation to a wide range of environments. Hence the need to identify and characterise genes that are able to withstand biotic and abiotic stresses and develop stress tolerant crops for food security.

1.9 Problem statement

The role of heme oxygenase 1 as a stress responsive protein has been identified and characterised in few plants including *Arabidopsis thaliana* (Gisk *et al.,* 2010), *Zea mays (*Han *et al.,* 2012), *Triticum aestivum* (Xu *et al.,* 2011), *Medicago sativa* L (Fu *et al.,* 2011), and *Brassica rapa* (Jin *et al.,* 2012). Upon induction by various environmental stresses, heme oxygenase 1 confers protection against oxidative damage and tissue injuries. To date, the role of heme oxygenase 1 (HO1) has not been identified and characterised in *Sorghum bicolor*, an important cereal crop. Therefore, identifying and characterising the role of heme oxygenase 1 in *Sorghum bicolor* would pave the way towards a better understanding of the molecular and biological role of HO1 in sorghum plants upon various stress conditions. Data generated would then be used to generate transgenics lines towards crop improvement.

2.0 The aim of the study

The aim of this research was to characterise the heme oxygenase-1 gene from *Sorghum bicolor* and examine its role in conferring biotic and abiotic stress tolerance to plants. The following objectives were followed:

- To analyse the physico-chemical parameters of the *Sb*HO-1 gene using bioinformatics tools
- To over-express *Sb*HO1 into *E. coli* BL 21 codon plus strain, purify the protein and conduct enzyme activity assay
- To analyse the expression pattern of *Sb*HO-1 using quantitative real-time PCR under biotic and abiotic stresses.

CHAPTER 2

In Silico Analysis of Sorghum Bicolor Heme Oxygenase Genes

ABSTRACT: Heme oxygenase is an enzyme that produces biliverdin, carbon monoxide and iron by oxidative catalysis of heme. In mammals, isoforms HO1, HO2 and HO3 of heme oxygenase have been identified and characterised. In *Arabidopsis thaliana* and other plants, two HO subfamilies have been identified namely; the HO1-like subfamily (HY1/HO1, HO3, and HO4) and HO2-like subfamily (HO2).To date, only the HO1 and HO2 have been sequenced, but HO3 and HO4 still remain elusive. In addition, the physico-chemical properties and functional characterisation of sorghum HO genes has not yet been done. In this study, the physicochemical properties, multiple sequence alignment, phylogenetic analysis, exon-intron structure, and conserved motif analysis of heme oxygenase genes and proteins were performed. A total of 43 HO homologous genes from 32 plant species were identified. Sequence analysis revealed that *Sb*HO1 belongs to the heme oxygenase 1 protein subfamily and encodes a protein of 21.3 kDa, with a coding sequence of 557 bp. Exon-intron organisation showed that *Sb*HO1 has 4 exons within its genomic DNA sequence. Multiple sequence alignment and conserved motif search identified the conserved heme oxygenase signature motif (QAFICHFYNI/V) as well as other amino acid sequence similarities between *Sb*HO1 and the other plant homologs. Phylogenetic analysis showed that the HO genes are grouped into specific clusters with *Sb*HO1, *Sb*HO3 and *Sb*HO4 clustered within the HO1-like subfamily and is more closely related to *Os*HO1. These bioinformatics results provide information for the identification of functional HO genes in plants and also provide a foundation for understanding stress responses mediated by HO1 in sorghum.

Keywords: *In silico*, phylogenetic analysis, conserved motif, exon-intron organization, heme oxygenase, signature motif.

2.1 INTRODUCTION

Biotic and abiotic stresses such as pathogen and herbivore attack, drought, salinity, temperature, heavy metals and UV radiation cause osmotic stress, which affects plant growth and development and lead to the increased production of reactive oxygen species (ROS) (Sharma *et al.*, 2017). These factors in turn lead to low food production and hence, food scarcity as the demand for nutritious food would increase. To prevent food scarcity, there is a need to develop stress tolerant crops. Plants have developed various mechanisms to cope with these stresses such as ion transport mediation, production of compatible solutes and production of antioxidants, which are responsible for protecting plants against ROS. Various antioxidant systems such as ascorbate peroxidase (APX), superoxide dismutase (SOD), glutathione peroxidase (GPX) and catalase (CAT) play important roles in conferring cytoprotection in animals and in plants (Xu *et al*., 2011). Heme oxygenase (HO) is also an antioxidant enzyme that catalyses the oxidative degradation of heme to produce biliverdin, carbon monoxide (CO) and iron (Fe). Heme oxygenase was first identified in rat liver (Tenhunen *et al*., 1968) as an enzyme that degrades heme and is localised in the endoplasmic reticulum (Morse & Choi, 2002). Three isoforms of heme oxygenase were identified in mammals namely; the inducible HO1 and the constitutive HO2 and HO3 isoforms. Heme oxygenase 1 is induced by its substrate, heme and various environmental stresses. These stresses leads to increase in gene expression and activity while heme oxygenase 2 and 3 are constitutively expressed (Shekhawat & Verma, 2010). In the model plant *Arabidopsis*, four heme oxygenase isoforms namely HO1, HO2, HO3 and HO4 have been identified and classified into the HO1 (HO1, HO3, HO4) subfamily and HO2 into the HO2 subfamily (Wang *et al*., 2014). While the role of heme oxygenase in mammals have been well characterised, its exact role in plants have not been well elucidated.

Bioinformatics are computer-based algorithms used to analyse and interpret biological processes (Eurich *et al.,* 2012). Bioinformatics is employed to better understand the biological role of a gene and can be employed for characterisation and phylogenetic analysis as well as determining the structural and physicochemical parameters of a protein to facilitate experimental decisions. Gene identification and sequence analysis gives a better understanding of the characteristic function of a gene or protein. The sequences are first retrieved from a public database and subjected to different tools that predict their function, evolutionary relationship and structure accurately (Mehmood *et al.,* 2014). The role of a protein can be predicted by determining the similarity of a protein sequence to that of a known protein sequence using tools like BLAST. These algorithms perform analysis tasks before further research can be undertaken and determine highly conserved sequences (Truong & Ikura, 2002).

Proteins that are evolutionarily related show characteristic functions and have a conserved tertiary structure. Online tools like ClustalW are able to show the level at which each member of a protein family is conserved. ClustalW aligns highly similar sequences with good alignment score progressively to produce global aligned sequences of these sequences. These sequences are used for phylogenetic analysis to group a gene in accordance to their level of similarity and taxa organization. A phylogenetic tree gives concise information about the origin, the evolution and the potential role of proteins (Satpathy *et al.,* 2013). Comparative analysis of exon-intron structure also gives an insight into the gene structure and organization, the functionality of a protein and evolutionary changes among different species. It also gives an understanding of the gains, losses and changes that occurred in a gene's structure, thereby bringing to light the mechanisms underlying the molecular evolution of genes and genomes (Wang *et al*., 2013).

This chapter describes the use of bioinformatics tools to analyse the physico-chemical parameters, exon-intron organization, conserved motifs, multiple sequence alignment, phylogenetic analysis, and 3D structure between *Sorghum bicolor* heme oxygenases and other plant HOs. Part of the work described in this chapter has been published in the Journal of Bioinformatics and Biology Insight (Mulaudzi-Masuku *et al*., 2019). In addition, SWISS-MODEL was used to predict the tertiary structure of *Sb*HO1.

2.2 MATERIALS AND METHODS

2.2.1 Identification and sequence analysis of heme oxygenase genes

To identify genes that encode heme oxygenase proteins, the *Arabidopsis thaliana* (*At*HO1, accession number BAA77759.1) and *Sorghum bicolor* (*Sb*HO1, accession number AF320026.1) protein sequences were obtained from the National Center for Biotechnology Information (NCBI) databases and were used as query sequences to perform a BlastP search (Altschul *et al.*, 1990). The obtained plant HO protein sequences were analysed using the Pfam database to identify the protein domain families and the CDD-search tool in the Conserved Domain Database of NCBI was used to confirm for the presence of the conserved heme binding domain. Physicochemical properties of the HO proteins such as the amino acid lengths, isoelectric point (*pI)*, instability index, aliphatic index, molecular weight and grand average of hydropathicity (GRAVY) were obtained using the Expasy ProtParam tool (Gasteiger *et al.*, 2005). Sub-cellular localisation was predicted by CELLO (Yu *et al*., 2006).

2.2.2 Gene structure and conserved motifs analysis

The Gene Structure Display Server (GSDS) online tool version 2.0 (Hu *et al.*, 2015) was used to analyse the exon-intron structure of HO genes with the corresponding cDNA sequences and genomic DNA sequences. Conserved motifs were identified and analysed using the Multiple Expectation Maximization for Motif Elicitation (MEME 5.0.2) online tool (Bailey *et al.*, 2009) with the maximum number of motifs = 5, minimum width = 6 and maximum width = 50 and other parameters at default settings. The motif sequences from the conserved motif search were analysed for functional annotation using the Conserved Domain Database (CDD) (Marchler-Bauer *et al*., 2011).

2.2.3 *Multiple sequence alignment and phylogenetic analysis of SbHO1*

Multiple sequence alignment and analysis of the HO genes among different plant species were obtained using the ClustalW2 program of the European Bioinformatics Institute (Larkin *et al.*, 2007). Phylogenetic analysis to determine the evolutionary relationship between *Sb*HO1 sequence and other plant HO1 genes was performed with MEGA: Molecular Evolutionary Genetics Analysis version 7.0 for bigger database (Kumar *et al*., 2015). The program was used to generate a boot-strapped data set of 1000 replicates. Pair-wise deletion and *p*-distance model by neighbor-joining (NJ) method were used.

2.2.4 *3D Structure prediction of SbHO1*

In order to generate the 3D model structure of *Sb*HO1, the retrieved sequence was submitted to the SWISS model workspace online server to formulate *Sb*HO1 homology models (Waterhouse *et al.*, 2018). Template search with BLAST (Camacho *et al*., 2009) and HHBlits (Remmert *et al*., 2012) was performed against the SWISS-MODEL template library. The template with the highest quality was used for model building based on the target template alignment using ProMod3.

2.3 RESULTS

2.3.1 Identification and sequence analysis of heme oxygenase (HO) genes

Public databases provide resources to identify new HO genes and perform comparative analyses among various plant species. In order to determine the biological role of the *Sb*HO1 gene, a homology search was performed in the NCBI database to retrieve 43 HO homologs from 32 plant species (Table 2.1). The HO genes were further analysed using the Pfam database and found to belong to the PF01126 protein family. The conserved heme binding domain was also detected in the predicted HO proteins by the NCBI conserved domain search tool, indicating that the HO proteins analysed have comparable function. Broad characteristics of the HO gene, including the protein domain family, gene ID, domain family description and physicochemical parameters are shown in Table 2.1. The CDS lengths varied from 278 - 1381 bp and encoded polypeptides of 184 - 338 amino acid residues (Table 2.1). The molecular weight ranged from 21.3 - 37.06 kDa with 5.39 - 9.19 *pI* values. Sub-cellular localisation from the various HO proteins was predicted to be in the chloroplast, nucleus, mitochondria and cytoplasm (Table 2.1).

Table 2.1: List of heme oxygenase enzyme homologs from 32 plant species and their primary protein features.

Species name	Phytozome gene ID	Protein domain family[a]	Exon no.	Protein length	CDS (bp)	MW (KDa)	pI	Localization CELLO[b]	Gravy	Aliphatic index	Instability index	EC
***Sorghum bicolor* HO1**	Sobic.3010G184600	PF01126	4	184	557	21.3	5.59	Cyto	-0.597	75.82	55.76	38055/37930
Sorghum bicolor HO2	Sobic.3001G347800	PF01126	4	328	987	36.43	5.39	Nucl/chl	-0.541	75.34	62.38	40130/39880
***Sorghum bicolor* HO4**	Sobic.3010G184800	PF01126	5	338	1017	37.06	8.58	Chlo	-0.185	80.09	46.08	42190/41940
***Sorghum bicolor* HO3**	Sobic.3010G184600	PF01126	4	288	867	31.88	6.42	Chlo	-0.360	78.68	56.64	43555/43430
***Arabidopsis thaliana* HO1**	AT2G26670	PF01126	3	282	849	32.69	6.50	Cyto/Chl	-0.589	76.81	45.13	40005/39880
***At*HO2**	AT2G26550	PF01126	5	299	900	34.90	5.80	Nucl	-0.795	79.20	50.50	37025/26900
***At*HO3**	AT1G69720	PF01126	5	227	684	25.60	8.24	Mito	-0.568	64.98	41.10	32110/31860
***At*HO4**	AT1G58300	PF01126	4	283	852	32.95	6.98	Cyto	-0.530	80.64	45.25	45630/45380
***Zea mays* HO1**	GRMZM2G101004	PF01126	4	285	1262	31.60	6.63	Chlo	-0.421	75.40	55.92	43555/43430
***Glycine max* HO1**	GLYMA_04GG147700	PF00126	4	282	282	32.11	8.63	Cyto	-0.484	80.99	47.08	37025/36900
***Glycine max* HO3**	GLYMA_06G221900	PF01126	4	282	282	32.07	8.83	Cyto	-0.496	79.22	48.98	37025/36900
***Oryza sativa* HO1**	LOC-Os6G40080	PF01126	4	289	870	31.91	6.28	Chlo	-0.426	72.35	55.34	45045/44920

Table 2.1 continued

Species name	Phytozome gene ID	Protein domain family[a]	Exon no.	Protein length	CDS (bp)	MW (KDa)	pI	Localization CELLO[b]	Gravy	Aliphatic index	Instability index	EC
***Oryza sativa* HO2**	LOC_Os3G27770	PF01126	4	330	993	36.54	4.92	Chlo	-0.433	79.30	56.99	38515/38390
***Brassica juncea* HO1**	LOC357966944	PF01126	NA	282	849	32.62	7.68	Chlo	-0.691	69.18	44.19	46995/46870
***Brassica juncea* HO2**	NA	PF01126	NA	232	699	26.40	6.97	Nucl	-0.544	75.22	44.63	24660/24410
***Brassica juncea* HO3**	NA	PF01126	NA	281	846	32.27	6.99	Cyto	-0.657	71.92	45.95	40005/39880
***Brassica napus* HO1**	Brara.G01278	PF01126	3	282	849	32.62	8.27	Chlo/Cyt	-0.656	69.89	44.61	46995/46870
***Medicago sativa* HO1**	NA	PF01126	NA	283	852	32.83	6.21	Cyto	-0.633	67.24	43.90	42985/42860
***Medicago sativa* HO2**	NA	PF01126	NA	290	870	33.59	8.67	Nucl	-0.576	84.66	43.82	42525/42400
***Brachypodium distachyon* HO1**	Bradi1g36640	PF01126	4	279	840	31.08	7.03	Chlo/Mit	-0.394	77.71	48.16	39535/39420
***Solanum lycopersicum* HO1**	Solyc12g009470	PF01126	4	278	837	31.96	6.98	Cyto/Mit	-0.580	72.27	42.95	35535/35410
***Solanum tuberosum* HO1**	LOC102600014	PF01126	4	278	837	32.00	7.66	Cyto/Mit	-0.605	72.27	39.66	35535/35410
***Seteria italica* HO1**	Seita.4G223200	PF01126	4	282	849	31.44	6.14	Chlo/Mit	-0.425	76.88	52.36	43555/43430

Table 2.1 continued

Species name	Phytozome gene ID	Protein domain family[a]	Exon no.	Protein length	CDS (bp)	MW (KDa)	Pi	Localization CELLO[b]	Gravy	Aliphatic index	Instability index	EC
***Hevea brasiliensis* HO1**	LOC110648797	PF01126	5	291	876	33.62	8.44	Cyto/Mit	-0.567	74.05	49.93	40130/39880
***Spinacia oleracea* HO1**	LOC110776560	PF01126	4	281	846	32.18	8.26	Cyto/Mit	-0.512	74.63	49.66	37025/36900
***Aegilops tauschii* HO1**	LOC109775269	PF01126	4	288	867	31.63	6.21	Chlo	-0.361	74.65	44.98	39535/39420
***Elaeis guineensis* HO1**	LOC105040158	PF01126	4	282	849	32.19	8.95	Cyto	-0.566	76.45	59.51	46535/46410
***Asparagus officinalis* HO1**	LOC109819496	PF01126	4	272	819	31.11	8.88	Mito/Cyt	-0.598	74.96	46.04	41035/40910
***Dendrobium catenatum* HO1**	LOC110104187	PF01126	5	285	858	32.41	8.74	Mito/Cyt	-0.575	74.60	49.24	38180/37930
***Ziziphus jujuba* HO1**	LOC107434821	PF01126	4	293	882	33.43	8.81	Mito/Cyt	-0.640	73.24	50.10	35535/35410
***Nicotiana tabacum* HO1**	LOC107818591	PF01126	4	278	837	32.27	8.50	Mito/Cyt	-0.710	68.09	46.09	38515/38390
***Gossypium hirsutum* HO1**	LOC107962617	PF01126	4	285	858	32.96	7.71	Mito/Cyt	-0.642	72.18	49.33	40005/39880
***Sesamum indicum* HO1**	LOC105162092	PF01126	4	272	819	31.18	7.73	Cyto	-0.526	74.63	36.90	35535/35410
***Jatropha curacas* HO1**	LOC105639364	PF01126	4	291	876	33.29	7.70	Chlo	-0.463	78.76	47.90	45505/45380

Table 2.1 continued

Species name	Phytozome gene ID	Protein domain family[a]	Exon no.	Protein length	CDS (bp)	MW (KDa)	Pi	Localization CELLO[b]	Gravy	Aliphatic index	Instability index	EC
Manihot esculenta HO1	Manes.14G132400	PF01126	4	289	870	33.30	8.72	Cyto/Chl	-0.539	76.92	47.10	42985/42860
Cucurbita maxima HO1	LOC111500260	PF01126	4	297	894	33.92	8.30	Chlo	-0.578	71.91	48.25	37025/36900
Amborella trichopoda HO1	AMTR_s00078p00062760	PF01126	4	305	918	34.89	9.19	Mito/Chl	-0.587	73.21	36.50	41495/41370
Chenopodium quinoa HO1	AUR62011131-RA	PF01126	4	280	843	32.18	8.72	Cyto/Mit	-0.537	76.29	42.53	38515/38390
Phalaenopsis equestris HO1	LOC110022387	PF01126	4	285	858	32.53	7.64	Cyto	-0.511	76.70	44.03	35660/35410
Curcurbita moschata HO1	LOC111441000	PF01126	4	297	894	34.02	8.61	Chlo	-0.588	71.58	51.95	37025/36900
Cucumis sativus HO1	LOC101214191	PF01126	3	291	1381	33.31	7.67	Chlo	-0.531	72.71	52.22	37025/36900
Triticum aestivum HO1	NA	PF01126	NA	288	867	31.65	6.41	Chlo	-0.370	73.65	47.29	39545/39420
Hordeum vulgare HO1	NA	PF01126	NA	288	867	31.62	6.41	Chlo	-0.339	75.00	42.60	39545/39420

2.3.2 Gene structure and conserved domain analysis of HO genes

The exon-intron structures of plant heme oxygenase genes were examined using the GSDS online tool based on the CDSs and the genomic DNA sequences corresponding to the heme oxygenase genes. This was done to better understand the structural diversity of plant HO genes (Figure 2.1). Analysis of the exon-intron structures showed that the 36 HO homologs had three to five exons; 28 HOs had four exons, 5 HOs had five exons and 3 HOs had three exons while introns ranged from two to four (Figure 2.1), *Sb*HO1 had 4 exons and 3 introns. *At*HO1, *Nt*HO1, *Cs*HO1 and *Os*HO1 had both the upstream and the downstream stream DNA sequences while *At*HO3, *Bd*HO1, *Sb*HO1 and *Sl*HO1 had either the upstream or downstream sequences. The online MEME tool was used to predict the conserved heme oxygenase motifs to better understand the protein evolution using default parameter settings (maximum number of motifs; 5, minimum motif width, 6 and maximum motif width, 50) (Figure 2.2). The sequence of each motif was verified using the NCBI protein database, motif 1 (FICHFYNIYFAHTAGGRMIGKKVAEKILBKKELEFYKWDGDLSQLLQNVR) and motif 2 (PWYAEFRNTGLERSEKLAKDLEWFKEQGYAIPEPSSPGVTY) encoded the heme oxygenase superfamily and was found to be present in all the HO homologs searched, while motifs 3, 4 and 5 did not encode any conserved domain (Figure 2.2). Motif 1 and 2 having been found in almost all heme oxygenase proteins provides a reliability of this identification and a functional similarity amongst them.

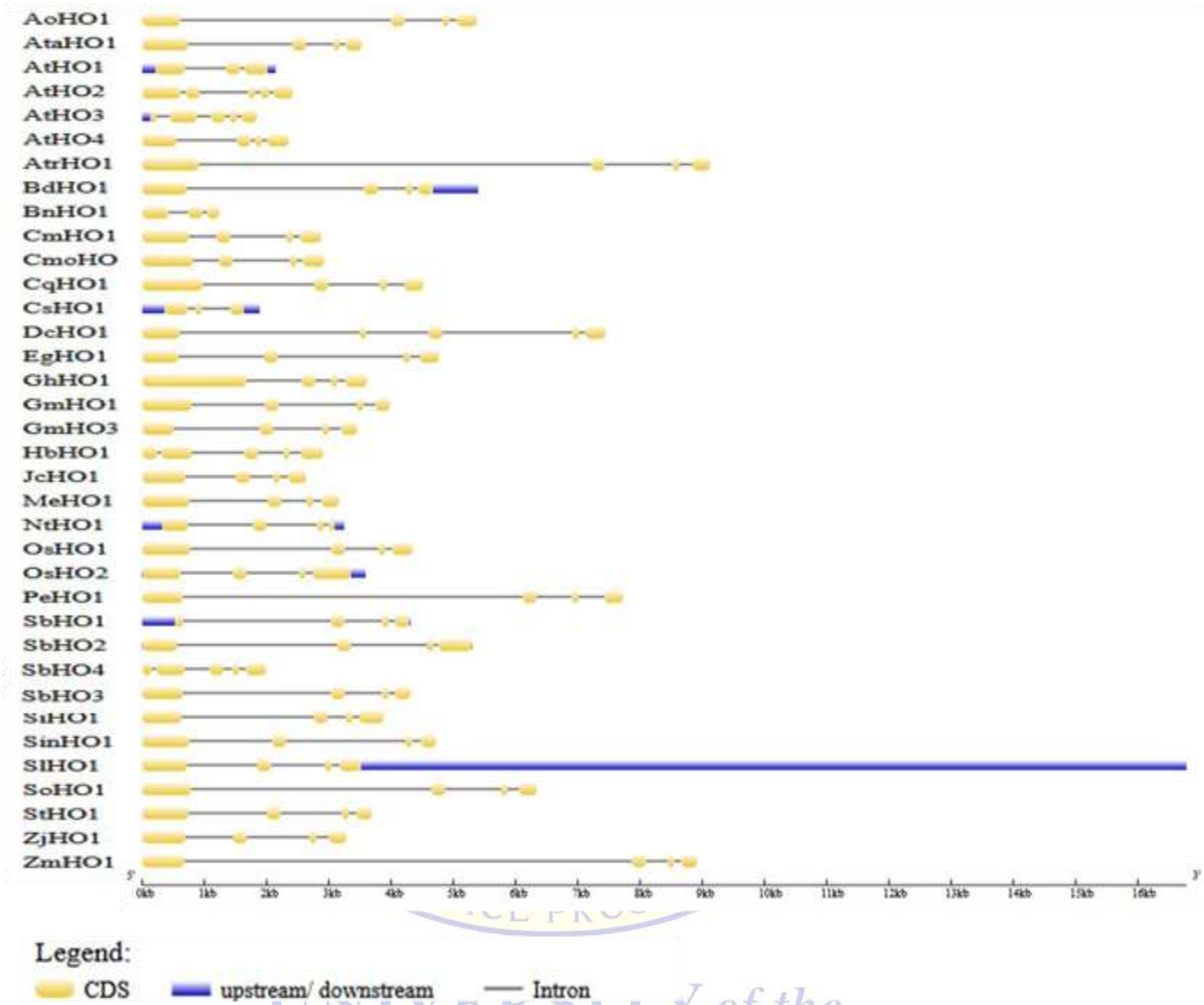

Figure 2.1: **Exon-intron organization of plant heme oxygenase genes using a GSDS server**. The species used are *Asparagus officinalis* (*Ao*HO1), *Arabidopsis thaliana* (*At*HO1, *At*HO2, *At*HO3, *At*HO4), *Aegilops tauschii* (AtaHO1), *Amborella trichopoda (Atr*HO1), *Brachypodium distachyon* (*Bd*HO1), *Brassica napus* (*Bn*HO1), *Cucurbita maxima* (*Cm*HO1), *Cucurbita moschata* (*Cmo*HO1), *Chenopodium quinoa* (*Cq*HO1), *Dendrobium catenatum* (*Dc*HO1), *Elaeis guineensis* (*Eg*HO1), *Glycine max* (*Gm*HO1, *Gm*HO3) *Gossypium hirsutum* (*Gh*HO1), *Hevea brasiliensis* (*Hb*HO1), *Jatropha curcas* (*Jc*HO1), *Manihot esculenta* (*Me*HO1), *Nicotiana tabacum* (*Nt*HO1), *Oryza sativa* (*Os*HO1, *Os*HO2), *Phalaenopsis equestris* (*Pe*HO1), *Sorghum bicolor* (*Sb*HO1, *Sb*HO2, *Sb*HO3, *Sb*HO4), *Setaria italica* (*Si*HO1), *Sesamum indicum* (*Sin*HO1), *Solanum lycopersicum* (*Sl*HO1), *Spinacia oleracea* (*So*HO1), *Solanum tuberosum* (*St*HO1), *Ziziphus jujuba* (*Zj*HO1), *Zea mays* (*Zm*HO1), *Cucumis sativus* (*Cs*HO1).

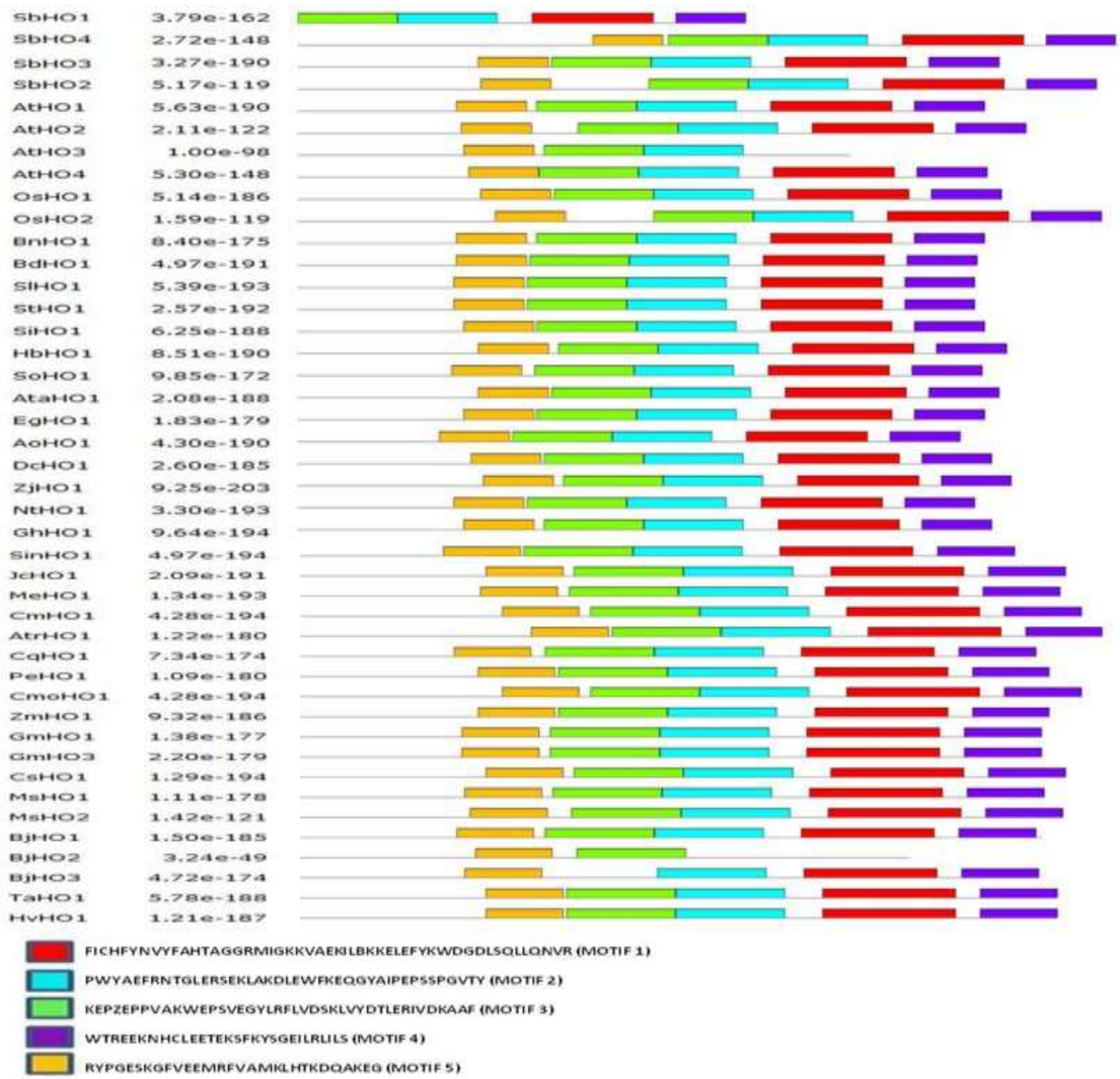

Figure 2.2: **Conserved motifs of heme oxygenase proteins**. Different motifs are shown by different colored boxes. The species searched are *Asparagus officinalis* (*Ao*HO1), *Arabidopsis thaliana* (*At*HO1, *At*HO2, *At*HO3, *At*HO4), *Aegilops tauschii* (AtaHO1), *Amborella trichopoda (Atr*HO1), *Brachypodium distachyon* (*Bd*HO1), *Brassica napus* (*Bn*HO1), *Cucurbita maxima* (*Cm*HO1), *Cucurbita moschata* (*Cmo*HO1), *Chenopodium quinoa* (*Cq*HO1), *Dendrobium catenatum* (*Dc*HO1), *Elaeis guineensis* (*Eg*HO1), *Glycine max* (*Gm*HO1, *Gm*HO3) *Gossypium hirsutum* (*Gh*HO1), *Hevea brasiliensis* (*Hb*HO1), *Jatropha curcas* (*Jc*HO1), *Manihot esculenta* (*Me*HO1), *Nicotiana tabacum* (*Nt*HO1), *Oryza sativa* (*Os*HO1, *Os*HO2), *Phalaenopsis equestris* (*Pe*HO1), *Sorghum bicolor* (*Sb*HO1, *Sb*HO2, *Sb*HO3, *Sb*HO4), *Setaria italica* (*Si*HO1), *Sesamum indicum* (*Sin*HO1), *Solanum lycopersicum* (*Sl*HO1), *Spinacia oleracea* (*So*HO1), *Solanum tuberosum* (*St*HO1), *Ziziphus jujuba* (*Zj*HO1), *Zea mays* (*Zm*HO1), *Cucumis sativus* (*Cs*HO1), *Medicago sativa* (*Ms*HO1, *Ms*HO2), *Brassica juncea* (*Bj*HO1, *Bj*HO2, *Bj*HO3), *Triticum aestivum* (*Ta*HO1), *Hordeum vulgare* (*Hv*HO1).

2.3.3 Multiple sequence alignment and phylogenetic analysis of HO genes

Multiple sequence alignment and phylogenetic analysis were performed based on the amino acid sequences of HO1 to examine the conservation and diversity of the HO1 domain region (Figure 2.3 and 2.4). The alignment showed that the amino acid sequences are conserved in the HO signature sequence (QAFICHFYNI/V) (Figure 2.3) with *Sb*HO1's signature sequence (QAFICHFYNV) similar to that of the HO1-like sub-family. Isoform HO2 of *Oryza sativa*, *Medicago sativa, Sorghum bicolor*, *Arabidopsis thaliana* and *Brassica juncea,* HO3 of *Glycine max* and *Brassica juncea,* HO2, HO3 and HO4 of *Arabidopsis thaliana* were also included in both the alignment and phylogenetic analysis. The multiple sequence alignment showed that the HO1 sub-family members; HO1, HO3 and HO4 are more closely related and therefore shows higher sequence conservation than the HO2 sub-family (Figure 2.3). The HO2 lacks the histidine for heme-binding and catalysis, which is present in the HO1-like sub-family. The signature sequence of all HO3's from *Brassica juncea*, *Glycine max*, *Sb*HO3 share similarities with HO1s whereas HO4 signature sequence from *Arabidopsis thaliana* and *Sorghum bicolor* are different to the HO1s but similar to each other. The phylogenetic tree was constructed using the neighbor-joining method and clearly showed that the HO1 sub-family members are differently clustered from the HO2 sub-family and are conserved across species (Figure 2.4). *Sb*HO1, 3 and 4 are grouped into the HO1-like subfamily and *Sb*HO1 is more closely related to *Os*HO1. These results show that the HOs have conserved similarity across the plant species.

Figure 2.3

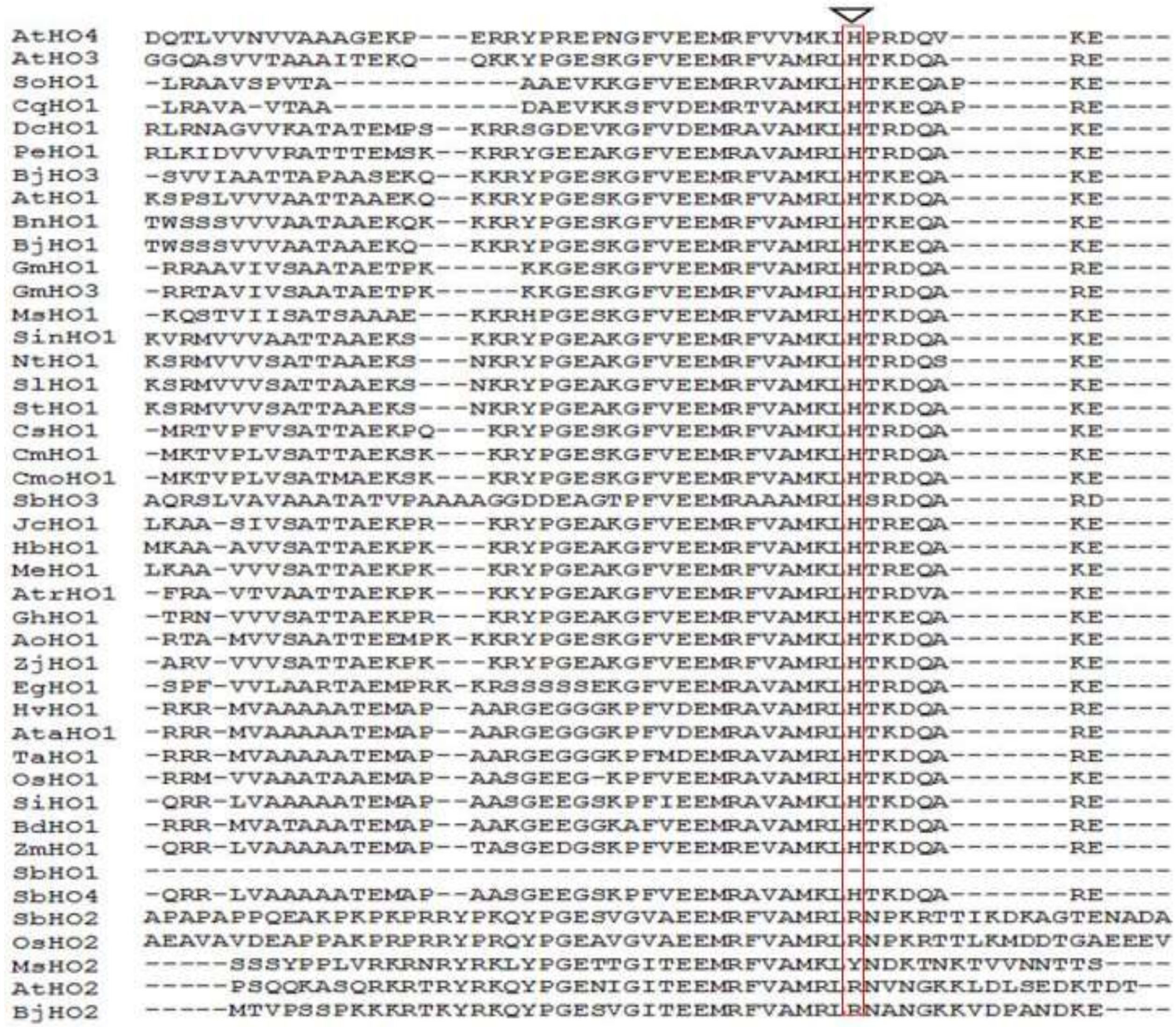
AtHO4 DQTLVVNVVAAAGEKP---ERRYPREPNGFVEEMRFVVMKIHPRDQV-------KE----
AtHO3 GGQASVVTAAAITEKQ---QKKYPGESKGFVEEMRFVAMRLHTKDQA-------RE----
SoHO1 -LRAAVSPVTA-----------AAEVKKGFVEEMRRVAMKLHTKEQAP------KE----
CqHO1 -LRAVA-VTAA-----------DAEVKKSFVDEMRTVAMKLHTKEQAP------RE----
DcHO1 RLRNAGVVKATATEMPS--KRRSGDEVKGFVDEMRAVAMKLHTRDQA-------KE----
PeHO1 RLKIDVVVRATTTEMSK--KRRYGEEAKGFVEEMRAVAMRLHTRDQA-------KE----
BjHO3 -SVVIAATTAPAASEKQ--KKRYPGESKGFVEEMRFVAMKLHTKEQA-------KE----
AtHO1 KSPSLVVVAATTAAEKQ--KKRYPGESKGFVEEMRFVAMRLHTKDQA-------KE----
BnHO1 TWSSSVVVAATAAEKQK--KKRYPGESKGFVEEMRFVAMRLHTKEQA-------KE----
BjHO1 TWSSSVVVAATAAEKQ---KKRYPGESKGFVEEMRFVAMRLHTKEQA-------KE----
GmHO1 -RRAAVIVSAATAETPK-----KKGESKGFVEEMRFVAMRLHTRDQA-------RE----
GmHO3 -RRTAVIVSAATAETPK-----KKGESKGFVEEMRFVAMRLHTRDQA-------RE----
MsHO1 -KQSTVIISATSAAAE---KKRHPGESKGFVEEMRFVAMRLHTKDQA-------KE----
SinHO1 KVRMVVVAATTAAEKS---KKRYPGEAKGFVEEMRFVAMKLHTRDQA-------KE----
NtHO1 KSRMVVVSATTAAEKS---NKRYPGEAKGFVEEMRFVAMKLHTRDQS-------KE----
SlHO1 KSRMVVVSATTAAEKS---NKRYPGEAKGFVEEMRFVAMKLHTKDQA-------KE----
StHO1 KSRMVVVSATTAAEKS---NKRYPGEAKGFVEEMRFVAMKLHTKDQA-------KE----
CsHO1 -MRTVPFVSATTAEKPQ---KRYPGESKGFVEEMRFVAMKLHTRDQA-------KE----
CmHO1 -MKTVPLVSATTAEKSK---KRYPGESKGFVEEMRFVAMKLHTRDQA-------KE----
CmoHO1 -MKTVPLVSATMAEKSK---KRYPGESKGFVEEMRFVAMKLHTRDQA-------KE----
SbHO3 AQRSLVAVAAATATVPAAAAGGDDEAGTPFVEEMRAAAMRLHSRDQA-------RD----
JcHO1 LKAA-SIVSATTAEKPR---KRYPGEAKGFVEEMRFVAMKLHTREQA-------KE----
HbHO1 MKAA-AVVSATTAEKPK---KRYPGEAKGFVEEMRFVAMKLHTREQA-------KE----
MeHO1 LKAA-VVVSATTAEKPK---KRYPGEAKGFVEEMRFVAMKLHTREQA-------KE----
AtrHO1 -FRA-VTVAATTAEKPK---KKYPGEAKGFVEEMRFVAMRLHTRDVA-------KE----
GhHO1 -TRN-VVVSATTAEKPR---KRYPGEAKGFVEEMRFVAMKLHTKEQA-------KE----
AoHO1 -RTA-MVVSAATTEEMPK-KKRYPGESKGFVEEMRFVAMKLHTKDQA-------KE----
ZjHO1 -ARV-VVVSATTAEKPK---KRYPGEAKGFVEEMRFVAMRLHTKDQA-------KE----
EgHO1 -SPF-VVLAARTAEMPRK-KRSSSSSEKGFVEEMRAVAMKLHTRDQA-------KE----
HvHO1 -RKR-MVAAAAATEMAP--AARGEGGGKPFVDEMRAVAMRLHTKDQA-------RE----
AtaHO1 -RRR-MVAAAAATEMAP--AARGEGGGKPFVDEMRAVAMRLHTKDQA-------RE----
TaHO1 -RRR-MVAAAAATEMAP--AARGEGGGKPFMDEMRAVAMRLHTKDQA-------RE----
OsHO1 -RRM-VVAAATAAEMAP--AASGEEG-KPFVEEMRAVAMRLHTKDQA-------KE----
SiHO1 -QRR-LVAAAAATEMAP--AASGEEGSKPFIEEMRAVAMKLHTKDQA-------RE----
BdHO1 -RRR-MVATAAATEMAP--AAKGEEGGKAFVEEMRAVAMRLHTKDQA-------RE----
ZmHO1 -QRR-LVAAAAATEMAP--TASGEDGSKPFVEEMREVAMKLHTKDQA-------RE----
SbHO1 --
SbHO4 -QRR-LVAAAAATEMAP--AASGEEGSKPFVEEMRAVAMKLHTKDQA-------RE----
SbHO2 APAPAPPQEAKPKPKPRRYPKQYPGESVGVAEEMRFVAMRLRNPKRTTIKDKAGTENADA
OsHO2 AEAVAVDEAPPAKPRPRRYPRQYPGEAVGVAEEMRFVAMRLRNPKRTTLKMDDTGAEEEV
MsHO2 -----SSSYPPLVRKRNRYRKLYPGETTGITEEMRFVAMKLYNDKTNKTVVNNTTS----
AtHO2 -----PSQQKASQRKRTRYRKQYPGENIGITEEMRFVAMRLRNVNGKKLDLSEDKTDT--
BjHO2 -----MTVPSSPKKKRTKYRKQYPGESVGITEEMRFVAMRLRNANGKKVDPANDKE----

Figure 2.3 continued

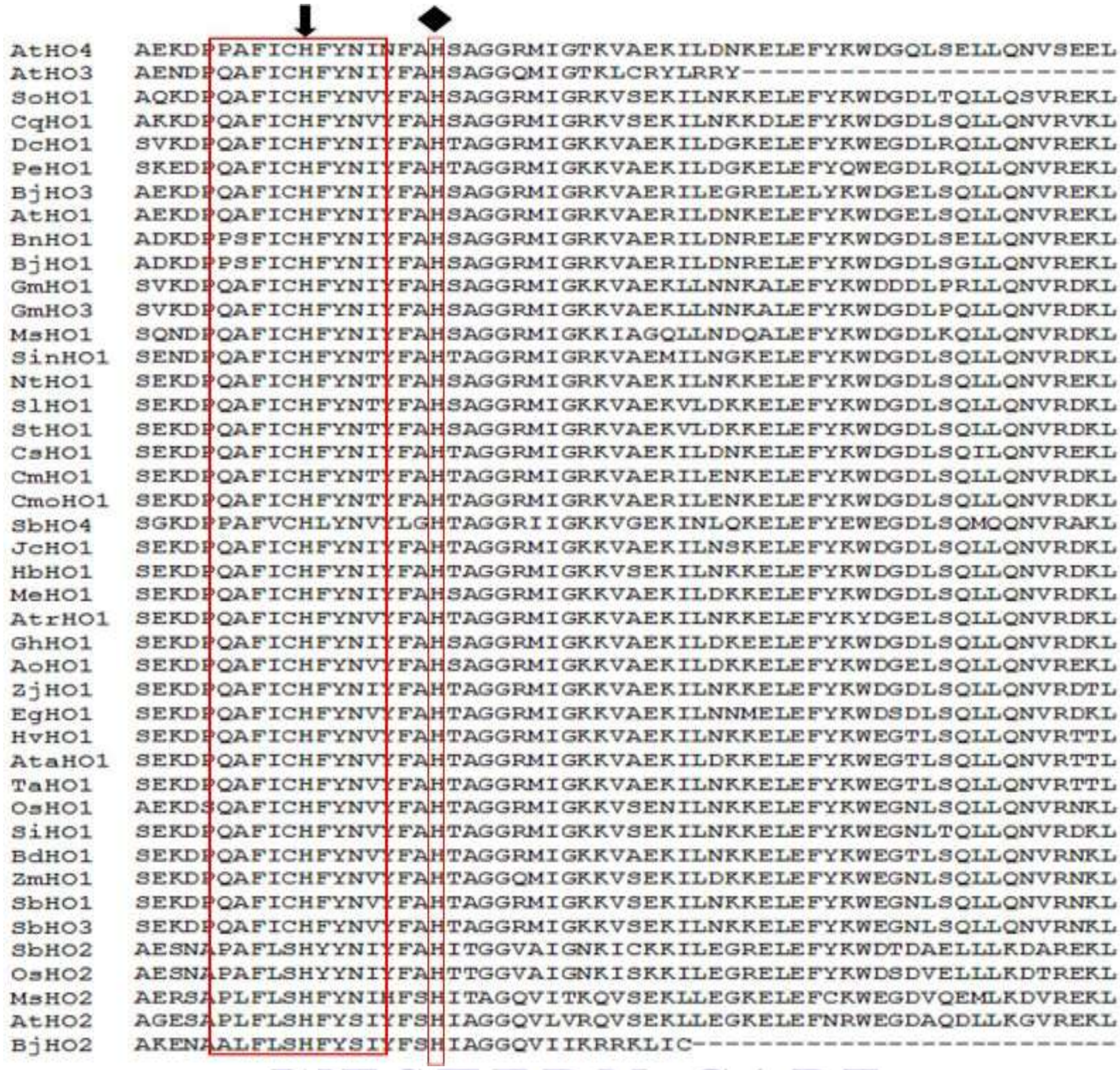

Figure 2.3: Multiple sequence alignment of *Sb*HO1 gene and other HO1/2/3/4 isoforms in plants using ClustalW2. The conserved HO amino acids are emphasized with red block. The black arrow pointing downwards is the conserved histidine residue for protein stability. The white reverse triangle shows the heme-iron binding and catalysis conserved histidine residue not present in HO2 sequences. The black diamond shows the conserved histidine residue that is involved in ascorbic acid binding. The species used are *Asparagus officinalis* (*Ao*HO1), *Arabidopsis thaliana* (*At*HO1, *At*HO2, *At*HO3, *At*HO4), *Aegilops tauschii* (AtaHO1), *Amborella trichopoda (Atr*HO1), *Brachypodium distachyon* (*Bd*HO1), *Brassica napus* (*Bn*HO1), *Cucurbita maxima* (*Cm*HO1), *Cucurbita moschata* (*Cmo*HO1), *Chenopodium quinoa* (*Cq*HO1), *Dendrobium catenatum* (*Dc*HO1), *Elaeis guineensis* (*Eg*HO1), *Glycine max* (*Gm*HO1, *Gm*HO3) *Gossypium hirsutum* (*Gh*HO1), *Hevea brasiliensis* (*Hb*HO1), *Jatropha curcas* (*Jc*HO1), *Manihot esculenta* (*Me*HO1), *Nicotiana tabacum* (*Nt*HO1), *Oryza sativa* (*Os*HO1, *Os*HO2), *Phalaenopsis equestris* (*Pe*HO1), *Sorghum bicolor* (*Sb*HO1, *Sb*HO2, *Sb*HO3, *Sb*HO4), *Setaria italica* (*Si*HO1), *Sesamum indicum* (*Sin*HO1), *Solanum lycopersicum* (*Sl*HO1), *Spinacia oleracea* (*So*HO1), *Solanum tuberosum* (*St*HO1), *Ziziphus jujuba* (*Zj*HO1), *Zea mays* (*Zm*HO1), *Cucumis sativus* (*Cs*HO1), *Medicago sativa* (*Ms*HO1, *Ms*HO2), *Brassica juncea* (*Bj*HO1, *Bj*HO2, *Bj*HO3), *Triticum aestivum* (*Ta*HO1), *Hordeum vulgare* (*Hv*HO1).

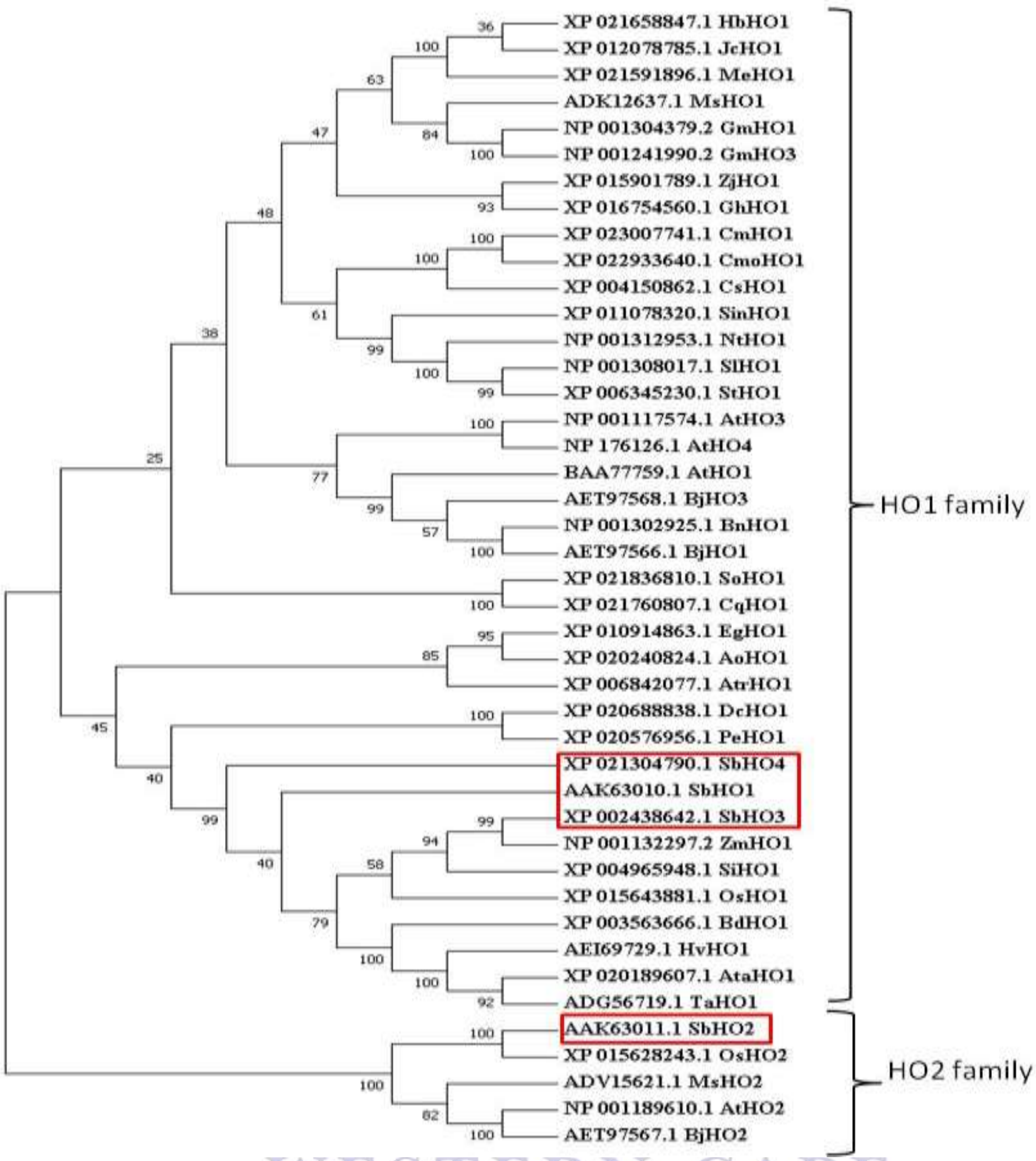

Figure 2.4: Phylogenetic tree showing evolutionary relationship between *Sb*HO1 sequence and other HO1/2/3/4 sequence from plant. The protein sequence of *Sb*HO1 was aligned with 24 other HO1/2/3/4 sequence from plant using ClustalW2 and analyzed using MEGA 7 program by neighbor-joining method with 1000 bootstrap replicate. The species used are *Asparagus officinalis* (*Ao*HO1), *Arabidopsis thaliana* (*At*HO1, *At*HO2, *At*HO3, *At*HO4), *Aegilops tauschii* (AtaHO1), *Amborella trichopoda (Atr*HO1), *Brachypodium distachyon* (*Bd*HO1), *Brassica napus* (*Bn*HO1), *Cucurbita maxima* (*Cm*HO1), *Cucurbita moschata* (*Cmo*HO1), *Chenopodium quinoa* (*Cq*HO1), *Dendrobium catenatum* (*Dc*HO1), *Elaeis guineensis* (*Eg*HO1), *Glycine max* (*Gm*HO1, *Gm*HO3) *Gossypium hirsutum* (*Gh*HO1), *Hevea brasiliensis* (*Hb*HO1), *Jatropha curcas* (*Jc*HO1), *Manihot esculenta* (*Me*HO1), *Nicotiana tabacum* (*Nt*HO1), *Oryza sativa* (*Os*HO1, *Os*HO2), *Phalaenopsis equestris* (*Pe*HO1), *Sorghum bicolor* (*Sb*HO1, *Sb*HO2, *Sb*HO3, *Sb*HO4), *Setaria italica* (*Si*HO1), *Sesamum indicum* (*Sin*HO1), *Solanum lycopersicum* (*Sl*HO1), *Spinacia oleracea* (*So*HO1), *Solanum tuberosum* (*St*HO1), *Ziziphus jujuba* (*Zj*HO1), *Zea mays* (*Zm*HO1), *Cucumis sativus* (*Cs*HO1), *Medicago sativa* (*Ms*HO1, *Ms*HO2), *Brassica juncea* (*Bj*HO1,*Bj*HO2, *Bj*HO3), *Triticum aestivum* (*Ta*HO1), *Hordeum vulgare* (*Hv*HO1).

2.3.4 Structure modelling of SbHO1

The *Sb*HO1 sequence was used to search against the Swiss-Model template library and the template with the highest quality was selected for model building using ProMod3 (Figure 2.5). Conserved coordinates between the target and the template was used to model the tertiary structure of *Sb*HO1. The search generated about 50 templates, however the templates with the highest sequence identity used to build the model were the HO D136E mutant from *Corynebacterium diphtheriae* (HmuO) (1wnx.1.A) (Figure 2.6) and rat heme oxygenase (HO-1) in complex with heme binding to dithiothreitol (DTT) (3i9t.1.A) (Appendix I: Figure 1). HmuO showed 25.29 % sequence identity to *Sb*HO1, while rat HO-1 showed 22.54 % sequence identity to *Sb*HO1 (Appendix I: Figure 1). The models built are monomers with no ligands, with GMQE (Global Model Quality Estimation) scores of 0.64 and 0.62, which indicates a higher reliability of the search and a QMEAN (Qualitative Model Energy Analysis) score of -3.22 and -3.63 respectively, which indicates the degree of "nativeness" of the model globally (Appendix I: Figure 1) suggesting that *Sb*HO1 model that was generated was of high quality. A comparison plot with a non-redundant set of PDB structures showed the QMEAN4 (Qualitative Model Energy Analysis 4) Z score (Figure 2.6) of a combination of the c-beta atoms for residual level implementation, solvation energy for burial status of residues, all-atom energy for capturing model and torsion angle for local geometry (Appendix I: Figure 1).

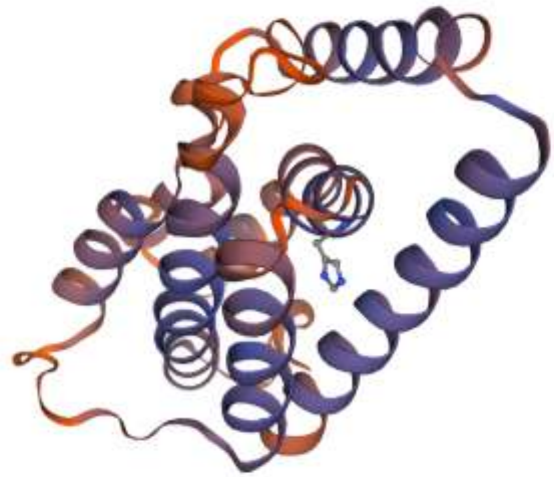

Figure 2.5: Structural model of *Sb*HO1 generated by SWISS-Model using *Corynebacterium diphtheria* HmuO as a template (https://swissmodel.expasy.org/interactive).

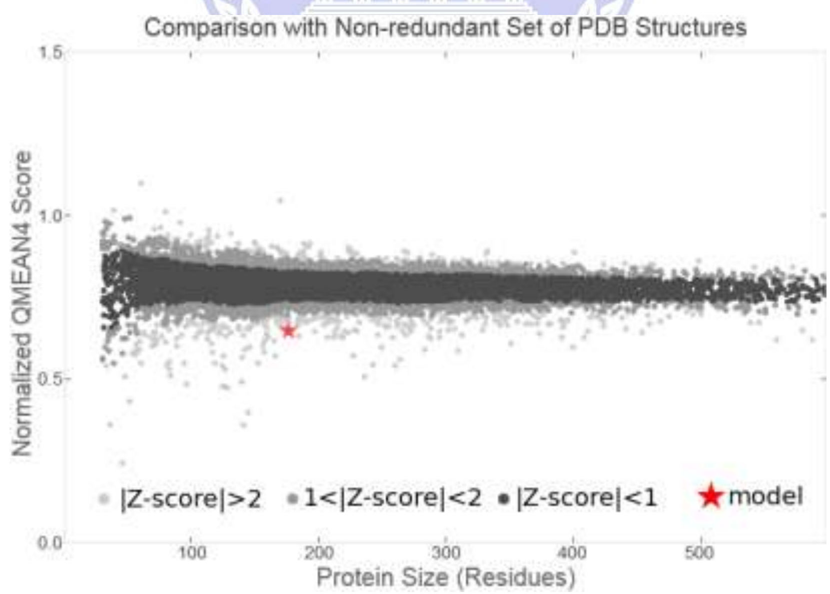

Figure 2.6: QMEAN4 Z score estimation of absolute model quality from SWISS-MODEL work space for *Sb*HO1: using structural coordinate for *Corynebacterium diphtheria* HmuO https://swissmodel.expasy.org/interactive .

2.4 DISCUSSION

Heme oxygenases in plants are comprised of the HO1-like sub-family that includes the HO1, HO3 and HO4 genes and the HO2 sub-family, based on their amino acid sequences (Shekhawat & Vema, 2010). Heme oxygenase genes have been identified in *Arabidopsis thaliana,* barley, tomatoe, potatoe, maize, soybean, wheat and rice, among other crops (Shekhawat & Verma, 2010). Heme oxygenase plays various roles in protecting plants from oxidative damages (Shekhawat & Verma, 2010) but its functional role in *Sorghum bicolor* has not been characterised. To understand the protective mechanism of *Sb*HO1 and its role in stress defence, *Sb*HO1 was identified and characterised in comparison to 42 other heme oxygenase homologs from 32 plant species. These homologs included 4 genes from *Arabidopsis,* 4 from *Sorghum bicolor,* 3 from *Brassica junea,* 2 from *Oryza sativa* and *Medicago sativa* and 1 each from other plant species (Table 2.1). The characteristic features of *Sb*HO1 and other plant HOs such as the gene structure (gene ID, protein family domain, exon count) and physical parameters (instability index, aliphatic idex, extinction coefficient, protein length, and molecular weight) are detailed in Table 2.1. The instability index of the heme oxygenase genes varied from 36.50 to 62.38, aliphatic index ranged from 64.98 to 84.66, GRAVY ranged from -0.185 to -0.795 and the extinction coefficient ranged from 32110/31860 to 46995/46870 (Table 2.1). The instability index is a measure of the half life of a protein *in vivo* and a protein with an instability index of more that 40 has a half-life of less than 5 hours, while a protein with an instability index of less than 40 has a half life of more than 16 hours (Indicula-Thomas & Balaji, 2004). *Sb*HO1 is composed of 180 amino acid residues with a molecular weight of 21.3 kDa, an instability index of 55.76 (thus it is predicted to be unstable) and a pI of 5.59, which is acidic. *Sb*HO1 has an aliphatic index of 75.82, indicative that it is highly occupied by aliphatic chains with increased thermal stability. *Sb*HO1 has a GRAVY of -0.597, which indicates that it is interactible with water making it a soluble protein as confirmed by SOSUI and an extinction coefficient of 38055/37930 (Table 2.1).

Gene structure analysis gives an insight on how genes evolves. It determines a gene family's evolutionary history, providing insights into the evolution of gene families. The positions, phases, or loss or gain of an intron aid in understanding evolution (Wu *et al.,* 2017). As shown in Figure 2.1, the exon-intron structure from the GSDS server confirmed the exon count from the NCBI database (Table 2.1) of the HO homologs, which have 3 - 5 exons with a varied number of introns. *Sb*HO1 specifically contains 4 exons with 3 intron between the exons.

Motifs enables a clear understanding of a protein's evolution and functionality and also plays a significant role in transcriptional regulation. Protein networks are controlled by specific peptide motifs, which is a linker to the importance of motif to a protein's function and structure (Mittal *et al.,* 2018). To understand the diversity and similarity of gene motifs in different HO genes, five conserved motifs were identified. In this study, two motifts were found namely; motif 1 (FICHFYNIYFAHTAGGRMIGKKVAEKILBKKELEFYKWDGDLSQLLQNVR) and motif 2 (PWYAEFRNTGLERSEKLAKDLEWFKEQGYAIPEPSSPGVTY), which encoded the heme binding domain, and a characteristic of the heme oxygenase superfamily as it is present in almost all HO homologs, while motifs 3 - 5 had no putative conserved domains (Figure 2). However, *Bj*HO2 lacked motifs 1 and 2 and *At*HO3 lacked motif 1. These conserved motifs found in relation with the HO family mean that the HO sequences are conserved at these positions between species. Search results for conserved motifs can be used to identify signaling pathways, assess gene expression patterns and develop gene resistant markers.

Multiple sequence alignments indicated that *Sb*HO1 showed high similarity to heme oxygenase-1 (HO1) from other plant species (Figure 2.3). The HO1 signature sequence (QAFICHFYNI/V) is conserved across the plant species while HO2 (PLFLSHFYSIYF) showed few sequence differences from the HO signature sequence (Figure 2.3). The signature sequence for *At*HO3 of (QAFICHFYNI) showed similarity to *At*HO1, whereas *At*HO4 (PAFICHFYNI) had a single amino acid sequence difference as compared to the HO1 signature sequence (highlighted in red). The HO1-like signature sequence has a conserved histidine needed for heme-iron binding and catalysis; this conserved histidine is not present in the HO2 sub-family. It was reported that the amino acid spacer between 34 - 55 residues in HO2 replaces a conserved area found in the HO1 sequence and is the major difference between the HO1 and HO2 sub-families (Davis *et al.*, 2001). In Figure 2.3, it can be seen that the histidine residue (indicated by the open triangle) involved in heme-iron binding and catalysis present in the HO1 subfamily is replaced by arginine and tyrosine residues in the HO2 subfamily.

A phylogenetic tree using the neighbor-joining method showed that *Sb*HO1, *Sb*HO3 and *Sb*HO4 are clustered under the HO1 sub-family while the *Sb*HO2 is clustered with the HO2 sub-family (Figure 2.4). The phylogenetic tree also shows that *Sb*HO1 and *Sb*HO4 are more closely related to *Os*HO1 and *Bj*HO1. *Sb*HO2 is closely related to *Os*HO2 (Figure 2.4) while *Sb*HO3 is closely related to *Zm*HO1. These results indicate that the HO1-like sub-family might have less similarity to the HO2-like sub-family after species divergence and this is in agreement with previous studies (Zhu *et al*., 2014; Xu *et al*., 2011).

The Swiss-Model server was used to predict the 3D structure of *Sb*HO1 using the D136E mutant of heme oxygenase from *Corynebacterium diphtheriae* (HmuO) (1wnx.1. A) and rat heme oxygenase (HO-1) in complex with heme binding dithiothreitol (DTT) (3i9t.1.A) as templates.

The predicted models had high sequence identity of 25.29 % and 22.54 % and 1.8 Å and 2.1 Å angle resolutions respectively (Appendix I: Figure 1). The models have GMQE scores of 0.64 and 0.62, which indicates a higher reliability of the search and a QMEAN of -3.22 and -3.63 respectively, indicating a degree of nativeness of the model globally (Figure 2.6). Global Model Quality Estimation (GMQE) score was between 0 and 1 and shows the accuracy of a model build with that alignment and template and the coverage of the target. A higher number means the model has a higher reliability. The QMEAN Z-score is indicative of the model compared to the expected outcome from experimentally determined structures with similar size and scores of -4.0 and below indicates that the models are of a low quality (Benkert *et al*., 2011). QMEAN Z-score for the models indicates that of high quality as expected from experimental structure of same size. These findings suggest that *Sb*HO1 and other HO1 in plants have a conserved role in plant responses against stress and have similar structures.

CHAPTER 3

Expression and Purification of Sorghum bicolor Heme Oxygenase-1 (SbHO1)

ABSTRACT: Heme oxygenase-1, the enzyme that oxidatively catalyses the formation of biliverdin from heme has been identified and characterised in a few plant species as stress-responsive when induced by abiotic stresses. However, the molecular and enzymatic characterisation of heme oxygenase from *Sorghum bicolor* has not been performed. The aim of this chapter was to express and purify *Sb*HO1 protein and to perform enzymatic assays to confirm that *Sb*HO1 is a *bona fide* heme oxygenase. The *Sb*HO1 gene was cloned into the pTrcHis-TOPO vector (TA) and successfully over-expressed in *E. coli* BL21 cells under the induction with isopropyl-1-thio-D-galactopyranoside. Purification was done under denaturing conditions and the protein properly refolded as shown by an intact band at 25.1 kDa, which corresponds to 21.3 kDa *Sb*HO1 protein size plus the 6xHis tag which has a molecular weight of 3.8 kDa. Enzyme activity assays were performed to determine the ability of *Sb*HO1 to convert heme to biliverdin, thus providing an insight into the molecular processes of *Sb*HO1. The results showed that *Sb*HO1 is a true heme oxygenase that is able to convert heme to biliverdin as observed by soret bands at 405 nm and 610 nm, which correspond to the heme-enzyme (HO) complex and billiverdin respectively. In conclusion this study has identified and experimentally characterised a *Sorghum bicolor* heme oxygenase-1 and showed that it degrades heme to form billiverdin.

Keywords: Biliverdin, expression, heme, *Sorghum bicolor*, denaturing, purification.

3.1 INTRODUCTION

Protein expression involves the use of molecular techniques to produce target proteins and to determine its structural and functional properties. Recombinant protein expression can be conducted using prokaryotic, eukaryotic or *in vitro* systems (Jia & Jeon, 2016). Expression plasmids carrying suitable cDNA are transformed into a suitable expression host (Wingfield, 2016). *E. coli* is often used as an expression host for production of proteins of either plant or animal origin, because it is time and cost effective, easy to genetically modify and also gives high protein yields (Jia & Jeon, 2016).

An expression vector suitable for cloning of the target gene with features for overexpression of the recombinant protein is important. The pTrcHis-TOPO® expression vector used in this study contains a *trc* promoter, which has a -10 region from the *lacUV5* promoter and a -35 region from the *trpB* promoter and they both enable increased levels of expression *in E. coli* (Brosius *et al*., 1985). This vector contains the *lac* operator sequence to which the *lac* repressor binds and prevents transcription from occurring in the absence of IPTG, however, when IPTG is present, it binds to the repressor, reducing its binding affinity for the operator and induces expression (Jacob & Monod, 1961). The vector also contains a *rrnB* anti-termination sequence that decreases early transcription termination (Li *et al*., 1984), a T7 gene enhancer sequence that enhances effective translational initiation (Olins *et al*., 1988) and a mini-cistron for enhanced translational efficiency in prokaryotes (Schoner *et al*., 1986). Additional features of the pTrcHis-TOPO vector are a HisG epitope containing N-terminal peptide, Xpress™ epitope, a 6X His tag for identification and purification of recombinant proteins and an N-terminal peptide remover as well as an enterokinase recognition site.

Subsequent to a successful expression of the desired protein into a suitable host cell, a purification system is needed for the purification of the protein of interest. The Immobilized Metal Affinity Chromatography (IMAC) is a purification system used to purify recombinant His-tagged proteins on the basis of the interaction between the negatively charged His and transition metals on a matrix (Young *et al*., 2012). Ni (II) nitrilotriacetic acid (Ni^{2+} NTA) shows an increased affinity for histidine residues and a matrix that can withstand reuse and allows the dissociation of a bound recombinant protein by an imidazole gradient, metal chelating molecules or pH changes (Hefti *et al*., 2001).

Following expression and purification of a recombinant protein, it is necessary to confirm that the protein is active or not. Enzyme activity assays are performed following purification to determine if the enzyme is active (Bisswanger, 2014). The heme oxygenase enzyme activity assay is used to determine the ability of a putative heme oxygenase to bind to its substrate hemin and subsequently produce the antioxidant biliverdin. The heme oxygenase assay relies on the formation of biliverdin by monitoring spectrophotometrically the increase in absorbance at 650 nm that shows the successful degradation of heme (Jin *et al*., 2012). This chapter describes the recombinant expression and purification of the recombinant *Sb*HO1 protein under denaturing conditions and the refolding of the denatured protein. The ability of *Sb*HO1 to produce biliverdin from heme is also demonstrated.

3.2 MATERIALS AND METHODS

3.2.1 PCR amplification of SbHO1 gene

The expression construct, pTrcHis-TOPO-*Sb*HO1, was provided by Dr. A. Faro (Department of Biotechnology, University of the Western Cape, MSB laboratory). To verify the correct *Sb*HO1 insert, PCR amplification was conducted. Primers for PCR amplification were manually designed based on the *Sb*HO1 mRNA sequence (Accession number, AF320026.1) obtained from the NCBI database. The forward primer *Sb*HO1-FW (5'-GTACGGATCCATGCAGAGTTCCGGAACACT-3') and reverse primer *Sb*HO1-RV (5'-GTACCTCGAGTCAGGTGAATATATGGCGGAG-3') were designed to contain the *Bam*HI and the *Xho*I restriction sites respectively. Primers were synthesised at Inqaba Biotechnical Industries (PTY) LTD, South Africa. PCR amplification was carried out in a 25 µl reaction containing 12.5 µl of 2X DreamTaq Green PCR mastermix (Thermo Scientific USA), 0.2 µM, forward and reverse primers, 0.05 µg template DNA. The final volume of 25 µl was made up with nuclease free water. PCR tubes were briefly centrifuged, transferred to a thermocycler and amplification performed as shown in Table 3.1. The PCR product was analysed on a 1 % agarose gel and viewed using an ENDURO™ GDS (Labnet International, UK) UV transilluminator.

Table 3.1: Thermocycling conditions for PCR amplification of *Sb*HO1 gene

Steps	Temperature (°C)	Time (min)	Number of cycles
Initial denaturation	96	2	1
Denaturation	94	1	30
Primer annealing	50	1	
Extending step	72	1.5	
Final extension	72	10	1
Hold	4	Till use	~

3.2.2 Bacterial strains

E. coli strain XL GOLD competent cells were used to propagate plasmids, while *E. coli* BL21 Codon plus cells were used for expression of recombinant pTrcHisTOPO-*Sb*HO1.

3.2.3 Transformation of pTrcHisTOPO-SbHO1construct into competent cells

Competent cells were thawed on ice for 5 minutes and 2 µl pTrcHisTOPO-*Sb*HO1 was added to 50 µl of *E. coli* XL Gold competent cells in 1.5 ml Eppendorf tubes and incubated on ice for 30 minutes. Cells were heat shocked at 42 °C for 45 seconds and further incubated on ice for 2 minutes. After incubation, 450 µl of pre-warmed Luria Bertani (LB) media was added and the tubes were incubated at 37 °C for 1 hour with shaking at 225 rpm. Following incubation, 100 µl of the transformation mixture was plated on LB agar plates containing 100 µg/ml ampicillin and incubated at 37 °C overnight. For controls, untransformed cells were plated on LB agar plates with and without ampicillin.

3.2.4 Plasmid DNA isolation of pTrcHis-TOPO-SbHO1 expression construct

From the plates containing *E. coli* strain XL GOLD cells transformed with pTrcHisTOPO-SbHO1, a single colony was picked and inoculated into 10 ml LB media containing 100 µg/ml ampicillin and then incubated at 37 °C with shaking overnight. The following day, 5 ml of bacterial culture was centrifuged at 11,000 g for 1 minute to pellet cells and glycerol stocks were made with the remaining 5 ml (1 ml stock each) and stored at -80 °C. The plasmid was isolated based on the alkaline lysis method (Bimboim and Doly, 1979) using the FavorPrep™ plasmid extraction kit (Favorgen, Taiwan) following the manufacturer's protocol. The sample concentration was determined using the NanoDrop spectrometer (Thermo Scientific, Waltham, MA USA).

3.2.5 DNA sequencing

Plasmid DNA extracted in section 3.2.4 was sent for sequencing at the DNA sequencing facility at the Stellenbosch University (Cape Town, South Africa). Gene specific primers designed in section 3.2.1 were used for sequencing of the construct.

3.2.6 Expression and isolation of recombinant SbHO1

Single colonies from the *E. coli* BL21 Codon Plus plates transformed with *pTrcHis*TOPO-*Sb*HO1 were inoculated into 20 ml LB broth containing 100 µg/ml ampicillin and 1 % glucose. The culture was incubated overnight at 37 °C with shaking at 225 rpm. The following morning, the overnight culture was scaled up to 200 ml with LB broth media containing100 mg/ml ampicillin and was incubated at 37 °C with shaking until an OD_{600nm} between 0.4 - 0.6 was reached. The culture was then induced with 1 mM isopropyl-1-thio-D-galactopyranoside (IPTG) and incubated at 30 °C overnight. Bacterial cells were harvested after 2, 4, 5 hours and overnight induction by centrifugation at 4300 rpm for 10 minutes at 4 °C and the supernatant was discarded. Following the test expression, the same expression conditions were chosen for large scale protein expression. Large scale expression was performed in a final volume of 1.5 L and the cultures were induced at 30 °C overnight. The cultures were centrifuged at 4300 rpm for 10 minutes and the pellet was lysed.

3.2.7 Preparation of the soluble and insoluble clear lysate

The cell pellet was lysed under native conditions to collect the soluble fraction by resuspending in 10 ml lysis buffer [1 X PBS pH 7.4, 1 mM β-mercaptoethanol, 5 mM imidazole, 1 mM PMSF, 0.1 % Triton X-100, 100 mg/ml lysozyme, and 2000 U/ml DNAse 1]. The resuspended cells were incubated at room temperature for 30 minutes with shaking. Cells were sonicated for 4 minutes (30 seconds pulsing and 30 seconds chilling on ice) and were centrifuged at 4300 rpm for 30 minutes. The supernatant (soluble fraction) was then collected and stored at -20 °C until further use.

The remaining pellet from the native lysis was further lysed under denaturing conditions to collect the insoluble fraction (inclusion bodies) by re-suspending in 10 ml of urea lysis buffer [1 X PBS pH 7.4, 1 mM β-mercaptoethanol, 5 mM imidazole, 1 mM PMSF, 0.1 % Triton X-100, 100 mg/ml lysozyme, 4 M urea and 2000 U/ml DNAse 1]. The resuspended cells were incubated at room temperature for 30 minutes with shaking. The cells were sonicated for 4 minutes (30 seconds pulsing and 30 seconds chilling on ice) and centrifuged at 4300 rpm for 30 minutes. The supernatant (insoluble fraction) was then collected and stored at -20 °C until use.

3.2.8 Purification of SbHO1

Purification of *Sb*HO1 was carried out on an immobilized metal affinity chromatography column. The column was first washed with 10 column volume (CV) of distilled H_2O and then equilibrated with 3 CV of equilibration buffer [1X PBS pH 7.4, 1 mM β-mercaptoethanol, 10 mM imidazole]. The cell lysate was added to the column and the flow through was collected. The column was then washed with 3 CV of wash buffer [1 X PBS pH 7.4, 1 mM β-mercaptoethanol, 10 mM imidazole] and the flow through was collected. The protein was eluted with 2 CV elution buffer [1X PBS pH 7.4, 1 mM β-mercaptoethanol, 250 mM imidazole] and the elution fraction was collected. The column was finally washed with 3 CV of 1 M NaCl and 1 X PBS and flow through was collected. The column was then stored at 4 °C in 20 % ethanol to prevent microbial growth. To confirm that the protein was successfully expressed and purified, the samples collected from the purification process were analysed on a 12 % SDS PAGE using the protocol in Appendix II: Table 1.

3.2.9 Refolding of the purified SbHO1 protein

The purified denatured protein was dialysed before refolding it to eliminate the imidazole used during the purification. The protein elute of 10 ml was poured into a Snakeskin Dialysis Tubing tube (Thermo Fisher Scientific, USA, catalogue # 68700). The dialysis was performed in 2 L dialysis buffer [1 X PBS, 1 mM β-mercaptoethanol, 5 % glycerol] while stirring at 180 rpm for 48 hours at 4 °C. Following dialysis, the immobilised metal affinity chromatography column was washed with 5 CV distilled H_2O, equilibrated with 3 CV equilibration buffer [1 X PBS, 1 mM β-mercaptoethanol]. The dialysed denatured protein was added to the column and the flow-through was collected. About 10 CV refolding buffer [200 mM NaCl, 50 mM Tris-Cl pH 8.0, 0.05 %

(w/v) PEG, 500 mM glucose, 4 mM reduced glutathione, 0.4 mM oxidized glutathione and 0.5 mM phenylmethanesulfonylfluoride (PMSF)] was added to the column and flow-through was collected. The refolded protein was then eluted with 3 CV elution buffer containing 1 X PBS, 250 mM imidazole and dialysed in 1 X PBS and 1 mM β-mercaptoethanol. The refolded, dialysed protein was analysed on a 12 % SDS PAGE.

3.2.10 Protein concentration determination using the Bradford assay

A Bradford protein assay was performed to determine the concentration of the refolded *Sb*HO1 protein. A protein standard curve ranging from 0 – 2 mg/ml bovine serum albumin (BSA) was prepared using 1 X PBS buffer, the same buffer contained in the protein sample. To a microplate, 5 µl of the sample and 250 µl Bradford reagent was added in triplicate and incubated at room temperature for 5 minutes. The absorbance was measured at 595 nm with a spectrophotometer and the data obtained was averaged and was used to plot a standard curve. The protein sample was not diluted as the concentration as determined using a NanoDrop spectrometer fell within the standard curve range; 5 µl of the protein sample and 250 µl of the Bradford 1X dye reagent was prepared in triplicate and incubated at room temperature for 5 minutes. The absorbance was measured at 595 nm, averaged and the protein concentration was calculated using the equation derived from the standard curve (Appendix III: Figure 2).

3.2.11 Heme oxygenase activity assay

Heme oxygenase activity assays were performed to measure the conversion of heme to biliverdin as previously described (Verma *et al*., 2015). The assay reaction, in a final volume of 250 µl, contained 0.6 µM recombinant *Sb*HO1, 10 mM potassium phosphate pH 7.4 and 200 nM hemin. The reaction was started by adding NADPH to a final concentration of 800 nM and the absorbance was recorded using spectral wavelengths between 310 - 700 nm for 25 minutes at 25 °C.

3.3 RESULTS

In order to study the role of *Sb*HO1 at a molecular level, *Sb*HO1 was cloned into pTrcHis-TOPO TA vector system and was verified by re-amplification. The expression construct was used to transform *E. coli* BL21 Codon Plus host cells and expressed under induction with 1 mM IPTG. The *Sb*HO1 protein accumulated in inclusion bodies and was extracted and purified under denaturing conditions using a Ni-NTA chromatography column. The denatured *Sb*HO1 protein was refolded using the on-column method and was subsequently used to perform the heme oxygenase enzyme activity assay for functional characterisation.

3.3.1 PCR re-amplification of SbHO1 insert

In order to verify that the insert was present, PCR amplification of the *Sb*HO1 coding sequence was performed using the pTrcHisTOPO-*Sb*HO1 construct. Forward and reverse primers for *Sb*HO1 were designed manually using the annotated *Sorghum bicolor* HO1 mRNA sequence (accession number AF320026.1) obtained from NCBI. Primers were designed to contain *Bam*HI and *Xho*I restriction sites. The amplified insert was analysed on a 1 % agarose gel, which showed a band at the expected size of 557 bp as shown in lane 2 Figure 3.1.

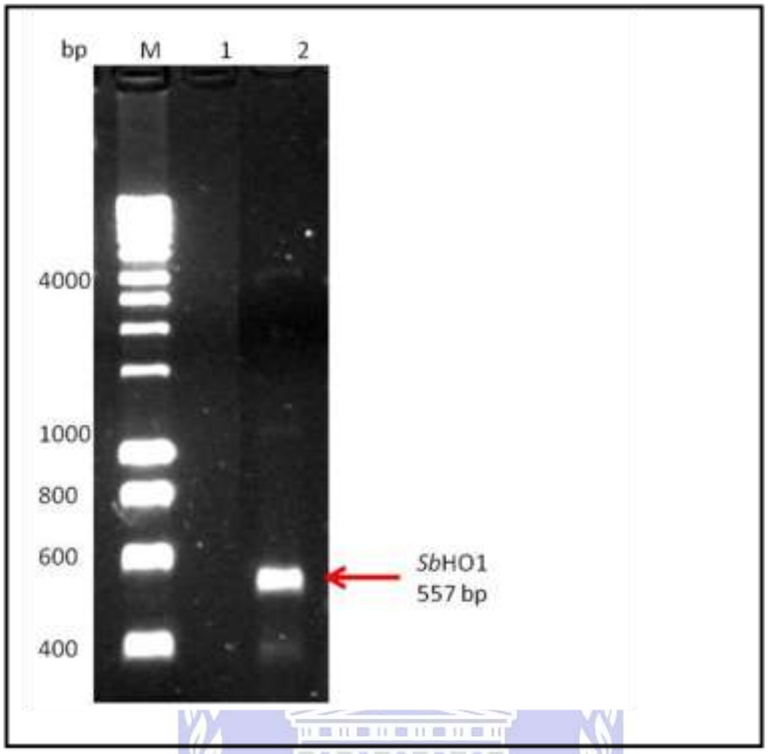

Figure 3.1: A 1 % agarose gel electrophoresis analysis of *pTrcHis*-TOPO-*Sb*HO1 PCR product. Lane M: 12 kb DNA marker (High range DNA ladder), lane 1: negative control, lane 2: amplified PCR product of *Sb*HO1.

3.3.2 DNA sequencing

The pTrcHisTOPO-*Sb*HO1 expression construct was sent for sequencing at the DNA sequencing facility Stellenbosch University (South Africa).

3.3.3 Recombinant expression and purification of SbHO1

To confirm that *Sb*HO1 encoded a functional protein, the pTrcHis-TOPO-*Sb*HO1 construct was transformed into *E. coli* BL21 Codon Plus cells and expression induced at 30 °C on a small-scale, time-course experiment. Cells were harvested at different time intervals until overnight (Figure 3.2). Figure 3.2 shows the result of the small-scale time-course experiment indicating thick bands at 25.1 kDa in the induced lanes 2 - 5. The expression experiment was then upscaled to obtain more of the recombinant *Sb*HO1 protein under the same conditions. The induced 1.5 L overnight culture was harvested and lysed under both native and denaturing conditions by sonication. The soluble and insoluble cell lysate were purified using the Ni-NTA purification system and analysed on a 12 % SDS-PAGE gel (Figure 3.3A & 3.3B respectively). The expected size of the recombinantly expressed *Sb*HO1 protein was 25.1 kDa, which includes the size of the *Sb*HO1 protein of 21.3 kDa plus the 6xHis tag epitope and the Xpress™ epitope of ~ 3.8 kDa. Figure 3.3A showed that the protein was present in the cell lysate and flow-through but not in the eluted fraction. However, after purification of the insoluble fraction, it can be seen in figure 3.3B that the protein was present in the eluted fraction, although in low quantity. The denatured *Sb*HO1 protein was dialysed and concentrated prior and after refolding the protein using the on-column method as described in Section 3.2.9. Figure 3.4 shows the SDS-PAGE of the concentrated *Sb*HO1 protein (lane 1) and the refolded purified protein (lane 5).

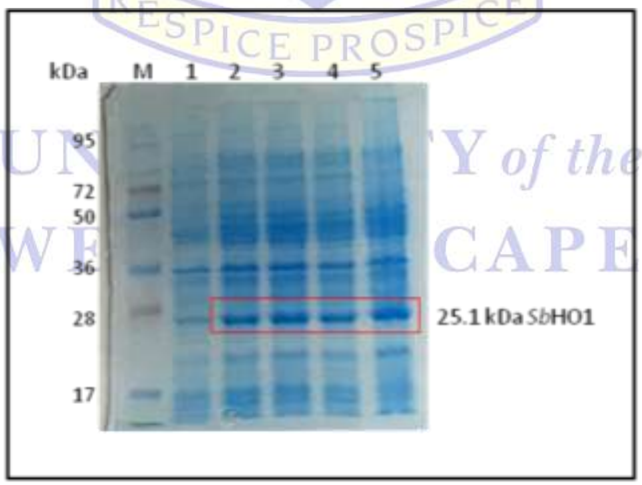

Figure 3.2: A 12 % SDS PAGE gel of a time-course expression analysis of *Sb*HO1. Lane M: 250 kDa protein marker (Thermo Scientific, USA), Lane 1: un-induced *Sb*HO1, Lanes 2-5: 2 hours, 4 hours, 5 hours and overnight induction of *Sb*HO1 at 30 °C respectively.

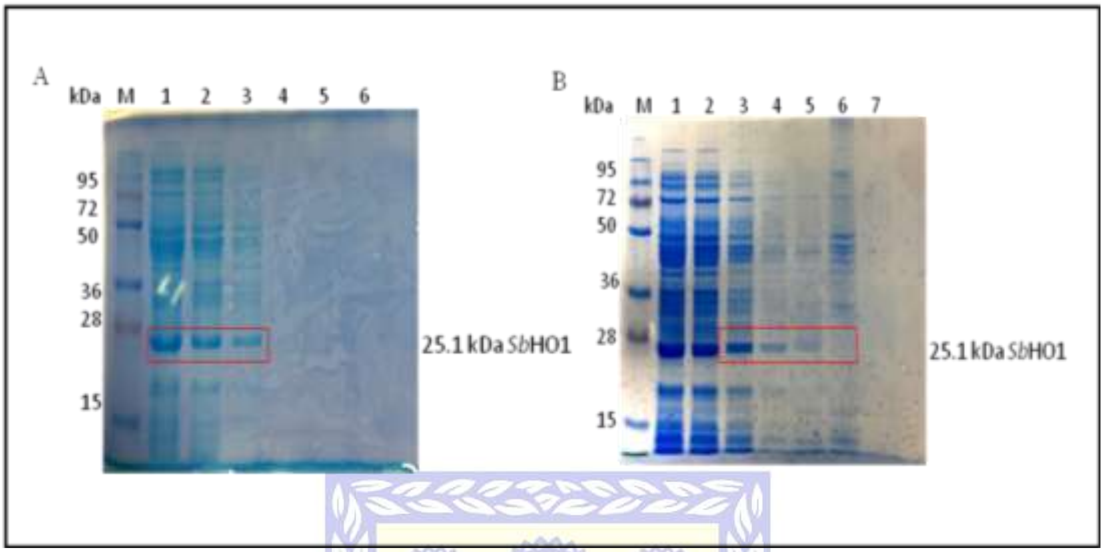

Figure 3.3: A 12 % SDS-PAGE gel showing the native and denatured *Sb*HO1 protein. **(A) Purification of native *Sb*HO1:** Lane M= 250 kDa protein marker (Thermo Scientifc, USA), Lane 1= cell lysate, Lane 2= flow-through, Lane 3= wash 1, Lane 4= wash 2, Lane 5= elute. **(B) Purification of denatured *Sb*HO1:** Lane M= 250 kDa protein marker (Thermo Scientifc, USA), Lane 1= denatured cell lysate, Lane 2= flow-through, Lane 3= wash 1, Lane 4= wash 2, Lane 5= elute, Lane 6= NaCl wash, Lane 7= bead.

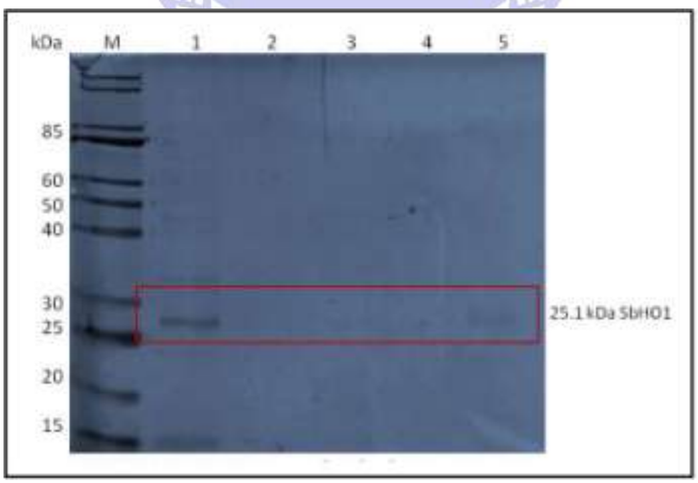

Figure 3.4: A 12 % SDS-PAGE gel showing the refolded purified *Sb*HO1 protein. Lane M= 200 kDa molecular marker (unstained protein ladder, New England Biolabs), lane 1= concentrated *Sb*HO1 protein, lane 2= flow-through, lane 3= wash 1, lane 4= wash 2, lane 5= refolded *Sb*HO1 protein.

3.3.4 Protein concentration determination using the Bradford assay

The purified refolded *Sb*HO1 protein was concentrated to a final volume of 1.3 ml using a Macrosep® Advance Centrifugal device concentrate (PALL Life Sciences, USA). The concentration of *Sb*HO1 protein was determined using the Bradford assay as described in Section 3.2.10. A protein standard curve using a stock solution of BSA (Bovine serum albumin) at a concentration of 2 mg/ml was prepared as shown in Appendix II: Table 3.1. The reaction mix was transferred to a 96 well microplate and the reaction was incubated at room temperature for 5 minutes. The absorbance was measured at 595 nm and the Bradford standard protein absorbance values were used to draw a standard curve (Appendix III: Figure 2). The concentration of the protein was calculated using the equation in Appendix III: Figure 2 to determine the concentration of the *Sb*HO1 protein, which was 0.078 mg/ml.

3.3.5 Heme oxygenase enzyme activity

The activity of the refolded *Sb*HO1 protein was measured spectrophotometrically by observing absorbance changes associated with the conversion of hemin to biliverdin (BV) induced by *Sb*HO1 as described in Section 3.2.11. As shown in Figure 3.5B, in the presence of both the *Sb*HO1 protein and the substrate hemin, the formation of the heme-*Sb*HO1 complex at 405 nm and BV formation at 610 nm was observed. In contrast, Figure 3.5A shows that in the absence of hemin, no heme-enzyme (*Sb*HO1) complex or BV formation was observed. This result clearly indicates that the recombinant protein was able to degrade heme to produce the antioxidant BV.

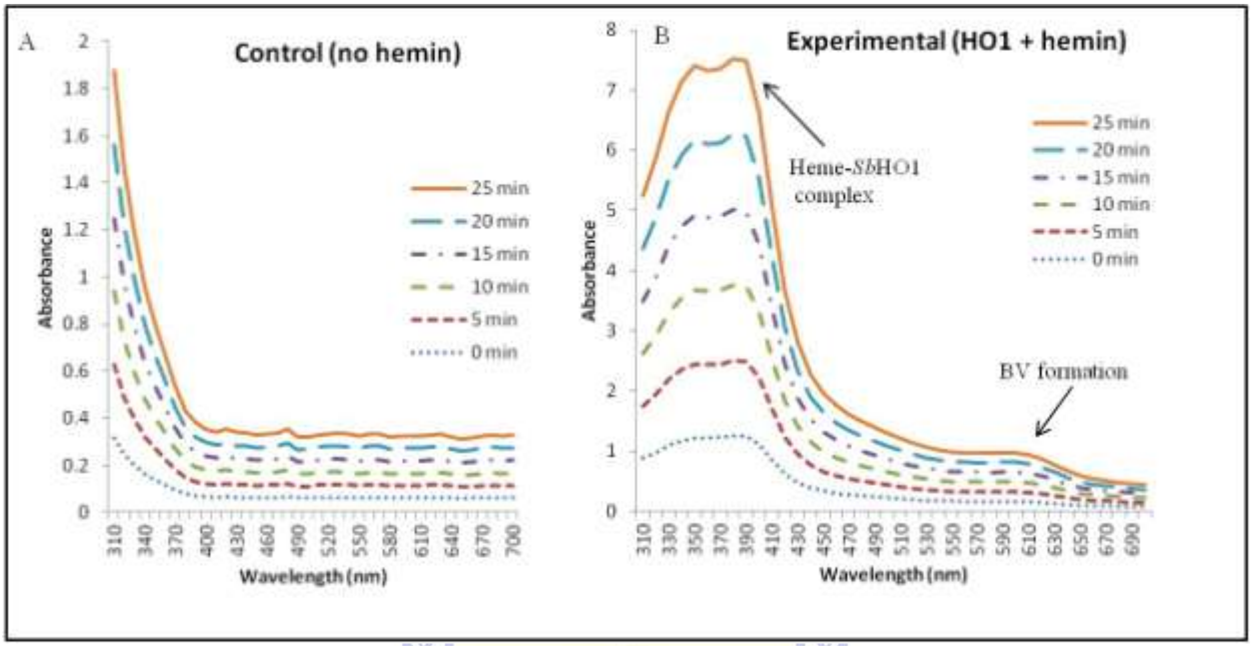

Figure 3.5: Biochemical characterisation of purified recombinant *Sb*HO1 protein. A: Absorption spectra of heme oxygenase activity in the presence of *Sb*HO1 only (Control) **B:** Absorption spectra following the conversion of heme to BV by recombinant *Sb*HO1 between 310 nm and 700 nm at 0, 5, 10, 15, 20 and 25 minutes after the addition of NADPH. Arrows indicate the complex formed at 405 nm and biliverdin formed at 610 nm over the course of the measurements.

3.4 DISCUSSION

The aim of this chapter was to express and purify *Sb*HO1 protein and to perform enzymatic assays to confirm that *Sb*HO1 is a *bona fide* heme oxygenase. The pTrcHis-TOPO-*Sb*HO1 construct was verified by PCR re-amplification, which yielded an amplicon of 557 bp (Figure 3.1).

Time-dependent expression analysis showed the successful overexpression of *Sb*HO1 in *E. coli* BL21 Codon Plus cells using the pTrcHis-TOPO vector. SDS PAGE gel analysis confirmed the presence of an overexpressed 25.1 kDa protein, the expected size of recombinant *Sb*HO1 (Figure 3.2). Large scale expression of *Sb*HO1 protein was performed and *Sb*HO1 was expressed as an insoluble protein and purified using the Ni-NTA affinity chromatography system under denaturing conditions (Figure 3.3B). The purified, denatured protein was dialysed, concentrated and successfully refolded as described previously (Cabrita & Bottomley, 2004; Santos *et al*., 2012; Ruzvidzo *et al*., 2013). Purifying a refolded protein has its constraints as the protein yield is always less after refolding (Graslund *et al*., 2008). The purified refolded protein had a relatively low yield (Figure 3.4). Nonetheless, sufficient recombinant *Sb*HO1 was obtained for subsequent enzyme assays.

The refolded purified recombinant *Sb*HO1 protein was used to test for heme ring cleavage activity by measuring the conversion of heme to biliverdin (BV) spectrophotometrically. The heme cleavage mechanism is conserved among members of the HO1 subfamily (HO1, HO3, and HO4) from *A. thaliana*, bacteria and mammals (Gisk *et al*., 2010). In this study, hemin was used as a substrate for heme oxygenase enzymatic activity. Figure 3.5A, which shows the control reaction lacking the substrate hemin, showed no complex formation or BV production. The enzyme *Sb*HO1 first forms a complex with the substrate, heme, which results in a maximum absorbance of the heme-*Sb*HO1 complex at 405 nm (Figure 3.5B). Over a 30 minutes time-course, a decrease in the peak from 405 nm was observed as a result of the conversion of heme to free biliverdin, as seen by the formation of a peak at 610 nm. *Sb*HO1 showed similarity in the catalytic activity of heme cleavage as previously characterised for recombinant HYI from *Arabidopsis* (Muramoto *et al*., 2002), *Ta*HO1 in wheat (Xu *et al*., 2011), *Os*HO1 in rice (Wang *et al*., 2014), and *Br*HO1 in Chinese cabbage (Jin *et al*., 2012). The results in this study are in agreement with other studies which showed the formation of the heme-HO1 complex at 405 nm and the production of biliverdin between 600 to 660 nm (Fu *et al*., 2011; Jin *et al*., 2012; Wang *et al*., 2014). This result indicated that the purified and refolded *Sb*HO1 protein was active and able to degrade heme. This also confirms that *Sb*HO1 is a true heme oxygenase and is a member of the HO1 subfamily.

CHAPTER 4

Functional Analysis of Sorghum Bicolor Heme Oxygenase 1

ABSTRACT: Biotic and abiotic stresses affect plant growth and productivity, which leads to increased production of reactive oxygen species (ROS). Heme oxygenase is a novel antioxidant enzyme that plays a role in cell protection through scavenging/detoxifying ROS to facilitate osmotic adjustment. Heme oxygenase genes are transcriptionally active and among them HO1 is the most expressed transcript, followed by HO2 while HO3 and HO4 are expressed at relatively low levels. HOs can be induced by heme, UV radiation, salinity, heavy metals and osmotic stress. The aim of this chapter was to study the expression profiles of S*b*HO1 following the exposure of plants to stress, using quantitative real time polymerase chain reaction (qRT-PCR). Before the expression of *Sb*HO1 gene could be studied, the expression profiles of other *Sb*HO (*Sb*HO2, *Sb*HO3, and *Sb*HO4) genes were determined. Gene expression profiles indicated that *Sb*HO1, *Sb*HO2, *Sb*HO3 and *Sb*HO4 were expressed at different levels in the leaves, stems and roots under non-stress conditions, but more significantly, their transcript levels were induced by osmotic stress. Since the *Sb*HO1 expression level was higher than the other *Sb*HO genes under osmotic stress in the leaves, its expression was further investigated under heme, oxidative (H_2O_2), heavy metal ($CuCl_2$) and nitric oxide (Sodium nitroprusside) stress. The expression level of *Sb*HO1 in leaves was up-regulated by its substrate hemin, H_2O_2, $CuCl_2$ and no significant up-regulation by nitric oxide was observed. The results obtained suggest a possible functional role for *Sb*HO genes in stress tolerance mechanisms in plants.

Keywords: Expression profile, transcript, tolerance, ROS, osmotic stress, quantitative real-time PCR.

4.1 INTRODUCTION

Pathogen attack, salinity, drought, and temperature are factors that affect plant growth and development and hence lead to low crop production (Pandey *et al.,* 2015). These factors cause osmotic stress to plants leading to high concentrations of reactive oxygen species (ROS) that results in enzyme inactivation, DNA-protein cross-links, increase in membrane fluidity and permeability and nutrient imbalance, which are lethal to plants and are not easily reparable (Das & Roychoudhury, 2014). Plants have adapted defence mechanisms to respond to osmotic stress, which include stomatal regulation, osmotic adjustment and ROS detoxification through antioxidant mechanisms.

Antioxidant mechanisms, both enzymatic and non-enzymatic, play a significant role in scavenging ROS formed during oxidative stress in plants. Heme oxygenase is another enzyme that degrades heme into carbon monoxide, free iron and biliverdin. Biliverdin is further reduced to bilirubin by biliverdin reductase and both compounds have antioxidative properties. Heme oxygenase genes are transcriptionally active with significantly overlapping levels of expression; HO1 being the most expressed followed by HO2, whereas HO3 and HO4 are expressed at low levels (Xu *et al*., 2011). HO1 is induced by heavy metals (Noriega *et al*., 2004), UV radiation (Yannarelli *et al*., 2006), salinity (Zill *et al*., 2008), glutathione depletion (Cui *et al*., 2011), heme, paraquat (Jin *et al*., 2012) and nitric oxide (NO) (Santa-Cruz *et al*., 2010). HO2 is induced by hemin, salinity (Gisk *et al*., 2010), paraquat (Wang *et al*., 2014) and NO (Fu *et al*., 2011). The induction of the HO genes in plants under different stress conditions suggests the role they play in mediating cytoprotection against oxidative damage.

For a better insight of an enzyme's biological roles, expression patterns of genes involved in signaling and metabolic pathways are required (Maroufi, 2016). To detect the expression level of

HO genes, real time polymerase chain reaction (PCR) is one of the suitable tools. Quantitative real-time PCR (qRT-PCR) is a technique that detects and quantifies DNA or RNA and the gene expression profile of specific genes by measuring at each cycle the amplified product in a PCR reaction (Gachon *et al.*, 2004). Quantitative RT-PCR involves the incorporation of fluorescent reagents in a PCR reaction; florescence is emitted as the amplification of double stranded product is produced. The quantity of florescence emitted is quantified in real time by assessing the increased concentration of the amplicon after each cycle (Fitzgerald & McQualter, 2013).

Quantitative RT-PCR is highly sensitive, accurate and has a high specificity making it a reliable technique for detecting foreign DNA or RNA and gene expression analysis (Qu *et al*., 2019). Though it is a tool for quantifying gene expression profiles, qRT-PCR performance and productivity are affected by the quality and integrity of the RNA used, efficiency of cDNA synthesis and variation in the amount of the RNA used (Andrade *et al.*, 2017). These factors are avoided by normalization of genes expressed to correct variability in experimental procedures by using reference genes. Housekeeping genes such as phosphoenolpyruvate carboxylase (*PEPC*), elongation factor 1 alpha (*EF-Iα*), glyceraldehydes-3-phosphate (*GAPDH*), actin (*ACT*) and ubiquitin (*UBQ*) that are involved in cellular processes are considered as stably expressed genes (Li *et al*., 2017). These reference genes are used to obtain biologically meaningful expression values; however, if the reference genes are unstable, there is bias and expression data can be misinterpreted (Zhang *et al*., 2017).

In this study, the expression profiles of HO genes from sorghum tissues including leaves, stems and roots, under osmotic stress treatment were determined. Also, the expression level of *Sb*HO1 using leaves under hemin (its substrate), H_2O_2 (hydrogen peroxide), $CuCl_2$ (copper (II) chloride) and SNP (sodium nitroprusside, a nitric oxide donor) stresses was measured. Knowledge of the functional gene expression profile will enable better insight into the role of HO genes in the metabolic and regulatory mechanism during oxidative stress.

4.2 MATERIALS AND METHODS

4.2.1 Plant growth and treatment

Sorghum bicolor seeds (Red sorghum) purchased from Agricol, Brackenfell, South Africa, were surface sterilized with 70 % ethanol for 1 minute followed by 20 % sodium hypochlorite solution for 20 minutes and rinsed extensively with autoclaved distilled water. The seeds were germinated in plant tissue culture vessels containing half strength Murashige Skoog (MS) media composed of 2.2 g/l MS, 1 % (w/v) sucrose, 5 mM MES and 0.4 % (w/v) plant agar, pH 5.8. The plant culture vessels were incubated at 25 °C under a 16 hours light/8 hours dark photoperiod for 14 days. After growing for 14 days, sorghum seedlings were transferred to half strength MS media supplemented with 250 mM mannitol (to induce osmotic stress), 10 µM hemin, 10 µM H_2O_2, 200 µM $CuCl_2$ or 100 µM SNP (sodium nitroprusside) as stressors and these were incubated for 0 (untreated seedling as control), 3, 6, 12 and 24 hours for expression pattern analysis. For tissue-specific analysis, roots, leaves and stems of treated seedlings were harvested and immediately frozen in liquid nitrogen and stored at -80 °C until further analysis. Three independent experiments were performed in triplicate.

4.2.2 Total RNA extraction and reverse transcriptions

Total RNA was extracted from 0.1 g of 2-week-old roots, leaves and stems of sorghum seedlings using the Favorgen plant mini RNA extraction kit (Favorgen Biotech Corp., Ping-Tung, Taiwan) according to the manufacturer's instructions. To remove genomic DNA, the extracted RNA was treated with RNase-free DNase set (New England Biolabs, Massachusetts) and was analysed on a 1 % agarose gel. Concentration and purity of the genomic DNA free extract was checked using a NanoDrop spectrophotometer (Thermo Scientifc, USA). About 1 µg of the total extracted RNA was used for synthesis of first-strand cDNA using the SuperScript™ III First-Strand synthesis kit (Invitrogen, Carlsbad, California, USA) according to the manufacturer's instructions.

4.2.3 Quantitative real-time PCR

Quantitative real-time PCR was used to analyse the expression profiles of HO genes in leaves, stem, and root of *Sorghum bicolor*. The experiment was performed on a Light cycler®480 instrument, the reaction mix contained 1 µL template cDNA, 5 µL 2X SYBR Green I Master mix (Roche Applied Science, Germany), varying concentrations of each primer and distilled H_2O added to a final volume of 10 µL. The reactions were subjected to 95 °C for 10 minutes, 45 cycles at 95 °C for 10 seconds, 55 °C for 10 seconds, and 72 °C for 20 seconds. A melting curve analysis was also performed using default parameters on the LightCycler® 480 instrument. Primer data of *Sb*HO target genes and the reference genes ubiquitin (UBQ) and phosphoenolpyruvate carboxylase (PEPC) used for real-time PCR are shown in Table 4.1. Expression levels of the *Sb*HO genes were normalised to the reference genes and analysed using the LightCycler® 480 SW (version 1.5) data analysis software. A standard curve was used to quantify the expression level of serially diluted cDNA templates by relative quantification methods (Pfaffl, 2001). Each reaction was performed in triplicate, inclusive of 3 non-template controls.

Table 4.1: Gene names and their accession numbers used to design primers for the quantitative real-time PCR analysis.

GENE NAME	FORWARD PRIMER	REVERSE PRIMER	ACCESSION NUMBER
*Sb*HO1	5’-TTCCAGACGCTCGAAGACAT-3’	5’CCTGGGGATCCTTCTCAGAC-3’	AF320026.1
*Sb*HO2	5’-GGAAAAGTGGTTTGGAGCGT-3’	5’-AACTCCAGCTCCCTTCCTTC-3’	AF320027.1
*Sb*HO3	5’TTCCAGACGCTCGAAGACAT-3’	5’-CCTGGGGATCCTTCTCAGAC-3’	XM_002438597.2
*Sb*HO4	5’-TTCCTCGTCGATAGCAAGCT-3’	5’-TTCCCAGACAGCTCTTCCAG-3’	XM_021449115.1
UBQ	5’-GCCAAGATTCAGGATAAG-3’	5’-TTGTAATCAGCCAATGTG-3’	XM_002452660
PEPC	5’-GAAGAATATCGGCATCAA-3’	5’CTATGTAATACTTGGTAACTTT-3’	XM_002438476

4.3 RESULT

4.3.1 Expression pattern analysis of SbHO genes

In order to understand the role of sorghum HO genes (*Sb*HO1, *Sb*HO2, *Sb*HO3 and *Sb*HO4), their expression profile was investigated using different tissues including leaves, stems and roots (Figure 4.1) using qRT-PCR. *Sb*HO transcripts were detected in all the tissues analysed (Figure 4.2A), with different levels of expression under non-stressed conditions (Figure 4.1). In untreated plants, the pattern of expression was consistent in all the *Sb*HO transcripts and showed higher expression in the stem, followed by the leaves and the roots, which had low levels (Figure 4.1). The result also showed that the expression level was high in the stem, leaves and the roots for *Sb*HO1 respectively (Figure 4.1).

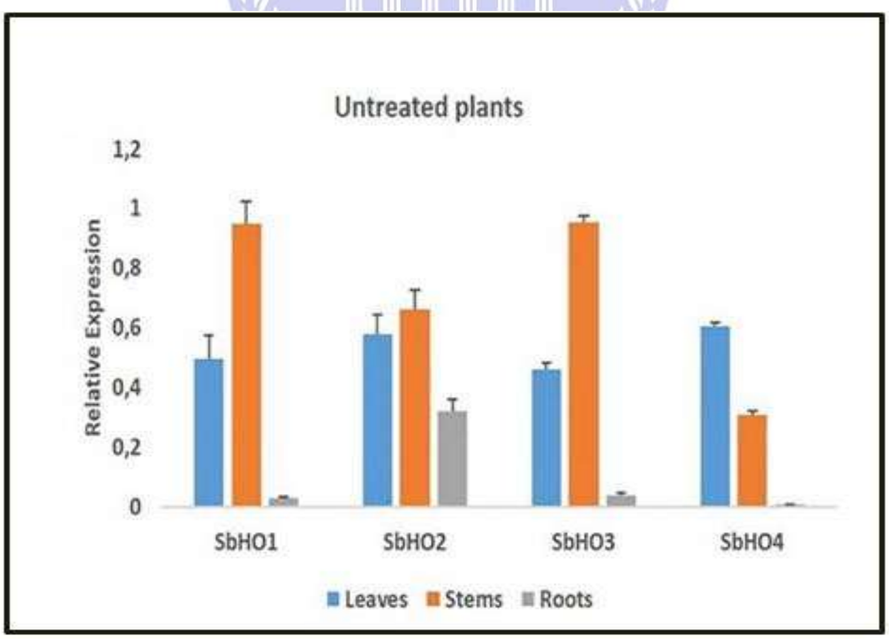

Figure 4.1: Quantitative RT-PCR analysis of the expression profiles of *Sorghum bicolor* HO gene superfamily in various tissues under normal conditions. Gene names are shown on the x-axis and the expression levels on the y-axis. Different tissues of sorghum are shown in different colours.

4.3.2 Expression analysis of SbHO genes in response to osmotic stress

Heme oxygenase (HO) genes are involved in cytoprotective responses to various stresses (He & He, 2014). Therefore, 250 mM mannitol treatment was used to induce osmotic stress and hence oxidative stress. The transcript levels of HO genes in response to the mannitol treatment were investigated by performing qRT-PCR on plant derived cDNA from time points of 0, 3, 12 and 24 hours (Figure 4.2 B-D), where time point zero represent the untreated control plants. As shown in Figure 4.1, *Sb*HO transcripts were differentially expressed in the leaves, stems and roots. Upon stress treatment, the transcript level of *Sb*HO1 in leaves was significantly ($P \leq 0.01$) increased at 3 hours compared to the control (Figure 4.2B), while no significant increase was observed in the stem (Figure 4.2C). A slight increase was observed in the roots (4.2D) at 3 and 12 hours compared to the control. After 3 and 12 hours of stress treatment, *Sb*HO2 was increased in the leaves compared to the control (Figure 4.2B) whereas, no significant increase was observed in the stems. *Sb*HO2 transcript levels, however, showed a significant ($P \leq 0.01$) increase in the roots (Figure 4.2D) at 12 hours with a 5-fold increase compared to the control. The *Sb*HO3 transcript was down-regulated in the leaves and the stem and showed a significant ($P \leq 0.01$) 12-fold increase in the roots at 12 hours of stress treatment compared to the control. The *Sb*HO4 transcript was slightly induced in the leaves at 24 hours and showed a 3-fold increase in the stem at 3 hours, while a slight increase in the root at 12 and 24 hours was observed.

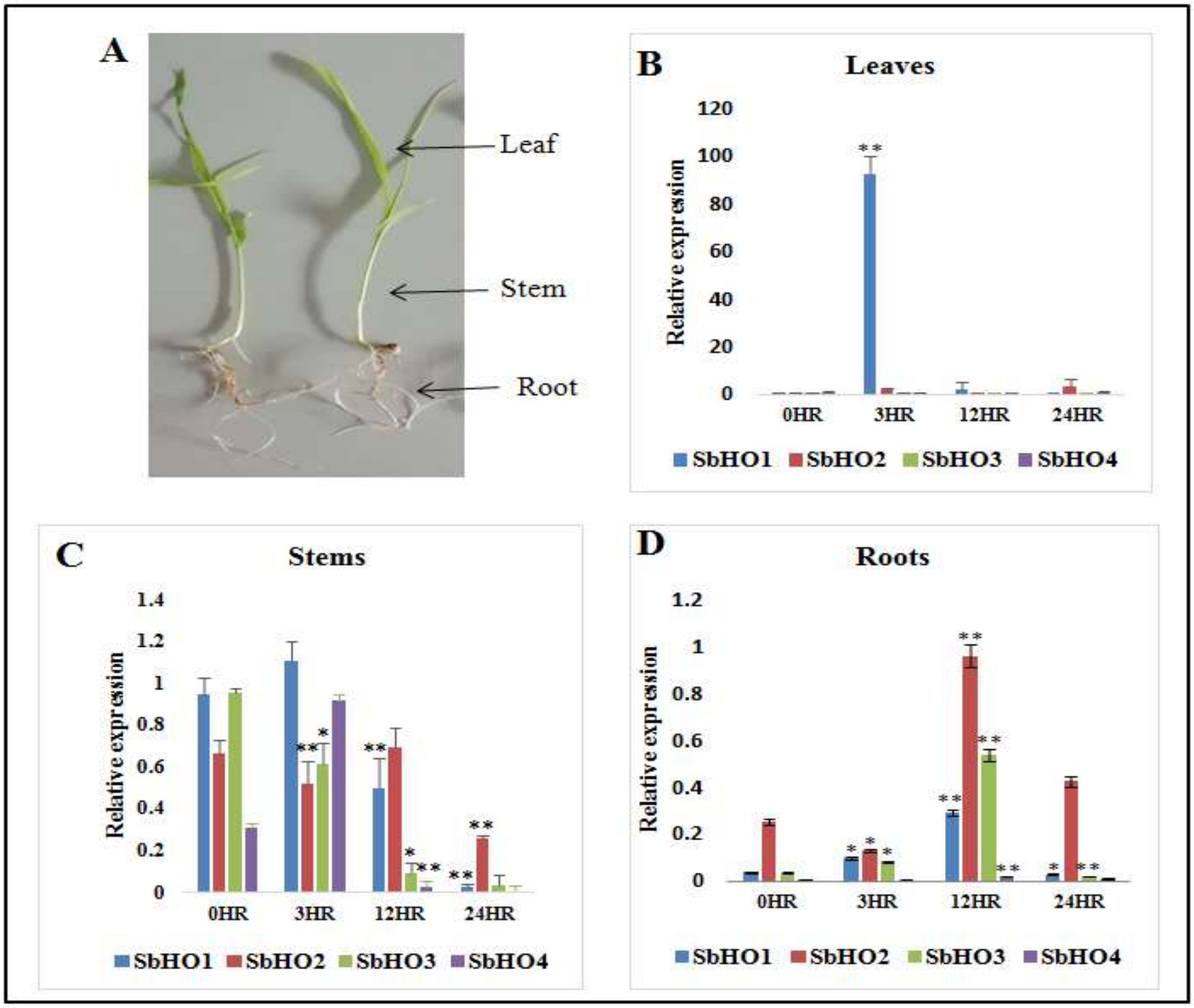

Figure 4.2: Quantitative real-time polymerase chain reaction (qRT-PCR) analysis of expression profiles of *Sb*HO gene superfamily in various tissue of sorghum under osmotic stress at different time points of 0, 3, 12, 24 hours. Different HO genes of sorghum are shown in different colours. Error bars represents the SD calculated from three biological replicates and significant differences between control and treated plants were determined using t-test shown as $^{**}P \leq 0.01$ and $^{*}P \leq 0.05$.

4.3.3 Expression analysis of the SbHO1 gene in response to different stresses

From the result in Figure 4.2B, it can be seen that *Sb*HO1 had the highest level of expression in the leaves. Therefore the expression profile of the *Sb*HO1 gene was further studied using qRT-

PCR in the leaves treated with different concentrations of exogenous chemicals including hemin, H_2O_2, $CuCl_2$ and SNP (a nitric oxide donor) (Figure 4.3). Time course expression analysis showed that the *Sb*HO1 transcript was differentially induced by hemin, H_2O_2, $CuCl_2$ and SNP (Figure 4.3). The *Sb*HO1 transcript was upregulated at 3 and 6 hours by hemin (Figure 4.3A), at 3 and 12 hours by H_2O_2 (Figure 4.3B) and at 3 and 12 hours by $CuCl_2$ (Figure 4.3C). The SNP did not elicit any significant increase in the transcript levels of *Sb*HO1 (Figure 4.3D).

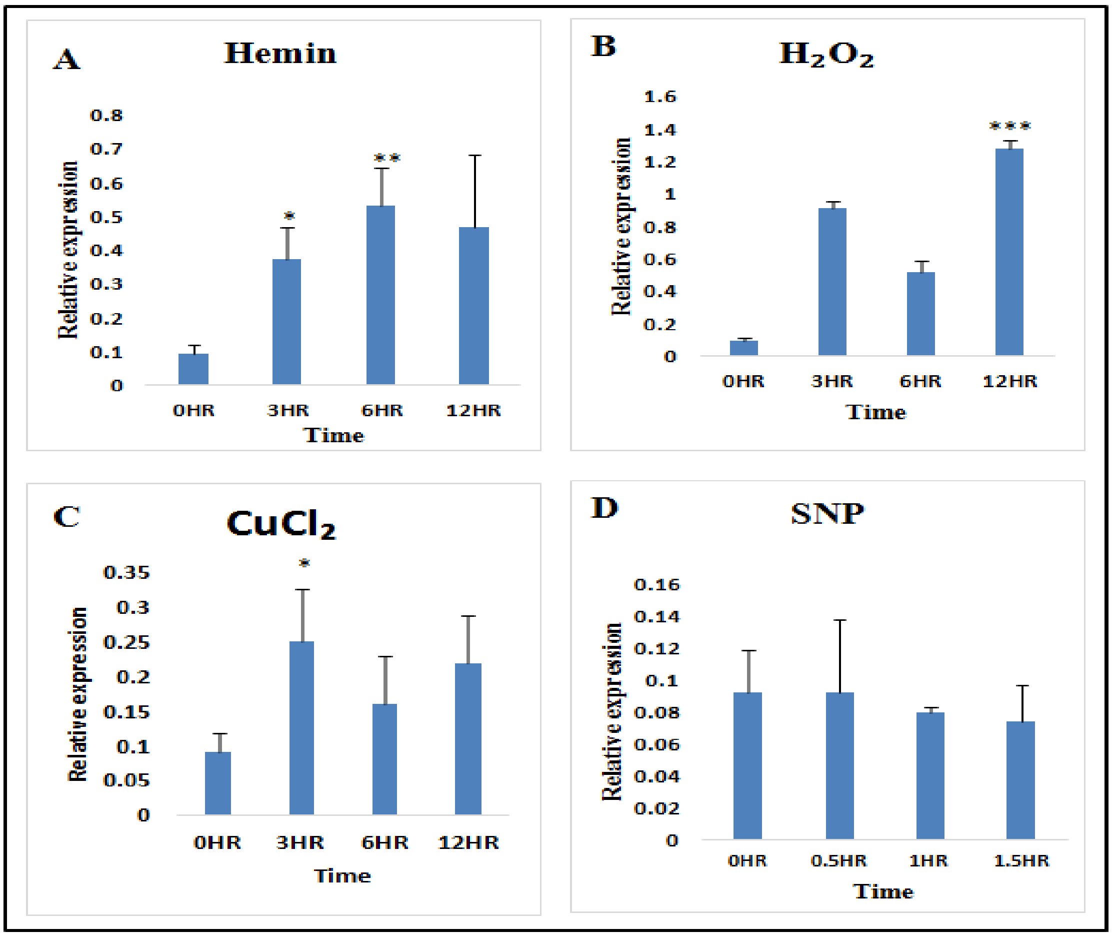

Figure 4.3: Quantitative RT-PCR analysis of the expression profiles of *Sb*HO1 gene in the leaves of sorghum in response to 10 µM hemin (A), 10 µM H_2O_2 (B), 200 µM $CuCl_2$ (C) at 0, 3, 6 and 12 hours, and 100 µM SNP (D) at 0, 0.5, 1 and 1.5 hours. The expression levels were presented as values relative to the control at 0 hour respectively. Error bars represents the SD calculated from three biological replicates and significant differences between control and treated plants were determined using t-test shown as ***$P \leq 0.001$, **$P \leq 0.01$ and *$P \leq 0.05$.

A comparison of the stressors used in this study, showed that compared to the control, H_2O_2 had the greatest effect on *Sb*HO1 transcript levels, followed by hemin and $CuCl_2$ (Figure 4.4).

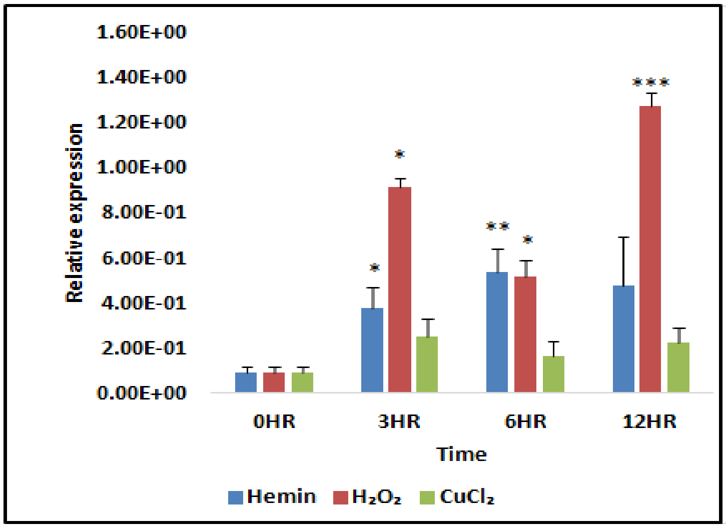

Figure 4.4: Comparative analysis of the expression profiles of *Sb*HO1 gene in leaves in response to hemin, H_2O_2 and $CuCl_2$ stress treatments. After various treatments, sorghum seedling leaves were harvested at time intervals of 0, 3, 6 and 12 hours. The expression levels were presented as values relative to the control at 0 hour respectively. Error bars represents the SD calculated from three biological replicates and significant differences between control and treated plants were determined using t-test shown as $***P \leq 0.001$, $**P \leq 0.01$ and $*P \leq 0.05$.

4.4 DISCUSSION

Biotic and abiotic stresses cause oxidative damage but there are antioxidant enzymes that induce stress tolerance against oxidative stress (Parihar *et al*., 2015). Heme oxygenase is a novel enzyme identified from *Sorghum bicolor* and characterised in this study to determine its possible role in stress responses. The biological roles of HO genes in plants are believed to be linked to an adaptive and defensive mechanism against osmotic stress (Xu *et al*., 2011), heavy metal (Noriega *et al*., 2004) and UV radiation (Yannarelli *et al*., 2006). In the present study, the expression profiles of the *Sb*HO genes in leaves, stems and roots of sorghum subjected to osmotic stress were analysed by qRT-PCR. In the untreated plants (Figure 4.1), *Sb*HO transcripts (*Sb*HO1, *Sb*HO2, *Sb*HO3 and *Sb*HO4) were expressed in all tissues but at different levels. The expression level of *Sb*HO1 was the highest in the stem, followed by the leaves and root, while the expression level of *Sb*HO2 was highest in the stem, followed by the leaves and the root (Figure 4.1). The expression level of *Sb*HO3 was highest in the stem, followed by the leaves and lowest in the root. *Sb*HO4 transcript level was highest in the leaves compared to *Sb*HO1 and *Sb*HO3 genes, then in the stem and in the root (Figure 4.1). In summary, the expression level of *Sb*HO transcripts was observed to be highest in the stem and leaves with lower levels in the roots, suggesting it to be required under normal conditions for plant growth and development. These results correlate with previous studies as demonstrated in *Brassica napus* (cotyledon, hypocotyls, leaf, stem and root) which revealed that *Bn*HO1, *Bn*HO2 and *Bn*HO3 are differentially expressed in all tissues analysed under normal conditions (Shen *et al*., 2011). Additionally, gene expression profiles of HOs in *Oryza sativa* (*Os*HO1 and *Os*HO2) (Wang *et al*., 2014) and *Medicago sativa* L. HO1 (Fu *et al*., 2011a), *Ms*HO2 (Fu *et al*., 2011b) (leaves, stems, roots and germinating seeds) revealed differential expression profiles under normal conditions.

The expression of HO genes in different tissues under osmotic stress conditions was analysed. Time-course analysis of the HO gene expression in sorghum treated with 250 mM mannitol showed that *Sb*HO genes could be differentially induced in all tissues tested by oxidative stress (Figure 4.2). A significant increase in the expression level was observed in the leaves for *Sb*HO1 at 3 hours with a 100-fold increase, followed by a slight increase of *Sb*HO2 at 3 and 24 hours, *Sb*HO4 at 24 hours while *Sb*HO3 was down-regulated (Figure 4.2B). In the root, *Sb*HO2 was the most expressed at 12 hours with a 2-fold increase compared to the control followed by *Sb*HO3 at 12 hours with a 12-fold increase, *Sb*HO1 slightly increased at 12 hours while *Sb*HO4 transcript was low at 12 hours of stress treatment (Figure 4.2D). In the stem, no significant increase was observed for *Sb*HO1, *Sb*HO2 and *Sb*HO3 transcripts as compared to the control (Figure 4.2C). There was a 3-fold increase for *Sb*HO4 transcript in the stem at 3 hours compared to the control. These results show consistency with the HO genes from the model plant *Arabidopsis thaliana*, which are transcriptionally active with different levels of expression and confer cell protection upon induction by oxidative stress (Xie *et al*., 2011). The expression profiles of HO genes has also been studied in *Brassica napus* (HO1, HO2, HO3) (Shen *et al*., 2011), and in *Oryza sativa* (HO1 & HO2) (Wang *et al*., 2014) and showed increase in response to abiotic stresses.

Expression levels of *Sb*HO1 in sorghum seedling leaves treated with different concentrations of exogenous chemicals and hemin was also analysed (Figure 4.3). Time course gene expression analysis showed that *Sb*HO1 was upregulated by its substrate (hemin), oxidative stress (H_2O_2) and heavy metal ($CuCl_2$) (Figure 4.3). Hemin plays a role in physiological functions in animals, and is also a potent inducer of root formation (Xuan *et al*., 2012; Lin *et al*., 2012). Treatment of sorghum leaves with 10 µM hemin, showed an upregulation in the gene expression level of

*Sb*HO1 at 3 and 6 hours (Figure 4.3A) as compared to the control exhibiting a protective role against hemin induced oxidative damage.

Hydrogen perioxide is a metabolic product from cellular processes, which can be toxic to plants in excess; however, an appropriate concentration improves antioxidant activity (Hasanuzzaman *et al*., 2017), enhances drought tolerance (Ashraf *et al*., 2014) and cold resistance (Iseri *et al*., 2013; Larkindale & Huang, 2004). Treatment with H_2O_2 (Figure 4.3B) and $CuCl_2$ (Figure 4.3C) showed an upregulation of *Sb*HO1 transcript at 3 hours and 12 hours for both treatments. These results support previous analysis indicating the role of HO1 as an antioxidant.

NO plays a role in intracellular and extracellular signaling such as stomatal closure, germination, growth and apoptosis (Noriega *et al*., 2007). The cytoprotective or cytotoxic effect of NO on plants depends on the concentration of NO, which is affected by the rate of production and efficiency of ROS detoxification. Exogenous application of 100 µM SNP, a NO donor, slightly decreased the *Sb*HO1 transcript as compared to the control (Figure 4.3D). Contrary to these results, 100 µM SNP protected the leaf tissues from oxidative stress by upregulating HO1 transcript level in soyabean leaves (Noriega *et al*., 2007). The downregulation of the expression level of *Sb*HO1 by NO might be as a result of the concentration of SNP used in this current study may not have been sufficient to activate ROS scavenging machinery and upregulate the expression of *Sb*HO1 gene. The effect of NO depends on its concentration (Shi *et al*., 2005) hence, at 100 µM SNP, the antioxidant defence mechanism of HO1 was inhibited.

The result also showed that *Sb*HO1 transcript was more induced by H_2O_2, followed by hemin and $CuCl_2$ (Figure 4.4). Previous reports showed that HO1 genes, *AtHO1* (Xie *et al*., 2011), *Ms*HO1 (Fu *et al*., 2011a), *Ta*HO1 (Xu *et al*., 2011), *Br*HO1 (Jin *et al*., 2012) and *Os*HO1 (Wang *et al*., 2014), transcript levels were differentially induced under different stress conditions such as PEG 6000 (simulates drought), NaCl, salinity, hemin, H_2O_2, gibberellic acid (GA), abscisic (ABA) and SNP. Heme oxygenase-1 in soyabean (*Gm*HO1) was found to be induced by salinity stress (Zilli *et al*., 2008) and UV-B irradiation (Yannarelli *et al*., 2006). These results suggest that *Sb*HO genes might have protective roles in sorghum and that *Sb*HO1 expression is induced by various oxidative stresses. However, the mechanism by which *Sb*HO1 confers a cytoprotective on plant cells was not a subject of the current study and still needs to be elucidated.

CHAPTER 5

Conclusion and Future Prospects

Biotic and abiotic factors affect crop quality and agricultural productivity which in turn threatens food security around the aspects of food availability, sustainability, utilization and affordability (Wang *et al.*, 2016). The world's population is increasing rapidly and is expected to reach 10 billion by the year 2050. This means that food production needs to be increased by at least 70 % to meet the growing demand for quality, nutritious and sustainable food (UN, 2015). Therefore, it is imperative to develop stress-tolerant crops with increased yield and improved tolerance against biotic and abiotic stresses. The identification and characterisation of genes that encode proteins that respond to stresses will pave the way towards a better understanding of the functional role of stress tolerance in plants. The role of heme oxygenase genes have been investigated in a few plant species such as *Arabidopsis thaliana* (Gisk *et al.*, 2010), *Zea mays (*Han *et al.*, 2012), *Triticum aestivum* (Xu *et al.*, 2011), *Medicago sativa* L (Fu *et al.*, 2011a), *Brassica napa* (Jin *et al.*, 2012) and *Sorghum bicolor* (Mulaudzi-Masuku *et al.*, 2019). These have shown that heme oxygenases respond to various stresses and confer protection against oxidative damage and tissue injuries.

In the current study, *in silico* analyses, enzymatic assays and gene expression analysis were used to elucidate the functional role of *Sb*HO1 in response to different stresses. *In silico* characterisation (Chapter 2), of the *Sb*HO1 gene indicated the presence of a heme-oxygenase conserved domain, similar to the highly conserved domain, referred to as the heme oxygenase signature motif, present in other HO1-like subfamily. The physicochemical properties, sequence similarities, conserved motifs and gene structure provided a clear understanding of the *Sb*HO1's diversity and similarity compared to other plant HO1's. To elucidate the functional role of *Sb*HO1, as described in chapter 3, *Sb*HO1 was recombinantly overexpressed in *E. coli* and purified. Partial denaturing and refolding revealed a possibility that a denatured protein can be refolded, however, only low amounts were recovered as previously described (Ruzvidzo *et al*., 2013). The enzyme activity assay revealed that the refolded recombinant *Sb*HO1 protein was active and formed a heme-*Sb*HO1 complex that produced biliverdin as was observed by a soret band at a wavelength of 610 nm.

Towards understanding the biological role of *Sb*HO1, gene expression analysis in response to various stresses was conducted as described in Chapter 4. The results indicated that the *Sb*HO1 transcript was expressed in all tissues, but higher levels were observed in the leaves. Additionally, other HO's genes were also expressed in all tissues, but their levels were low as compared to *Sb*HO1. A similar pattern was observed for HY1 in *Arabidopsis thaliana* which was highly expressed more that all HOs (Emborg *et al.,* 2006). The results showed that the *Sb*HO1 transcript was induced by osmotic (mannitol), oxidative (hemin, H_2O_2) and heavy metal ($CuCl_2$) but not by nitric oxide (SNP) stress. These results correlated with previous studies in other plant species (Noriega *et al*., 2008; Chen *et al*., 2009; Xu *et al*., 2011), suggesting a role of *Sb*HO1 in conferring stress tolerance.

In conclusion, besides *Arabidopsis thaliana*, *Sorghum bicolor* is the only plant species where all four HO's (HO1, HO2, HO3 and HO4) have been identified and their expression analysed. *Sb*HO1 was confirmed to be a *bona fide* heme oxygenase and a member of the HO1 subfamily based on the presence of the conserved HO signature sequence (QAFICHFYNI/V), and phylogenetic similarities with other plant HO1's. This was confirmed experimentally by determining its ability to degrade heme and produce billiverdin. Since the *Sb*HO1 transcript was increased in response to abiotic stress, results suggest a protective role in plants, but further analyses are required to confirm these findings. It is recommended in the future that the expression of *Sb*HO1 in response to biotic stress be investigated, since due to time it was not done in this thesis. To study the possible biological protective role of *Sb*HO1, it is recommended that transgenic knockout and overexpressing lines be generated in order to understanding the role of *Sb*HO1. With the knowledge that will be obtained from this ongoing project, development of high yield, stress tolerant crops is possible. This may contribute to sustainable agriculture to secure food production and meet the increase in demand for staple diets.

6 References

Agati, G., Azzarello, E., Pollastri, S & Tattini, M. 2012. Flavonoids as antioxidants in plants: location and functional significance. *Journal of Plant Science,* 196: 67-76.

Altschul, S.F., Gish, W., Miller, W., Myers, E.W. & Lipman, D.J. 1990. Basic local alignment search tool. *Journal of Molecular Biology,* 215: 403-410.

Andrade, L.A-de., Brito, M.dos-S., Junior, R.F.P., Marchiori, P.E.R., Nobile., P.M., Martins. A.P.B., Ribeiro, R.V & Creste, S. 2017. Reference genes for normalization of qPCR assays in sugarcane plants under water deficit. *Journal of Plant Methods,* 13: 28.

Apel, K & Hirt, H. 2004. Reactive oxygen species: metabolism, oxidative stress and signal transduction. *Annual Review Plant Biology,* 55: 373-399.

Arora, A., Sairam, R.K & Srivastava, G.C. 2002. Oxidative stress and antioxidative system in plants. *Current Science,* 82 (**10**): 1227-1238.

Asada, K. 2000. The water-water cycle as alternative photon and electron sinks. *Physiological Transactions of the Royal Society B Biological Sciences,* 355: 1419-1431.

Asada, K. 2006. Production and scavenging of reactive oxygen species in chloroplasts and their functions. *Journal of Plant Physiology,* 141: 391-396.

Ashraf, M.A., Rasheed, R., Hussaine, I., Iqbal, M., Haider, M.Z., Parveen, S., Muhammad, A.S. 2014.hydrogen perioxide modulates antioxidant system and nutrient relation in maize (*Zea mays* L.) under water-deficit conditions. *Journal of Agronomy and Soil Science,* 61: 507-523.

Bailey, T.M., Boden, M., Buske, F.A., Frith, M., Grant, C.E., Clementi, L., Ren, J., Li, W.W & Noble., W.S. 2009. MEME Suite tools for motif discovery and searching. *Nucleic Acids Research,* 37 (**2**): 202-208.

Balla, G., Jacog, H.S & Balla, J. 1992. Induction of endothelial ferritin: a cytoprotective antioxidant stratagem of the vessel wall. *Journal of Biological Chemistry,* 267: 18148-18153.

Bawa, I. 2016. Management strategies of Fusarium wilt disease of tomato incited by *Fusarium oxysporum f. sp. lycopersici* (*Sacc*.): A review. *International Journal of Advanced Academic Research*, 2 (**5**): 32-42.

Beale, S.I. 1993. Biosynthesis of phycobilins. *Chemistry Review*, 93: 785-802.

Benkert, P., Biasini, M. & Schwede, T. Towards the estimation of the quality of the individual protein structure models. *Journal of Bioinformatics* 27: 343-350.

Berger, S., Sinha, A. K., & Roitsch, T. 2007. Plant physiology meets phytopathology: Plant primary metabolism and plant-pathogen interactions. *Journal of Experimental Botany*, 58 (15–16), 4019–4026. https://doi.org/10.1093/jxb/erm298.

Berwal, MK & Ram, C. 2018. Superoxide dismutase: A stable biochemical marker for abiotic stress tolerance in higher plants, Abiotic and biotic stress in plants, Alexandre Bosco de Oliveira, *IntechOpen*, DOI: http://dx.doi.org/10.5772/intechopen.82079.

Brosius, J., Erfle, M & Storella, J. 1985. Spacing of the -10 and -35 regions of the tac promoter. *Journal of Biological Chemistry*, 260: 3539-3541.

Cabrita, L.D & Bottomley, S.P. 2004. Protein expression and refolding: A practical guide to getting the most out of inclusion bodies. *Biotechnology Annual Review*, 10: 31-50.

Camacho, C., Coulouris, G., Avagyan, V., Ma, N., Papadopoulos, J., Bealer, K & Madden, T.L. 2009. BLAST+: architecture and applications. *BMC Bioinformatics*: 10: 421-430.

Chen, D., Brown, J.D., Kawasaki, Y., Bommer, J & Takemoto, J.Y. 2012. Scalable production of biliverdin IXα by *Escherichia coli*. *Journal of Biotechnology*, 89 (**12**): 1-10.

Chen, X.Y., Ding, X., Xu, S., Wang, R., Xuan, W., Cao, Z.Y., Chen, J., Wu, H.H., Ye, M.B & Shen, W.B. 2009. Endogenous hydrogen peroxide plays a positive role in the upregulation of heme oxygenase and acclimation to oxidative stress in wheat seedling leaves. *Journal of Integrated Plant Biology*, 51: 951-960.

Choudhury, S., Panda, P., Sahoo, L & Panda, S.K. 2013. Reactive oxygen species signaling in plants under abiotic stress. *Plant Signaling Behavior*, 8 (**4**): e23681-6.

Choudhury, F.K., Rivero, R.M., Blumwald, E & Mittler, R. 2017. Reactive oxygen species, abiotic stress and stress combination. *The Plant Journal*, 90: 856-867.

Contour-Ansel, D., Torres-Franklin, M., Cruz, H., de Carvalho, M., D'arcy-Lameta, A & Zuily-Fodil, Y. 2006. Glutathione reductase in leaves of cowpea: cloning of two cDNAs, expression and enzymatic activity under progressive drought stress, dessication and abscisic acid treatment. *Annual Botany*, 98: 1279-1287.

Cui, W., Fu, G., Wu, H & Shen, W. 2011. Cadmium-induced heme oxygenase-1 gene expression is associated with the depletion of glutathione in the roots of *Medicago sativa. Journal of Biometals*, 24: 93-103.

Dalal, M., Mayandi, K & Chinnusamy, V. 2012. Sorghum: Improvement of abiotic stress tolerance *In* Tuteja, N., Gill, S.S., Tiburcio, A.F & Tuteja, R (Editions) Improving crop resistance to abiotic stress, Germany, Wiley-Blackwell, 924-949.

Das, K & Roychoudhury, A. 2014. Reactive oxygen species (ROS) and response of antioxidants as ROS-scavengers during environmental stress in plants. *Frontiers in Environmental Science*, 53 (**2**): 1-13.

Davis, S., Bhoo, S.H., Durski, A.M., Walker, J.M & Viersta, R.D. 2001. The heme oxygenase family required for phytochrome chromophore biosynthesis is necessary for proper photomorphogenesis in higher plants. *Journal of Plant Physiology*, 126: 656-669.

De Pinto, M.C & De Gara, L. 2004. Changes in the ascorbate metabolism of apoplastic and symplastic spaces are associated with cell differentiation. *Journal of Experimental Botany*, 55: 2259-2569.

Del Rio, L.A., Sandalio, L.M., Corpas, F.J., Palma, J.M & Barroso, J.B. 2006. Reactive oxygen species and reactive nitrogen species in peroxisomes: production, scavenging and role in cell signaling. *Journal of Plant Physiology*, 141: 330-335.

Dulak, J & Jozkowicz, A. Carbon monoxide: a "new" gaseous modulator of gene expression. *Journal of Acta Biochimica polonica*, 50: 31-47.

Duan, X., Dai, C., Li, Z., Zhou, H., Xiao, T., Xie, Y & Shen, W. 2016. Ectopic over-expression of *Bo*HO1, a cabbage heme oxygenase gene, improved salt tolerance in *Arabidopsis*: A case study on proteomic analysis. *Journal of Plant Physiology*, 196-197: 1-13.

Emborg, T.J., Walker, J.M., Noh, B & Vierstra, R.D. 2006. Multiple heme oxygenase family members contribute to the biosynthesis of the phytochrome chromophore in *Arabidopsis*. *Journal of Plant Physiology*, 140: 856-868.

Eurich, C., Fields, P.A & Rice, E. 2012. Proteomics: Protein identification using online databases. *The American Biology Teacher*, 74 (**4**): 250-255.

Food and Agricultural Organization of the United Nations. 2009. The Declaration of the World Summit on Food Security.

FAO. 2016. Sorgo Producción Mundial. Producción Mundial de Sorgo. Available from: https://www.produccionmundialsorgo.com/previous-year.asp.

Fedoroff, N.V., Battisti, D.S., Beachy, R.N., Cooper, P.J., Fischhoff, D.A., Hodges, C.N., Knauf, V.C.,Lobell, D., Mazur, B.J., Molden, Reynolds, M.P., Ronalds, P.C., Rosegrant, M.W., Sanchez, P.A., Vonshak, A & Zhu, J-K. 2010. Radically re-thinking Agriculture for the 21[st] Century. *Journal of Science*, 327, 833-834.

Filiz, E., Ozigit, I.I., Saracoglu, I.A., Uras, M.E., Sen, U & Yalcin, B. 2019. Abiotic stress-induced regulation of antioxidant genes in different *Arabidopsis* ecotypes: microarray data evaluation. *Journal of Biotechnology & Biotechnological Equipment*, 33 (**1**): 128-143.

Fitzgerald, T.L & McQualter, R.B. 2013. The quantitative real-time polymerase chain reaction for the analysis of plant gene expression *In*: Henry, R., & Furtado, A. (Editions) Cereal Genomics. Methods in Molecular Biology (Methods and Protocols), volume 1099. Human Press, Totowa, NJ.

Foyer, C.H., Lopez-Delgado, H., Dat, J.F & Scott, I.M. 1997 Hydrogen- peroxide and gluthathione-associated mechanisms of acclimatory stress tolerance and signaling. *Physiologia Plantarum*, 100 (**2**): 241–254.

Fu, G-Q., Xu, S., Xie, Y-J., Han, B., Nie, L., Shen, W-B & Wang, R. 2011a. Molecular cloning, characterization and expression of an alfalfa (*Medicago sativa* L.) heme oxygenase-1 gene, *Ms*HO1, which is pro-oxidants-regulated. *Journal of Plant Physiology and Biochemistry*, 49: 792-799.

Fu, G-Q., Jin, Q-J., Lin, Y-T., Feng, J-F., Shen, W-B & Zheng, T-Q. 2011b. Cloning and characterization of a heme xoygeanse-2 gene from alfalfa (*Medicago sativa* L.). *Journal of Applied Biochemistry and Biotechnology*, 165: 1253-1263.

Gachon, C., Mingam, A & Charrier, B. 2004. Real-time PCR: what relevance to plant studies? *Journal of Experimental Botany*, 402 (**55**): 1445-1454.

Garcia-Mata, C & Lamattina, L. 2013. Gasotransmitters are emerging as new guard cell signalling molecules and regulators of leaf gas exchange. *Journal of Plant Science*, 102: 11-16.

Gasteiger, E., Hoogland, C., Gattiker, A., Duvaud, S., Wilkins, M.R., Appel, R.D & Bairoch, A. 2005. *Protein Identification and Analysis Tools on the ExPASy Server In* John, M. Walker. (Editions), *The Proteomics Protocols Handbook*, Humana Press, 571-607.

Gill, S.S., Khan, N.A & Tuteja, N. 2011. Amelioration of cadmium stress in crop plants by nutrient management: morphological, physiological and biochemical aspects. *Journal of Plant Stress*, 5 (**1**): 1-23.

Gisk, B., Yasui, Y., Kohchi, T & Frankenberg-Dinkel, N. 2010. Characterization of the haem oxygenase protein family in *Arabidopsis thaliana* reveals a diversity of functions. *Biochemical Journal*, 425 (**2**): 425-434.

Glorieux, C & Calderon, P.B. 2017. Catalase, a remarkable enzyme: targeting the oldest antioxidant enzyme to find a new cancer treatment approach. *Journal of Biological Chemistry*, 398 (10): 1095-1108.

Gozzelino, R., Jeney, V & Soares, M.P. 2010. Mechanisms of cell protection by Heme oxygenase-1. *Annual Review of Pharmacology and Toxicology*, 50: 323-354.

Gräslund, S., Nordlund, P., Weigelt, J., Hallberg, B. M., Bray, J., Gileadi, O., ... Gunsalus, K. C. 2008. Protein production and purification. *Nature Methods*, 5 (**2**), 135-146. https://doi.org/10.1038/nmeth.f.202.

Gull, A., Lone, A.A & Wani, N.U.I. 2019. Biotic and abiotic stresses in plants. Alexandre Bosco de Oliveira, IntechOpen, DOI: 10.5772/intechopen.85832. Available from: https://www.intechopen.com/books/abiotic-and-biotic-stress-in-plants/biotic-and-abiotic stresses-in-plants.

Guo, K., Kong, W.W & Yang, Z.M. 2009. Carbon monoxide promotes root hair development in tomatoe. *Journal of Plant Cell Environment*, 32: 1033-1045.

Gupta, A.S., Heinen, J.L., Holaday, A.S., Burke, J.J & Allen, R.D. 1993. Increased resistance to oxidative stress in transgenic plants that overexpress chloroplastic Cu/Zn superoxide dismutase. *Proceedings of the National Academy of Sciences of the United States of America*, 90 (**4**): 1629-1633.

Halliwell, B. 2006. Reactive species and antioxidants: Redox biology is a fundamental theme of aerobic life. *Journal of Plant Physiology*, 141: 312-322.

Han, B., Yang, Z., Xie, Y., Nie, L., Cui, J & Shen, W. 2014. *Arabidopsis* HY1 confers cadmium tolerance by decrasing nitric oxide production and improving iron homeostasis. *Journal of Molecular Plant*, 7 (**2**): 388-403.

Han, Y., Xuan, W., Yu, T., Fang, W.B., Lou, T.L., Gao, Y., Chen, X.Y., Xiao, X & Shen, W.B. 2007. Exogenous hematin alleviates mercury-induced oxidative damage in the roots of *Medicago sativa. Journal of Integrated Plant Biology*, 49: 1703-1713.

Han, Y., Zhang, J., Chen, X.Y., Gao, Z.Z., Xuan, W., Xu, S., Ding, X & Shen, W.B. 2008. Carbon monoxide alleviates cadmium-induced oxidative damage by modulating glutathione metabolism in the roots of *Medicago sativa. Journal of New Phytology*, 177: 155-166.

Hasanuzzaman, M., Nahar, K., Gill, S.S., Alharby, H.F., Razafindrabe, B.H & Fujita, M. 2017. Hydrogen perioxide pretreatment mitigates cadmium-induced oxidative stress in *Brassica napus*

L.: An intrinsic study on antioxidant defense and glyoxalase systems. *Frontier in Plant Sciences* 8: 115.

He, H & He, L. 2014. Heme oxygenase 1 and abiotic stresses in plants. *Acta Physiologiae Pantarum,* 36: 581-588.

He, H & He, L. 2014. The role of carbon monoxide signalling in the responses of plants to abiotic stresses. *Nitric Oxide*, 42: 40-43.

Hefny, M & Abdel-Kadar, D.Z. 2009. Antioxidant-enzyme system as selection criteria for salt tolerance in forage sorghum genotypes (*Sorghum bicolor* L. Moench) *In* Ashraf, M., Ozturk, M & Athar, H.R, (Editions), *Salinity and water stress*, The Netherlands, Springer, 25-36.

Hernandez, J.A., Ferrer, M.A., Jimenez, A., Barcelo, A.R & Sevilla, F. 2001. Antioxidant systems andO^{2-}/H_2O_2 production in the apoplast of pea leaves, its relation with salt-induced necrotic lesions in minor veins. *Journal of Plant Physiology,* 127: 817-831.

Hu, B., Jin, J., Guo, A-Y., Zhang, H., Luo, J & Gao, G. 2015. GSDS 2.0: an upgraded gene feature visualization server. *Journal of Bioinformatics*, 31 (**8**): 1296-1297.

Ignacimuthu, S & Premkumar, A. 2014. Development of transgenic *Sorghum bicolor* (L) moench resistant to the *Chilo partellus* (Swinhoe) through agrobacterium-mediated transformation. *Journal of Molecular Biology and Genetic Engineering*, 2: 1-8.

Indicula-Thomas, S & Balaji, P.V. 2004. Understanding the relationship between the primary structure of proteins and its propensity to be soluble on overexpression in *Escherichia coli*. *Journal of Protein Science*, 14 (**3**): 582-592.

Iseri, O.D., Korpe, D.A., Sahin, F.I & Haberal, M. 2013. Hydrogen perioxide pretreatment of roots enhanced oxidative stress response of tomato under cold stress. *Journal of Plant Physiology*, 35: 1905-1913.

Jacob, F & Monod, J. 1961. Genetic regulatory mechanisms in the synthesis of proteins. *Journal of Molecular Biology*, 3: 318-328.

Jaleel, C.A., Manivannan, P., Wahid, A., Farooq, M., Somasundaram, R & Panneerselvam. 2009. Drought stress in plants: a review on morphological characteristics and pigments composition. *International Journal of Agricultural Biology*, 11: 100-105.

Jia, B & Jeon, C.O. 2016. High through-put recombinant protein expression in *Escherichia coli*: current status and future prospective. *Open Biology*, 6: 1-17.

Jin, Q-J., Yuan, X-X., Cui, W-T., Han, B., Fend, J-F & Xu, S. 2012. Isolation and characterization of a heme oxygenase-1 gene from Chinese cabbage. *Journal of Molecular Biotechnology*, 50: 8-17.

Jin, Q., Zhu, k., Cui, W., Xie, Y., Han, B & Shen, W. 2012. Hydrogen gas acts as a novel bioactive molecule in enhancing plant tolerance to paraquat-induced oxidative stress via the modulation of heme oxygenase-1 signalling system. *Journal of Plant, Cell and Environment*, 36:956-969.

Kader, S. 2010. Cytosolic calcium and pH signaling in plants under salinity stress. *Journal of Plant Signaling Behavior*, 5 (**3)**: 233-238.

Kumar, S., Stecher, G & Tamura, K. 2016. MEGA7: Molecular Evolutionary Genetics Analysis version 7.0 for bigger datasets. *Journal of Molecular Biology and Evolution*, 33: 1870-1874.

Karuppanapandian, T., Monn, J-C., Kim, C., Manoharam, K & Kim, W. 2011. Reactive oxygen species: their generation, signal transduction and scavenging mechanisms. *Australian Journal of Crop Science*, 5 (**6**): 709-725.

Larkin, M.A., Blackshields, G., Brown, N.P., Chenna, R., McGettigan, P.A., McWilliam, H., Valentin, F., Wallace, I.M., Wilm, A., Lopez, R., Thompson, J.D., Gibson, T.J & Higgins, D.G. 2007. Clustal W and Clustal X version. *Journal of Bioinformatics*, 23: 2947-2948.

Larkindale, J & Huang, B. 2004. Thermotolerance and antioxidant systems in *Agrotis stolonifera*: involvement of salicylic acid, abscisic acid, calcium, hydrogen perioxide and ethylene. *Journal of Plant Physiology*, 161: 405-413.

Li, S.C., Squires, C.L & Squires, C. 1984.Antitermination of *E. coli* rRNA transcription is caused by a control region segment containing Lambda nut-like sequences. *Cell* 38: 851-860.

Li, W., Zhang, L., Zhang, Y., Guodong, W., Song, D & Zhang, Y. 2017. Selection and validation of appropriate reference genes for quantitative real-time PCR normalization in staminate and perfect flowers of andromonoecious *Taihangia rupestris*. *Frontiers in Plant Science*, 8: 1-13.

Lin, Y., Huang, L., Shen, W & Ren, Y. 2012. Involvement of heme oxygenase 1 in β-cyclodextrin-hemin complex-induced cucumber adventitious rooting process. *Journal of Plant Cell Reports*, 31: 1563-1572.

Lobell, D.B., Schlenker, W & Coata-Roberts, J. 2011. Climate trends and global crop production since 1980. *Journal of Science*, 333: 616-620.

Maheshwari, R & Dubey, R.S. 2009. Nickel-induced oxidative stress and the role of antioxidant defence in rice seedlings. *Plant Growth Regulation*, 59 (**1**): 37-49.

Marchler-Bauer, A., Lu, S., Anderson, J.B., Chitsaz, F., Derbyshire, M.K., DeWeese-Scott, C., Fong, J.H., Geer, L.Y., Geer, R.C., Gonzales, N.R., Gwadz, M., Hurwitz, D.I., Jackson, J.D., Ke, Z., Lanczycki, C.J., Lu, F., Marchler, G.H., Mullokandov, M., Omelchenko, M.V., Robertson, C.L., Song, J.S., Thanki, N., Yamashita, R.A., Zhang, D., Zhang, N., Zheng, C & Bryant, S.H. 2011. CDD: a Conserved Domain Database for the functional annotation of proteins. *Nucleic Acids Research*, 39: 225-229.

Maroufi, A. 2016. Selection of reference genes for real-time quantitative PCR analysis of gene expression in *Glycyrrhiza glab*ra under drought stress. *Journal of Biologia Plantarum*, 60 (**4**): 645-654.

Matsumoto, F., Obayashi, T., Sasaki-Sekimoto, Y., Ohta, H., Takamiya, K-I & Masuda, T. 2004. Gene expression profiling of the tetrapyrrole metabolic pathway in *Arabidopsis* with a mini-array system. *Journal of Plant Physiology*, 135: 2379-2391.

Medina, S.M., Rodriguez, R.R., Gomez-kosky, R., Rodriguez, N.V., Vega, M.E.G., Castilo, O.S & Ardisana, F.H. 2019. Morphoagronomic characterization of surghum cultivar "CIAO 132R-05' obtained by somatic embryogenesis in the conversion phase using different substrates. Emirates. *Journal of Food and Agriculture*, 31 (**4**): 248-255.

Mehmood, AR., Sehar, U & Ahmad, N. 2014. Use of bioinformatics tools in different spheres of life sciences. *Journal of Data Mining in Genomics and Proteomics,* 5 (**2**): 1-13.

Mittal, S., Banduni, P., Mallikarjuna, M.M., Rao, A.T., Jain, P.A., Dash, P.K & Thirunavukkarasu, N. 2018. Structural, functional and evolutionary characterization of major drought transcription factors fsmilies in maize. *Frontiers in Chemistry,* 77 (**6**): 1-16.

Mittler, M. 2002. Oxidative stress, antioxidants and stress tolerance. *Trends in Plant Science,* 7: 405-410.

Moller, I.M., Jensen, P.E & Hansson, A. 2007. Oxidative modifications to cellular components in plants. *Annual Review Plant Biology*, 58: 459-481.

Morita, T., Perella, M.A., Lee, M.E., Kourembanas, S. 1995. Smooth muscle cell-derived carbon monoxide is a regulator of vascular cGMP. *Proceedings of the National Academy of Sciences of the United States of America,* 92 (**5**): 1475-1479.

Motterlini, R., Foresti, R., Bassi, R., Calabrese, V., Clark, J.E & Green, C.J. 2000. Endothelial haem oxygenase 1 induction by hypoxia. Modulation by inducible nitric oxide synthase and S-nitrosothiols. *Journal of Biological Chemistry*, 275: 13613-13620.

Mulaudzi-Masuku, T., Ikebudu, V.C., Muthevhuli, M., Faro, A., Gehring, C.A & Iwuoha, E. 2019. Characterization and expression analysis of heme oxygenase genes from *Sorghum bicolor*. *Journal of Bioinformatics and Biology Insights*, 13: 1-11.

Munns, R & Tester, M. 2008. Mechanisms of salinity tolerance. *Annual Review of Plant Biology*, 59: 651-681.

Muramoto, T., Kohchi, T., Yokota, A., Hwang, I & Goodman, H.M. 1999. The *Arabidopsis* photomorphogenic mutant *HYI* is deficient in photochrome chromophore biosynthesis as a result of a mutation in a plastic heme oxygenase. *The Plant Cell,* 11: 335-348.

Muramoto, T., Tsurui, N., Terry, M.J., Yokota, A & Kohchi, T. 2002. Expression and biochemical properties of a ferredoxin-dependent heme oxygenase required for phytochrome chromophore synthesis. *Journal of Plant Physiology*, 130: 1958-1966.

Murphy, M.P .2009. How mitochondria produce reactive oxygen species. *Biochemical Journal,* 417 (**1**): 1-13.

Nagesh, B.R & Devaraj, V.R. 2008. High temperature and salt stress response in French bean (*Phaseolus* vulgaris). *Australian Journal of Crop Science*, 2: 40-48.

Nay, M.M., Souza, T.L.P.O., Raatz, b., mukankusi, C.M., Goncalves-Vidigal, M.C., Aberu, A.F.B., Melo, L.C & Pator-Corrales, M.A. 2019. A review of angular leaf rot resistance in common beans. *Journal of Crop Science*, 59: 1376-1391.

Noriega, G.O., Balestrasse, K.B., Batlle, A & Tomaro, M.L. 2004. Heme oxygenase exerts a protective role against oxidative stress in soyabean leaves. *Journal of Biochemical and Biophysical Research Communications*, 323: 1003-1008.

Noriega, G.O., Yannarelli, G.O., Balestrasse, K.B., Batlle, A & Tomaro, M.L. 2007. The effect of nitric oxide on heme oxygenase gene expression in soyabean leaves. *International Journal of Plant Biology*, 5: 1155-1163.

Olins, P.O., Devine, C.S., Rangwala, S.H & Kavka, K.S. 1988. T7 phage gene 10 leader RNA, a Ribosome-binding site the dramatically enhances the expression of foreign genes in *Escherichia coli*. *Gene* 73: 227-235.

Ortiz de Montellano, P.R & Wilks, A. 2001. Heme oxygenase structure and mechanism. *Advanced Inorganic Chemistry*, 51: 359-407.

Otterbein, LE., Bach, F.H., Soares, M., Tao Lu, H., Wysk, M., Davis, R.J., Flavell, R.A & Choi, A.M. 2000. Carbon monoxide has anti-inflammatory effects involving mitogen-activated protein kinase pathway. *Nature Medicine*, 6 (**4**): 422-428.

Pandey, P., Ramegowda, V & Senthil-Kumar, M. 2015. Shared and unique responses of plants to multiple individual stresses and stress combinations: physiological and molecular mechanisms. *Frontier in Plant Science*, 6: 723.

Parihar, P., Singh, S., Singh, R., Singh, V. P., and Prasad, S. M. 2015. Effect of salinity stress on plants and its tolerance strategies: a review. *Environmental Science and Pollution Research*, 22 (**6**), 4056–4075. https://doi.org/10.1007/s11356-014-3739-1

Pfaffl, M.W. 2001. A new mathematical model for relative quantification in real time RT-PCR. *Journal of Nucleic Acids Research*, 29 (**9**): 2002-2007.

Qu, R., Miao, Y., Cui, Y., Cao, Y., Zhou, Y., Tang, X & Yang, J. 2019. Selection of reference genes for the quantitative real-time PCR normalization of gene expression in *Isatis indigotica* fortune. *Journal of Molecular Biology*, 20 (**9**): 1-12.

Rasool, S., Hameed, A., Azooz, A.A., Muneeb-u-Rehman., Siddiqi, T.O & Ahmad, P. 2013. Salt stress: causes, types and responses of plants. In: Ahmad, P., Azooz, M & Prasad, M. (Editions) *Ecophysiology and Responses of plants under salt stress*. Springer, New York, NY: 1-24.

Reddy, P.S., Reddy, D.S., Sivasakthi, K., Bhatnagar_Mathur, P., Vadez, V & Sharma, K.K. 2019. Evaluation of sorghum (*Sorghum bicolor* (L.)) reference genes in various tissues and under abiotic stress conditions for quantitative real-time PCR data normalization. *Frontiers in Plant Science*, 7: 529.

Redondo-Gómez, S. 2013. Abiotic and biotic stress tolerance in plants *in* Rout, G.R & Das, A.B. (Editions) *Molecular Stress Physiology of Plants*, Springer, India, 1-20.

Remmert, M., Biegert, A., Hauser, A & Soding, J. 2012. HHBlits: lightning-fast iterative protein sequence searching by HMM-HMM alignment. *National methods*, 9: 173-175.

Salehi-Lisar, S.Y & Bakhshayeshan-Agdam, H. 2016. Drought stress in plants: causes, consequences and tolerance. In: Hossain, M., Wani, S., Bhattacharjee, S., Burritt, D & Trans, L.S. (Editions) *Drought stress tolerance in plant*, Volume 1. Springer, Cham: 1-16.

Santa-Cruz, D.M., Pacienza, N.A., Polizio, A.H., Balestrasse, K.B., Tomaro, M.L & Yanarelli, G.G. 2010.Nitric oxide synthase-like dependent NO production enhances heme oxygenase up-regulation in ultraviolet-B-irradiated soyabean plants. *Journal of Phytochemistry*, 71: 1700-1707.

Sanghera, G.S., Wani, S.H., Hussain, W & Singh, N.B. 2011. Engineering cold stress tolerance in crop plants. *Journal of Current Genomics*, 12: 30-43.

Santos, C.A., Beloti, L.L., Szymanski De Toledo, M.A., Cruello, A., Favaro, M.T.P., Mendes, J.S., Santiago, A.S., Azzoni, A.R & Souza, A. P. 2012. A novel protein folding protocol for the solubilization and purification of recombinant peptidoglycan-associated lipoprotein from *Xylella fastidiosa* overexpressed in *Escherichia coli*. *Journal of Protein Expression and Purification*, 82 (**2**): 284-290.

Satpathy, R., Behera, R., Padhi, S.K & Guru, R.K. 2013. Computational phylogenetic study and data mining approach to laccase enzyme sequences. *Journal of Phylogentic Evolution Biology*, 1 (**2**): 1-7.

Schoner, B.E., Belagaje, R.M & Schoner, R.G. 1986. Translation of a synthetic Two-cistron mRNA in *Escherichia coli. Proeedings of the National Academy of Sciences* USA, 83: 8506-8510.

Selvaraj, K & Fofana, B. 2012. An Overview of Plant Photosynthesis Modulation by Pathogen Attacks, Advances in Photosynthesis - Fundamental Aspects, Dr Mohammad Najafpour (Ed.), ISBN: 978-953-307-928-8,http://www.intechopen.com/books/advances-in photosynthesisfundamental- aspects/an-overview-of-plant-photosynthesis-modulation-by-pathogen-attacks.

Sharma, M., Gupta, S.K., Deeba, F & Pandey, V. 2017. Effects of reactive oxygen species on crop productivity: an overview in Singh, V.P., Singh, S., Tripathi, D.K., Prasad, S.H & Chauhan, D.K (First Edition), Reactive oxygen species in plant: Boon or Bane-Revisiting the role of ROS, John Wiley & Sons Ltd, 117-136.

Sharma, P & Dubey, R.S. 2004. Ascorbate peroxidase from rice seedlings: properties of enzyme isoforms, effects of stresses and protective roles of osmolytes. *Plant Science*, 167: 541-550.

Sharma, P., Jha, A.B., Dubey, R.S & Pessarakli, M. 2012. Reactive oxygen species, oxidative damage & antioxidative defence mechanism in plants under stressful conditions. *Journal of Botany*, 1-27.

Shekhawat, G.S & Mahawar, L. 2017. Heme oxygenase: A functionally diverse enzyme of photosynthetic organisms and its role in phytochrome chromophore biosynthesis, cellular signalling and defence mechanisms. *Journal of Plant, Cell & Environment*, 41: 483-500.

Shekhawat, G.S & Verma, K. 2010. Heme oxygenase (HO): an overlooked enzyme of plant metabolism and defence. *Journal of Experimental Botany*, 61 (**9**): 2255-2270.

Shen, Q., Jiang, M., Li, H., Che, L.L & Yang, Z.N. 2011. Expression of a *Brassica napus* heme oxygenase confers plant tolerance to mercury toxicity. *Journal of Plant, Cell & Environment*, 34 (**5**): 752-763.

Shewfelt, R.L. 1992. Response of plant membranes to chilling and freezing. In: Plant membranes. Springer, Dordrecht, 192-219.

Shi, S., Wang, G., Wang, Y., Zhang, L & Zhang, L. 2005. Protective effect of nitric oxide against oxidative stress under ultraviolet-B radiation. *Nitric Oxide*, 13: 1-9.

Tan, C-M., Chen, R-J., Zhang, J-H., Gao, X-L., Li, L-H., Wang, P-R., Deng, X-J & Xu, Z-J. 2013. *OsPOP5,* A prolyl oligopeptidase family gene from rice confers abiotic stress tolerance in *E.coli*. *International Journal of Molecular Science*, 14: 20204-20219.

Tenhunen, R., Marver, H.S & Schmid, R. 1968. The enzymatic conversion of heme to bilirubin by microsomal heme oxygenase. *Proceedings of the National Academy of Sciences, USA* 61: 748-755.

Tenhunen, R., Marver, H.S & Schmid,R. 1969. Microsomal heme oxygenase: characterization of the enzyme. *Journal of Biological Chemistry*, 244: 6288-6394.

Tesfaw, A & Feyissa, T. 2014. Current trends in genetic manipulations to enhance abiotic and biotic stresses in tobacco. *African Journal of Biotechnology*, 13: 2095-2102.

Truong, K & Ikura, M. 2002. Identification and characterization of subfamily-specific signatures in a large protein subfamily by a hidden Markov model approach. *BMC Bioinformatics,* 3: 1-14.

Turrens, J.F. 2003. Mitochondrial formation of reactive oxygen species. *Journal of physiology*, 552 (**2**): 335-344.

UN 2015.The millennium development goals report. Department of Economic and Social Affairs of the United Nations Secretariat.

http://www.un.org.ezproxy.uwc.ac.za/millenniumgoals/2015_MDG_Report/pdf/MDG%202015%20rev%20(July%201).pdf.

Vellosillo, T., Vicente, J., Kulasekaran, S., Hamburg, M & Castresana, C. 2010. Emerging complexity in reactive oxygen species production and signaling during response of plants to pathogens. *Plant Physiology*, 154: 444-448.

Verma, K., Dixit, S., Shekhawat, G.S & Alam, A. 2015. Antioxidant activity of heme oxygeanse 1 in *Brassica juncea* (L.) Czern. (Indian mustard) under salt stress. *Turkish Journal of Biology*, 39: 540-549.

Vernoux, T., Sanchez-Fernandez, R & May, M. 2002. Glutathione biosynthesis in plants *in* Inze, D, (Editions), *Oxidative Stress in Plants*, M. V Montagu, London: Taylor and Francis, 297-311.

Vile, G.F & Tyrrell, R.M. 1993. Oxidative stress resulting from ultraviolet A irradiation of human skin fibroblasts leads to a heme oxygenase-dependent increase of ferritin. *Journal of Biological Chemistry*, 268: 14678-14681.

Wahsha, M., Bini, C., Fontana, S., Wahsha, A. & Zilioli, D. 2012. Toxicity assessment of contaminated soils from a mining area in Northeast Italy by using lipid peroxidation assay. *Journal of GeochemicalExploration*, 113: 112-117.

Wang, H., Wang, H., Shao, H & Tang, X. 2016. Recent advances in utilizing transcription factors to improve plant abiotic stress tolerance by transgenic technology. *Frontiers in Plant Science*, 67 (**7**): 1-13.

Wang, Y., Wisniewski, M., Meilam, R., Cui, M., Webb, R & Fuchigami, L. 2005. Overexpression of cytosolic ascorbate peroxidase in tomato confers tolerance to chilling and salt stress. *Journal of the American Society for Horticultural Science*, 130 (**2**): 167-173.

Wang, L., Ma, F., Xu, S., Zheng, T., Wang, R., Chen, H & Shen, W. 2014. Cloning and characterization of a heme oxygenase 2 gene from rice (*Oryza sativa* L.), and its expression analysis in response to some abiotic stresses. *Acta Physiologiae Plantarum*, 36: 893-902.

Wang, Y., You, F.M., Lazo, G., Luo, M.C., Thilmony, R., Gordon, S., Kianian, S.F & Gu, Y.Q. 2013. PIECE: a database for plant gene structure comparison and evolution. Journal of Nucleic Acids Research, 41: 1159-1166.

Wingfield, P.T. 2016. Overview of the purification of recombinant proteins. *Current Protocol of Protein Science*, 80: 1-50.

Wu, B., Gao, L., Gao, J., Xu, Y., Liu, H., Cao, X., Zhang, B & Chen, K. 2017. Genome-wide identification, expression patterns and functional analysis of UDP glycosyltransferase family in peach (*Prunus persica* L. Batsch). *Frontiers in Plant Science*, 389 (**8**): 1-14.

Wu, M., Huang, J., Xu, S., Ling, T., Xie, Y & Shen, W. 2011. Haem oxygenase delays programmed cell death in what aleurone layers by modulation of hydrogen peroxide metabolism. *Journal of Experimental Botany*, 62: 235-248.

Xie, Y-J., Cui, W.T., Yuan, X.X., Shen, W-B & Yang, Q. 2011. Haem oxygenase-1 is associated with wheat salinity acclimation by modulating reactive oxygen species homeostasis. *Journal of Integrated Plant Biology*, 53: 653-670.

Xie, Y-J., Xu, S., Han, B., Wu, M.Z., Yuan, X.X., Han, Y., Gu, Q., Xu, D.K., Yang, Q & Shen, W.B. 2011. Evidence of *Arabidopsis* salt acclimation induced by upregulation of *HYI* and the regulatory role of RbohD-derived reactive oxygen species synthesis. *Plant Journal*, 66 (**2**): 280-292.

Xu, D-K., Jin, Q-J., Xie, Y-J., Liu, Y-H., Lin, Y-T., Shen, W-B & Zhou, Y-J. 2011. Characterization of a wheat heme oxygenase-1 gene and its responses to different abiotic stresses. *International Journal of Molecular Sciences*, 12: 7692-7707.

Xu, S., Zhang, B., Cao, X.Y., Ling, T.F & Shen, W.B. 2010. Heme oxygenase is involved in cobalt chloride-induced lateral root development in tomato. *Journal of Biometal*, 24: 181-191.

Xu, S., Wang, R., Zhang, B., Han, B., Xie,Y.J., Yang, J., Zhong, W., Chen, H., Wang, R., Wang, N., Cui, W & Shen, W. 2012. RNAi knoeckdown of rice SE5 gene is sensitive to the herbicide methyl viologen by the down-regulation of antioxidant defence. *Journal of Plant Molecular Biology*, 80: 219-236.

Xuan, W., Huang, L.Q., Li, M., Huang, B.K., Xu, S., Liu, H., Gao, Y & Shen, W.B. 2007. Induction of growth eleongation n wheat root segments by heme molecules: a regulatory role of carbon monoxide in plants. *Journal of Plant Growth Regulation*, 52: 41-51.

Xuan, W., Xu, S., Li, M., Han, B., Zhang, B., Zhang, J., Lin, Y., Huang, J., Shen, W & Cui, J. 2012. Nitric oxide is involved in hemein-induced cucumber adventitious rooting process. *Journal of Plant Physiology*, 169 (**11**): 1032-1039.

Yadav, N & Sharma, S. 2016. Reactive oxygen species, oxidative stress and ROS scavenging system in plants. *Journal of Chemical and Pharmaceutical Research*, 8 (**5**): 595-604.

Yannarelli, G.G., Noriega, G.O., Batlle, A & Tomaro, M.L. 2006. Heme oxygenase up-regulation in ultraviolet-B irradiated soyabean plants involves reactive oxygen species. *Planta*, 224: 1154-1162.

Youn, C.L., Britton, Z.T & Robinson, A.S. 2012. Recombinant protein expression and purification: A comprehensive review of affinity tags and microbial applications. *Journal of Biotechnology*, 7: 620-634.

Yu, C.S., Chen, Y.C., Lu, C.H & Hwang, J.K. 2006. Prediction of protein subcellular localization. *Journal of Proteins Structure, Function and Bioinformatics*, 64: 643-651.

Zhu, K., Jin, Q., Samma, M.K., Lin, G & Shen, W. 2014. Molecular cloning and characterization of a heme oxygenase-1 gene from sunflower and its expression profiles in salinity acclimation. *Journal of Molecular Biology*, 41: 4109-4121.

Zhu, Jian-Kang. 2016. Abiotic stress signaling and responses in plants. *Cell*, 313-323.

Zilli, C.G., Balestrasse, K.B., Yannarelli, G.G., Polizio, A.H., Santa-Cruz, D.M & Tomaro, M.L. 2008. Heme oxygenase up-regulation under salt stress protects nitrogen metabolism in modules of soybean plants. *Journal of Environmental Experimental Botany*, 64: 83-89

7 APPENDICES

Appendix I:

A. Table 2.1: Predicted parameters of heme oxygenase genes

Specie name	Protein accession number	mRNA accession number
Sorghum bicolor HO1	AAK63010.1	AF320026.1
Sorghum bicolor HO4	XP_021304790.1	XM_021449115.1
Sorghum bicolor HO3	XP_002438642.1	XM_002438597.2
Sorghum bicolor HO2	AAK63011.1	AF320027.1
Arabidopsis thaliana HO1	BAA77759.1	AB021858
Arabidopsis thaliana HO2	NP_001189610.1	NM_001202681
Arabidopsis thaliana HO3	NP_001117574.1	NM_001124102
Arabidopsis thaliana HO4	NP_176126.1	NM_104610.2
Zea mays HO1	NP_001132297.2	NM_001138825.2
Glycine max HO1	NP_001304379.2	NM_001317450.2
Glycine max HO3	NP_001241990.2	NM_001255061.2
Oryza sativa Japonica Group HO1	XP_015643881	XM_015788395
Oryza sativa HO2	XP_015628243.1	XM_015772757
Brassica napus HO1	NP_001302925.1	NM_001315996
Brachypodium distachyon HO1	XP_003563666.1	XM_003563618
Solanum lycopersicum HO1	NP_001308017.1	NM_001321088
Solanum tuberosum HO1	XP_006345230.1	XM_006345168
Setaria italica HO1	XP_004965948.1	XM_004965891.2
Hevea brasiliensis HO1	XP_021658847.1	XM_021803155.1
Spinacia oleracea HO1	XP_021836810.1	XM_021981118.1
Aegilops tauschii HO1	XP_020189607.1	XM_020334018
Elaeis guineensis HO1	XP_010914863.1	XM_010916561.2
Asparagus officinalis HO1	XP_020240824.1	XM_020385235.1
Dendrobium catenatum HO1	XP_020688838.1	XM_020833179.1
Ziziphus jujuba HO1	XP_015901789.1	XM_016046303.2
Nicotiana tabacum HO1	NP_001312953.1	NM_001326024.1
Gossypium hirsutum HO1	XP_016754560.1	XM_016899071
Sesamum indicum HO1	XP_011078320.1	XM_011080018.2
Jatropha curcas HO1	XP_012078785.1	XM_012223395.2

Manihot esculenta HO1	XP_021591896.1	XM_021736204.1
Cucurbita maxima HO1	XP_023007741.1	XM_023151973.1
Amborella trichopoda HO1	XP_006842077.1	XM_006842014.3
Chenopodium quinoa HO1	XP_021760807.1	XM_021905115.1
Phalaenopsis equestris HO1	XP_020576956.1	XM_020721297.1
Cucurbita moschata HO1	XP_022933640.1	XM_023077872
Cucumis sativus HO1	XP_004150862.1	004150814.2
Medicago sativa HO1	ADK12637.1	HM212768
Medicago sativa HO2	ADV15621.1	HQ652868
Brassica junea HO1	AET97566.1	JN202587.1
Brassica junea HO2	AET97567.1	JN202588.1
Brassica junea HO3	AET97568.1	JN202589.1
Triticum aestivum HO1	ADG56719.1	HM14348.1
Hordeum vulgare HO1	AEI69729.1	JF913455.1

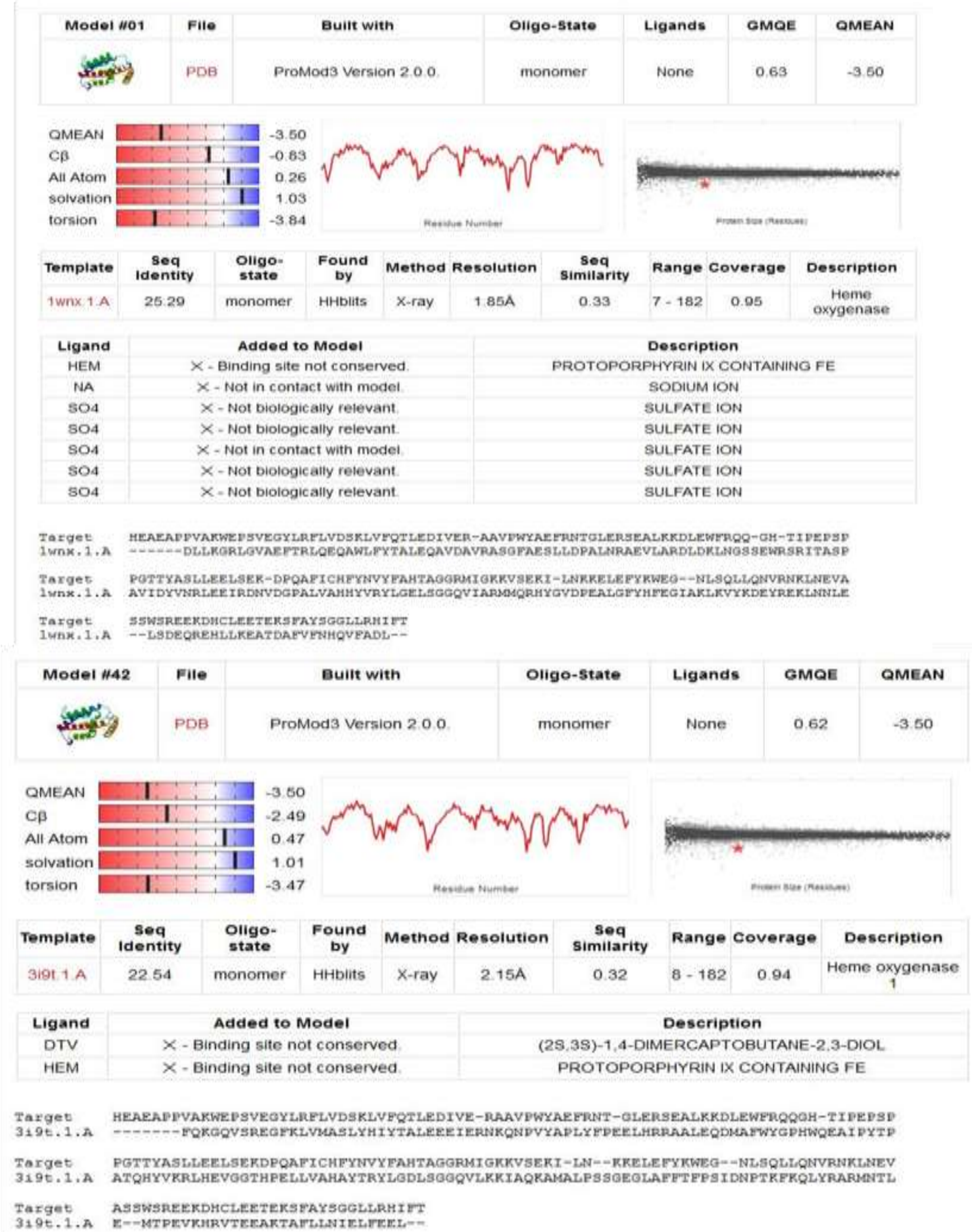

FIGURE 1: Comparison plot of *Sb*HO1 with non-redundant set of PDB structures. A combination of the c-beta atoms, solvation energy, all-atom energy and torison angle.

Appendix II: Stock solutions, gel preparations, bacterial strains and buffers

A. Stock solutions, media and buffer preparations

All reagents were supplied by ThermoFisher Scientific, Gene Direx, Thermo Scientific and New England Biolabs unless otherwise stated.

2 X SDS sample buffer: 10 % SDS, 1 M Tris-HCl pH 6.8, 0.5 % bromophenol blue, 200 mM β-mercaptoethanol and 20 % glycerol stored at -20 °C.

APS (Ammonium persulphate): 10 % APS was prepared by dissolving 100 mg in 1 ml distilled water and stored at -20 °C.

Bacterial strains: BL21 CODON Plus competent cells

Coomassie staining solution: 250 mg Coomassie Blue R-250, 45 % methanol and 10 % acetic acid made up to a final volume of 1000 ml with distilled water.

De-staining solution: for de-staining 30 % methanol, 10 % acetic acid in distilled water.

Electrophoresis buffer (SDS): 10 X stock solution was prepared by dissolving 30 g Tris-HCl, 144 g glycine, 10 g SDS and made up to a final volume of 1000 ml with distilled water.

Electrophoresis buffer (TBE): 10 x stock solution prepared by dissolving 108 g Tris, 55 g boric acid and 9.3 g EDTA made up to 1000 ml with distilled water.

Elution buffer: 1 X PBS containing 286.3 mM NaCl pH 7.4 and 250 mM Imidazole.

Equilibration buffer: 1 X PBS containing 286.3 mM NaCl pH 7.4, 10 mM Imadazole,

Glucose 20 %: 4 g of glucose in 20 ml distilled water.

Kanamycin: 50 mg/ml stock solution prepared in distilled water; 1 g of kanamycin in 10 ml of distilled water.

IPTG (Isopropyl-1-thio D-galactoside): 1 M stock solution prepared by dissolving 1.19 g IPTG in 50 ml distilled water. The prepared stock was filter-sterilized, aliquoted in 2 ml eppendorf tubes and was store at – 20 °C.

Luria Broth (LB): weighed 10 g tryptone, 5 g yeast extract, 10 g NaCl and dissolved in 1 L distilled water. The media was autoclaved at 121 °C for 20 minutes.

Lysis buffer: 1 X PBS pH 7.4, 286.3 mM NaCl,0.1.% Triton-X100, 0.1 mM β-mercaptoethanol, 5 mM imidazole,100 µg/ml of lysozyme, 1 mM PMSF (phenylmethylsulfonyl fluoride).

Nutrient agar: LB medium containing 15 g/l Bacteriological Agar.

Phenylmethylsulfonyl fluoride (PMSF): 1 mM PMSF in distilled water.

Primers: 100 µM stock solutions stored at -20 °C.

SDS: 10 % stock solution was prepared by adding 100mg of SDS dissolved in 1000 ml water and was stored at room temperature.

Separating gel (12 %): 1.5 M Tris pH 8.8, 30 % acrylamide. 10 % SDS, 10 % APS, 8 ul TEMED, 2.6 ml water.

Stacking gel (6 %): 0.5 M Tris pH 6.8, 30 % acrylamide. 10 % SDS, 10 % APS, 5 ul TEMED, 2.6 ml water.

Tris-Cl: 1.5 M stock solution prepared by dissolving 72.68 g in 200 ml distilled water, pH adjusted with HCl and make up to a final volume of 400ml with distilled water.

Tris-Cl: 0.5 M stock solution prepared by dissolving 12.1 g in 100 ml distilled water, pH adjusted with HCl and make up to a final volume of 200ml with distilled water.

Urea lysis buffer: 1 X PBS pH 7.4, 286.3 mM NaCl,5 mM β-mercaptoethanol, 4 M urea, 10 mM imidazole, 1 mM PMSF, 0.1% Triton X-100, 100 ug/ml lysozyme.

Wash buffer 1: 1 X PBS containing 286.3 mM NaCl pH 7.4, 0 mM imidazole.

Wash buffer 2: 1 X PBS containing 286.3 mM NaCl pH 7.4, 5 mM Imidazole.

Wash buffer 3:, 1 X PBS containing 286.3 mM NaCl pH 7.4, 10 mM Imadazole.

B: Preparation of 1 % agarose gel and DNA samples

One gram of agarose (Lab Unlimited, UK) was dissolved in 100 ml of 1 X TBE and microwaved for 1 minute to dissolve the agarose. It was allowed to cool after which it was poured into a casting tray with a comb. The comb was removed upon solidification. For molecular weight lane, 2 µl of loading dye and 4 µl DNA ladder (Clontech Laboratories and GeneDireX respectively) was aliquoted. Also, 2 µl of loading dye and 10 µl of the sample were mixed and loaded. The gel was electrophoresed at 80 V for 1 hour and the gel was viewed using ENDURO™ GDS (Labnet International, UK).

C: Preparation of a 12 % SDS-PAGE

SDS PAGE was prepared using the protocol in Table 1; the separating gel was 12 % and the stacking was 6 %. The separating gel was prepared first, poured between the spacer plates and enough space was left for the stacking gel. Isopropanol was dispensed on top the separating gel and the gel was left to set for 20 minutes at room temperature. Once solidified, the isopropanol was poured off on paper towel and the stacking gel was prepared and loaded on top of the separating gel. This was followed by immediately placing 1 mm well combs between the spacer plates to form wells.

Table 1: preparation of SDS PAGE for analysis of expressed *Sb*HO1 protein

Gel type	Stacking gel (6 %)	Separating gel (12 %)
dH_2O	2.6 ml	2.6 ml
Acrylamide 30 %	1 ml	3.2 ml
0.5 M Tris-HCl pH 6.8	1.25 ml	0 ml
1.5 M Tris-HCl pH 8.8	0 ml	2 ml
10 % SDS	0.05 ml	0.08 ml
10 % APS	0.05 ml	0.08 ml
TEMED	0.005 ml	0.008 ml

D: Protein sample preparation

The protein lysate of recombinant *Sb*HO1 were mixed with 2 X SDS-loading dye (10 % SDS, 0.2 M Tris, p H 6.8, 20 % glycerol, 0.5 % Bromophenol Blue, 200 mM beta-mercaptoethanol) followed by incubation at 95 °C for 5 minutes. The samples were then loaded on a 12 % 1D SDS-PAGE gel and ran at 100 V in 1X SDS running buffer from a 10x stock solution containing 30 g Tris-HCl, 144 g glycine, 10 g SDS. Following electrophoresis, the gels were stained with Coomassie Brilliant Blue staining buffer (2 g Coomassie blue R-250, 45 % methanol and 10 % glacial acetic acid made up to a final volume of 1000 ml with distilled water) for 20 minutes and then destained with a destaining solution (30 % methanol, 10 % glacial acetic acid made up to a final volume of 1000 ml with distilled water).

Appendix III: Determination of protein concentration using Bradford assay

Table 2: Bradford assay standards

Tube number	Standard volume (µl)	Source of standard (BSA)	Diluent Buffer 1 (µl)	Final protein concentration (mg/ml)
1	200	2 mg/ml	0	2
2	300	2 mg/ml	100	1.5
3	200	2 mg/ml	200	1
4	200	tube 2	200	0.75
5	200	tube 3	200	0.5
6	200	tube 5	200	0.25
7	200	tube 6	200	0.125
8 (blank)	–	–	200	0

Table 3: protein standard and Bradford reagent volumes added to a 96 well microplate

Assay	Volume of standard and sample	1 X bradford reagent
Microplate	5 µl	250 µl

Final protein concentration (mg/ml)	Absorbance @ 595 nm
2	0.73
1.5	0.68
1	0.43
0.75	0.34
0.5	0.21
0.25	0.10
0.125	0.06
0	0
*Sb*HO1	0.0515

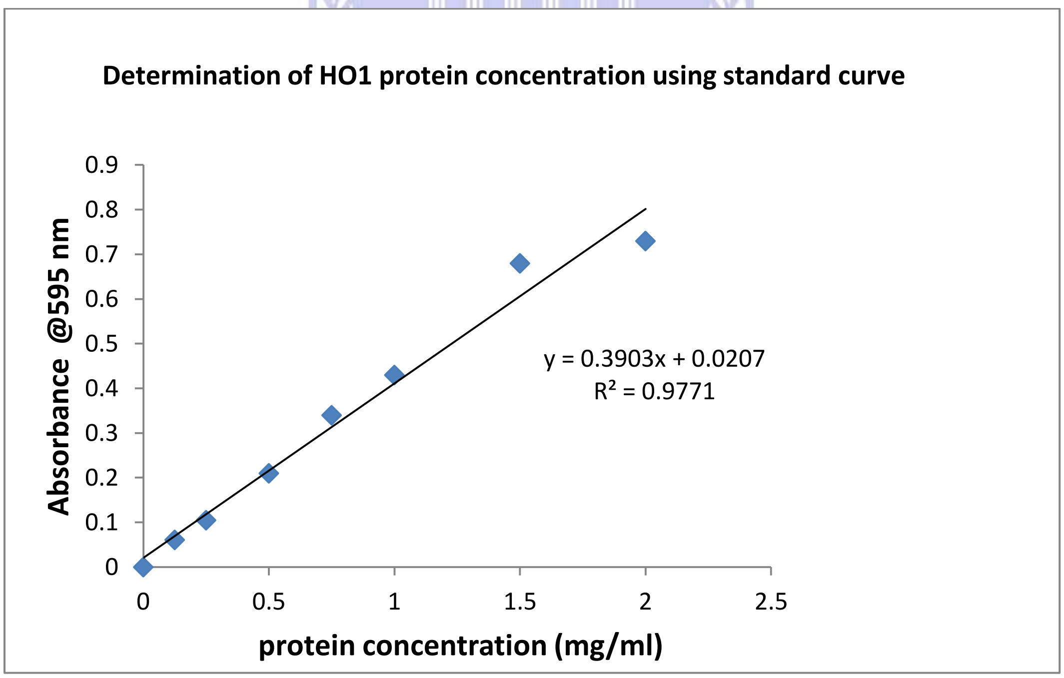

Figure 2: Standard curve of the BSA for the Bradford assay to determine the protein concentration of the recombinant *Sb*HO1 protein.

Using the equation above the protein concentration of *Sb*HO1 was calculated as shown below:

$Y= 0.3903x + 0.0207$

$0.0515= 0.3903x + 0.0207$

$0.3903x= 0.0515-0.0207$

$X= 0.078$ mg/ml